

# Statistical Geometry Image Examples

To the present time examples of these patterns as images have been rather scattered. It is the object here to collect as many of them as possible into a single document. Some of these images are technical in nature, while others belong more to "art". Each image is placed on a separate page, with supporting text. This is a big file, because the images must have reasonably good resolution if one is to see all the fine detail.

For the reader who would like more information, or who would like to construct his own computer code, the site ([john-art.com](http://john-art.com)) contains much technical information. Such readers are referred to the other documents on the site, or the last page of this document.

## Statistical Geometry Described

The first discovery of the algorithm was for circles. It was found that if the sizes of circles were made progressively smaller in a specific way, and new non-overlapping sites where a smaller circle could be placed were sought by random search, it is possible to continue placing ever-smaller circles indefinitely, i.e., "to infinity". The author has created patterns with a million circles with no sign that the process will stop. The process used here is always *space-filling*, i.e., with a sufficiently large number of circles space can be filled to an arbitrary degree of completion.

A surprising finding is that the algorithm appears to work for any shape, and is space-filling for any shape. It does not require that the shapes all be congruent to each other.

The algorithm is quite general and works in 1, 2, and 3 physical dimensions. Only the 2-dimensional case is presented here, as it is the easiest to grasp and the most useful for graphic arts, etc. It is emphasized that all of these images are made with the same algorithm. In going from one shape to another the only things which need to be changed in the computer code are (1) the formula(s) for the linear dimension(s) of the shape as a function of its area (e.g.,  $\text{radius} = \sqrt{\text{area}/\pi}$  for a circle), (2) the code which tests whether two shapes overlap each other.

In general the plan here is to proceed from the simpler cases to more complicated ones.

Fig. 9.1. Circles. Random color.  $c=1.27$ ,  $N=1$ , 2500 circles, fill 89.6%

This is quite typical of the ever-smaller-circle patterns. One of the challenges is to color the circles in such a way that the human eye sees all of them. With simple black-on-white the smaller circles tend to be seen as a blurry gray. Random color provides good contrast for even the tiniest circles.

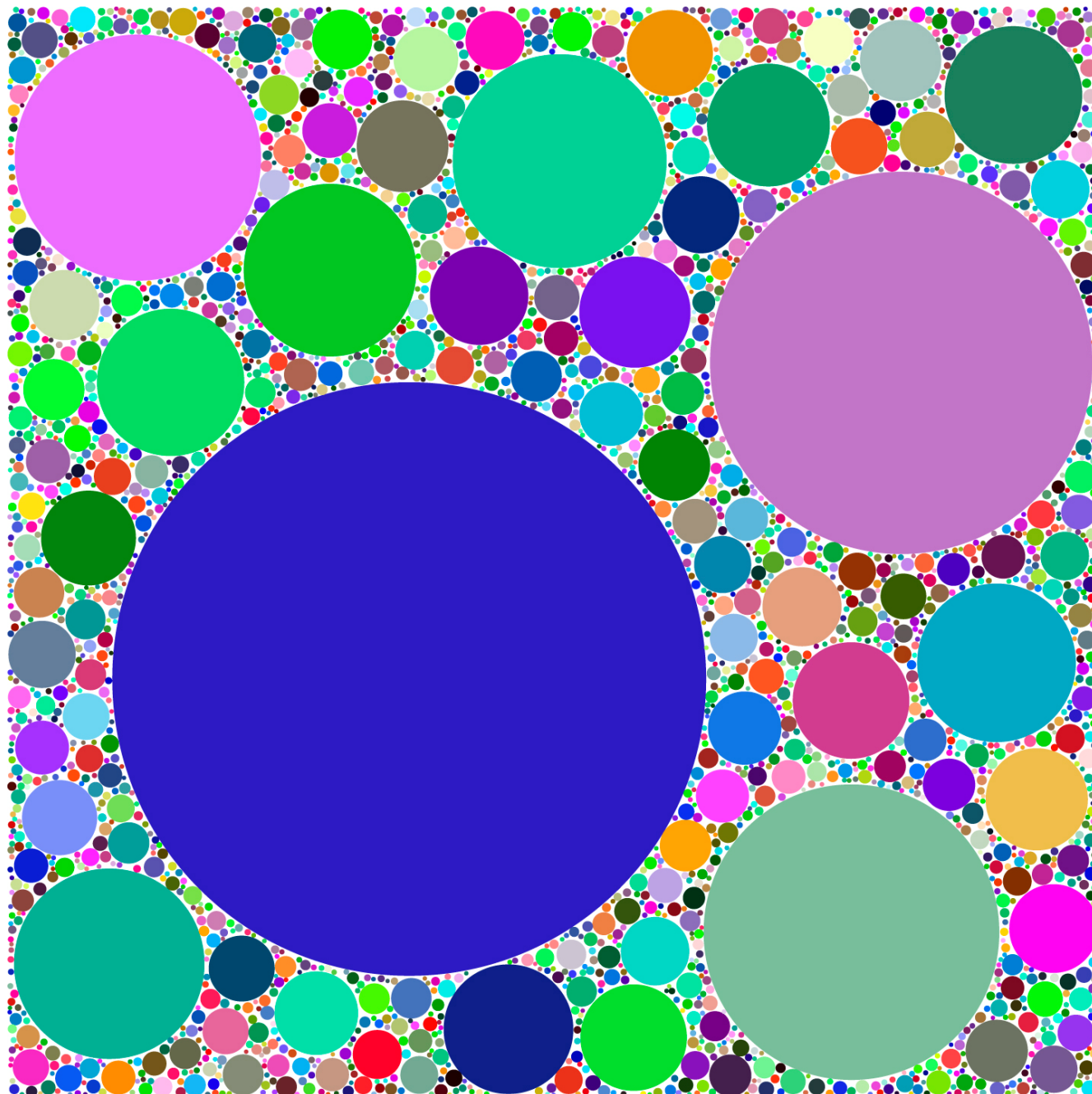


Fig. 9.2. Circles. Random color.  $c=1.40$ ,  $N=1,500$  circles, fill 93.3%

The parameter  $c$  has a big effect on the pattern. Higher  $c$  gives tighter packing. Here a mere 500 circles fill 93.3% of the available area. The trade-off is that the number of trial positions for placement is much higher for each placement.

Such an image can have a different appearance depending on how the circles are colored, and that is where art comes in.

A discerning viewer will see that this image is much more *ordered* than the previous one with  $c = 1.27$ . The average distance between circles (compared to the size of the smallest circle) is much smaller.

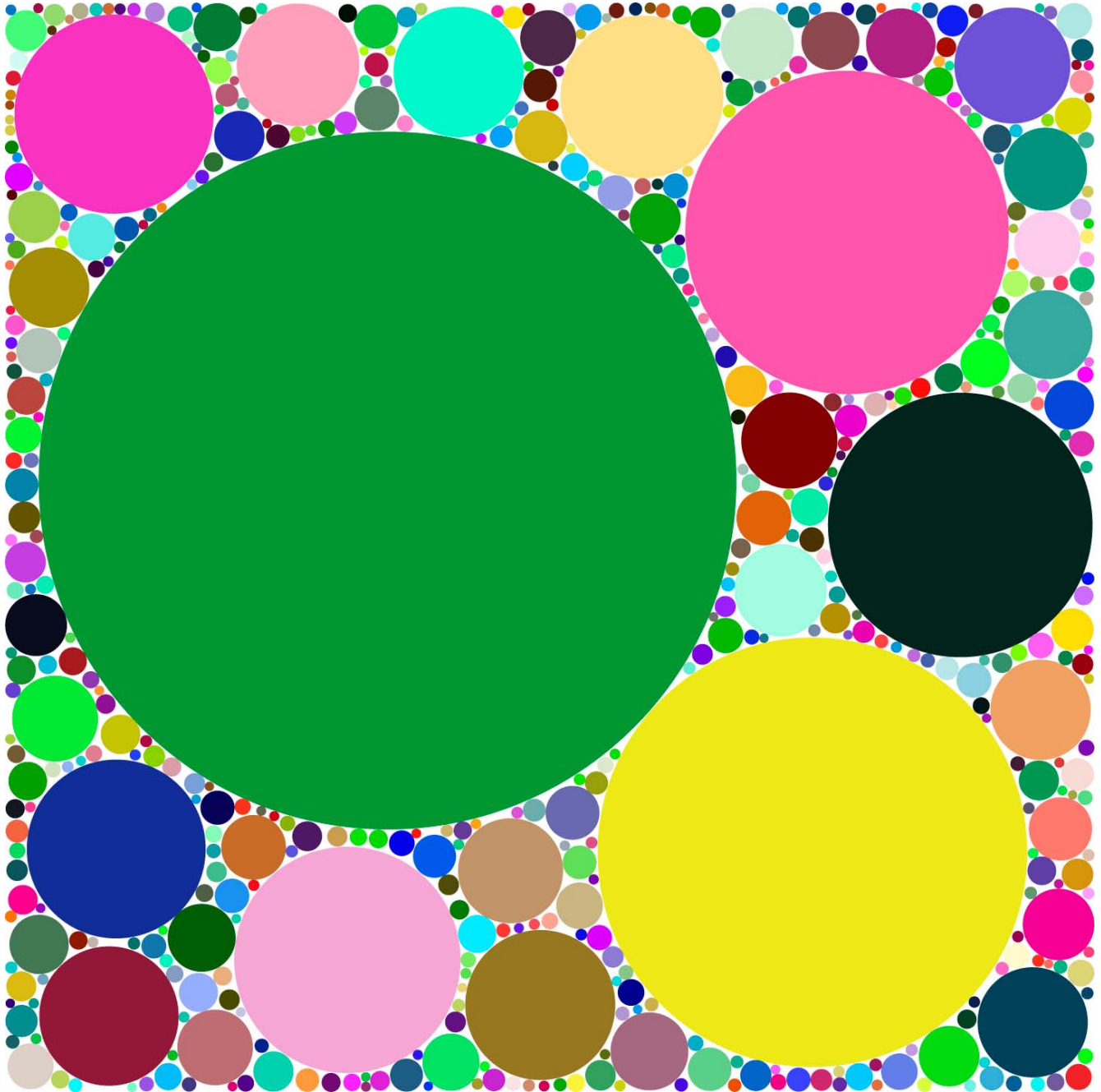


Fig. 9.3. Circles. Log-periodic color.  $c=1.28$ ,  $N=2$ , 5000 circles, fill 89.6%

The essence of this color scheme is that circles of about the same size have nearly the same color (each circle has a nominally different color). This helps to illustrate the idea of "statistical self-similarity" -- the same rules operating on an ever-smaller scale. The color sequence repeats, as close inspection will show.

Here the "gasket" (space between shapes) is black.

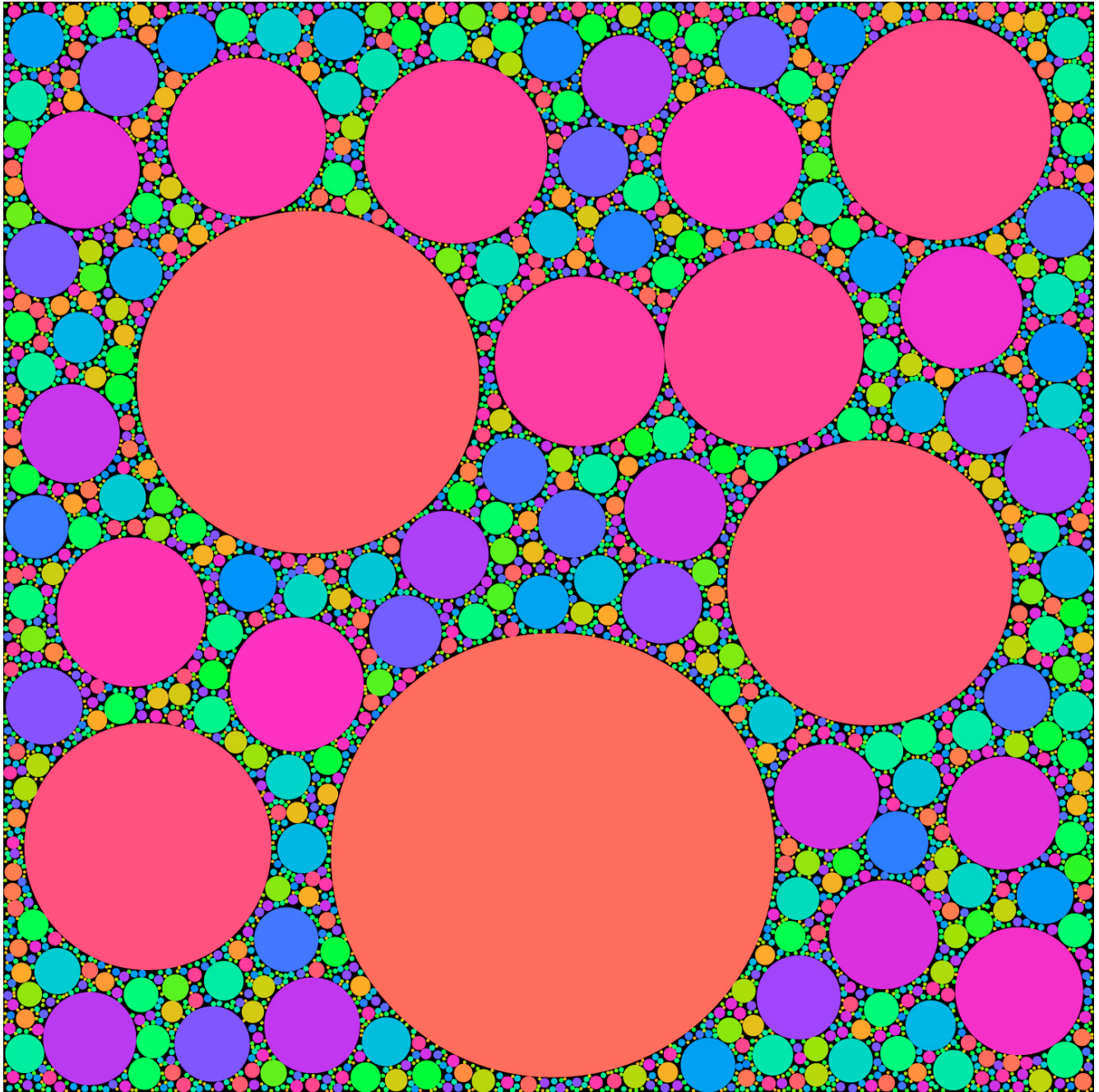


Fig. 9.4. Circles as yin-yang symbols.

This illustrates some of the possibilities for the use of these fractals in decorative art. One can place any circular shape within each circle. The author does not know what the symbolic Taoist interpretation of this image might be. I believe that red and blue are the customary colors in some east Asian traditions. "Smiley faces" could be another example.

While the examples shown here are all space-filling, for decorative purposes it may be desirable to set up the algorithm with less than 100% fill with a corresponding gain in visibility. This is easily done.

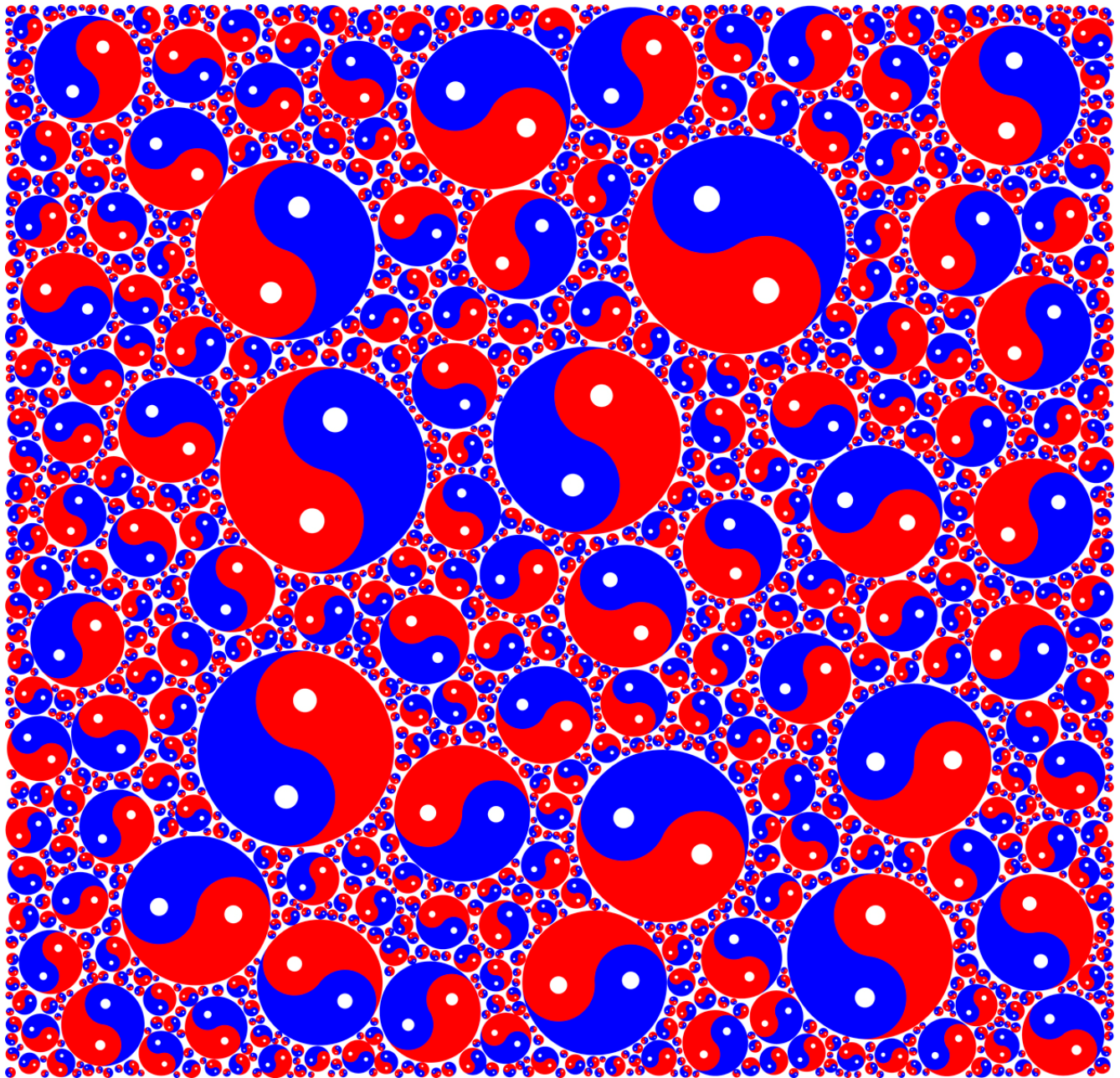
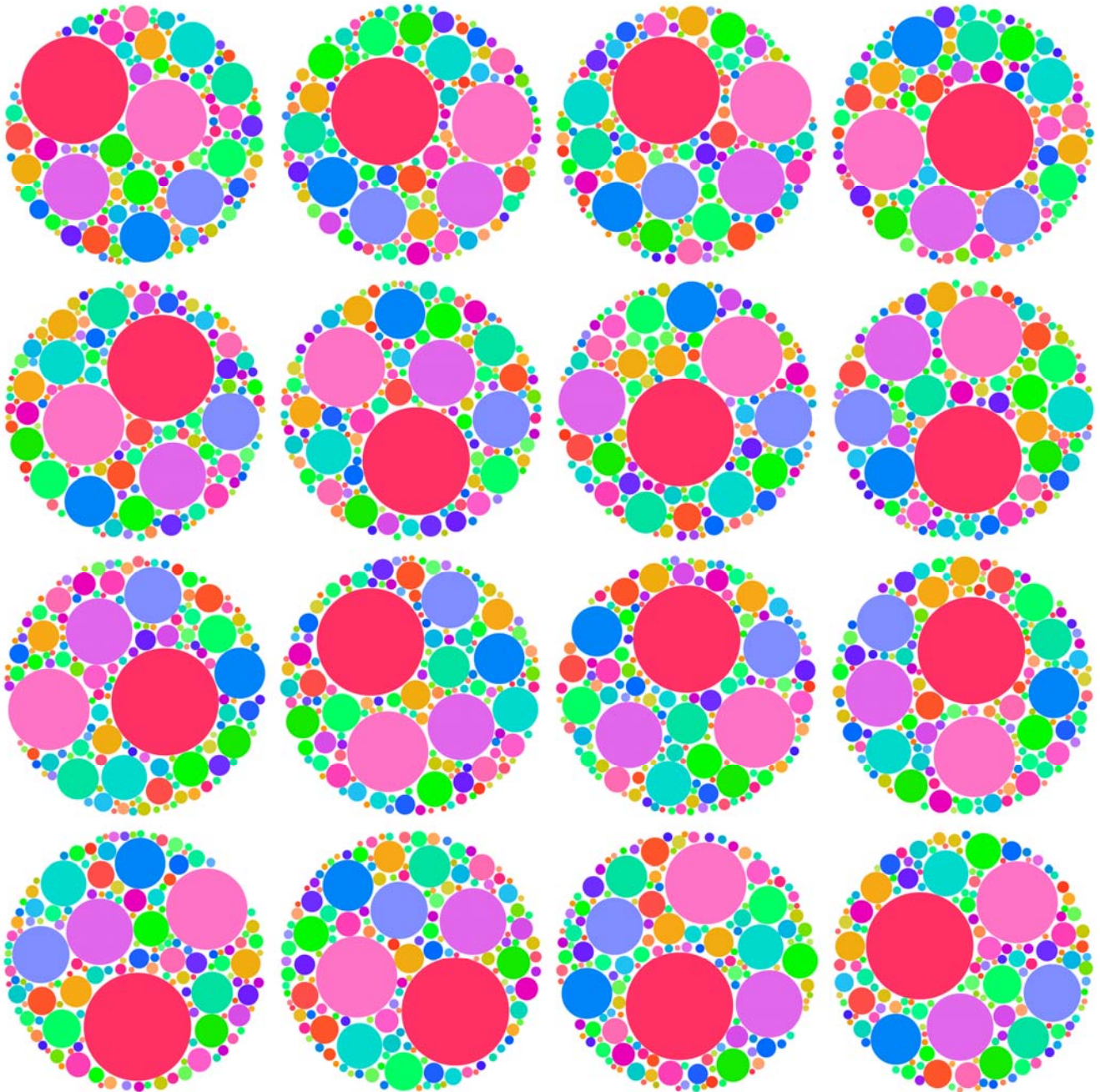


Fig. 9.5. Multiple case; circles-in-circle.

This shows circles placed within a circular boundary. The use of boundaries with varied shapes is one of the little-explored possibilities.

The algorithm has been re-run 16 times and drawn with the same color scheme in all cases (e.g., the biggest circle is always red). It is interesting how the eye perceives this -- most people have a hard time recognizing the difference between one example and another. It seems "all the same".



The algorithm repeated 16 times with the same color scheme

Fig. 9.6. Squares. Log-periodic color.  $c=1.42$ ,  $N=2$ , 6500 squares, fill 97%

Squares are the most "packable" of the shapes that have been studied, i.e., they require the fewest trials for a given number of placements. This can also be interpreted as "best fit". This quite high fill can only be achieved with fairly large  $c$  values. The white unfilled "gasket" area is so small that it is hard to see at this resolution.

It is perhaps worthy of note that the long rows of small squares between big squares are about the same color, i.e., placed at about the same time. This is an odd property of the algorithm that could use further study, and is seen at all length scales. Filling of such a "slot" appears to temporarily slow the algorithm.

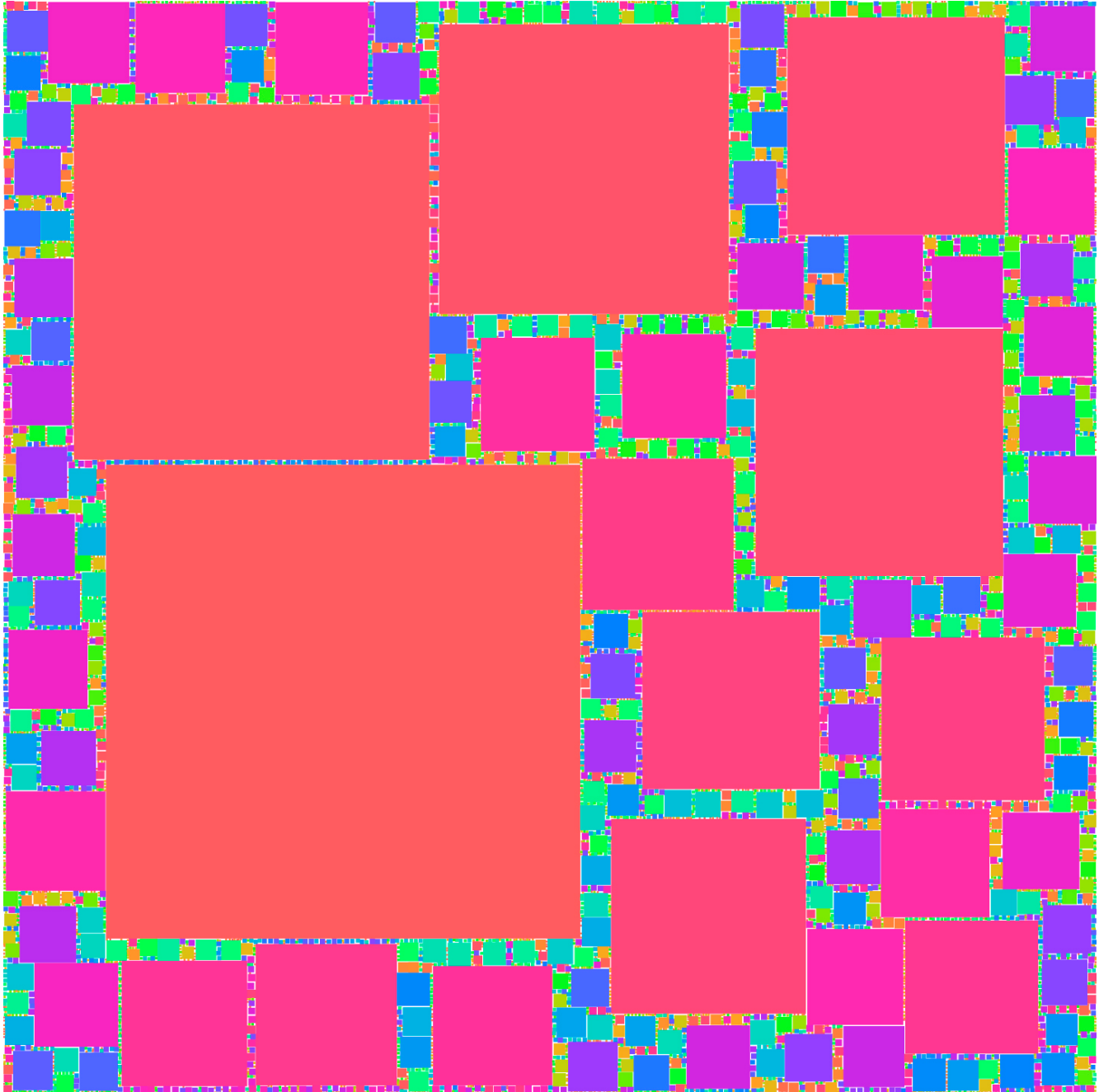


Fig. 9.7. Mixed rectangles. Black and white.  $c=1.30$ ,  $N=5$ , 4000 circles, fill 90.5%

The algorithm works with rectangles. In this case we have rectangles with a 2.5:1 aspect ratio, with the orientation changed after each placement. Those elongated horizontally are colored black and those elongated vertically are white. Red gasket. This is best viewed as two different shapes. The viewer can see that there is a strong correlation here. The black shapes are placed preferentially near other black shapes, and *vice versa* for white. The correlation becomes stronger for a larger aspect ratio, and the trials needed for placement of a given number of shapes rises sharply.

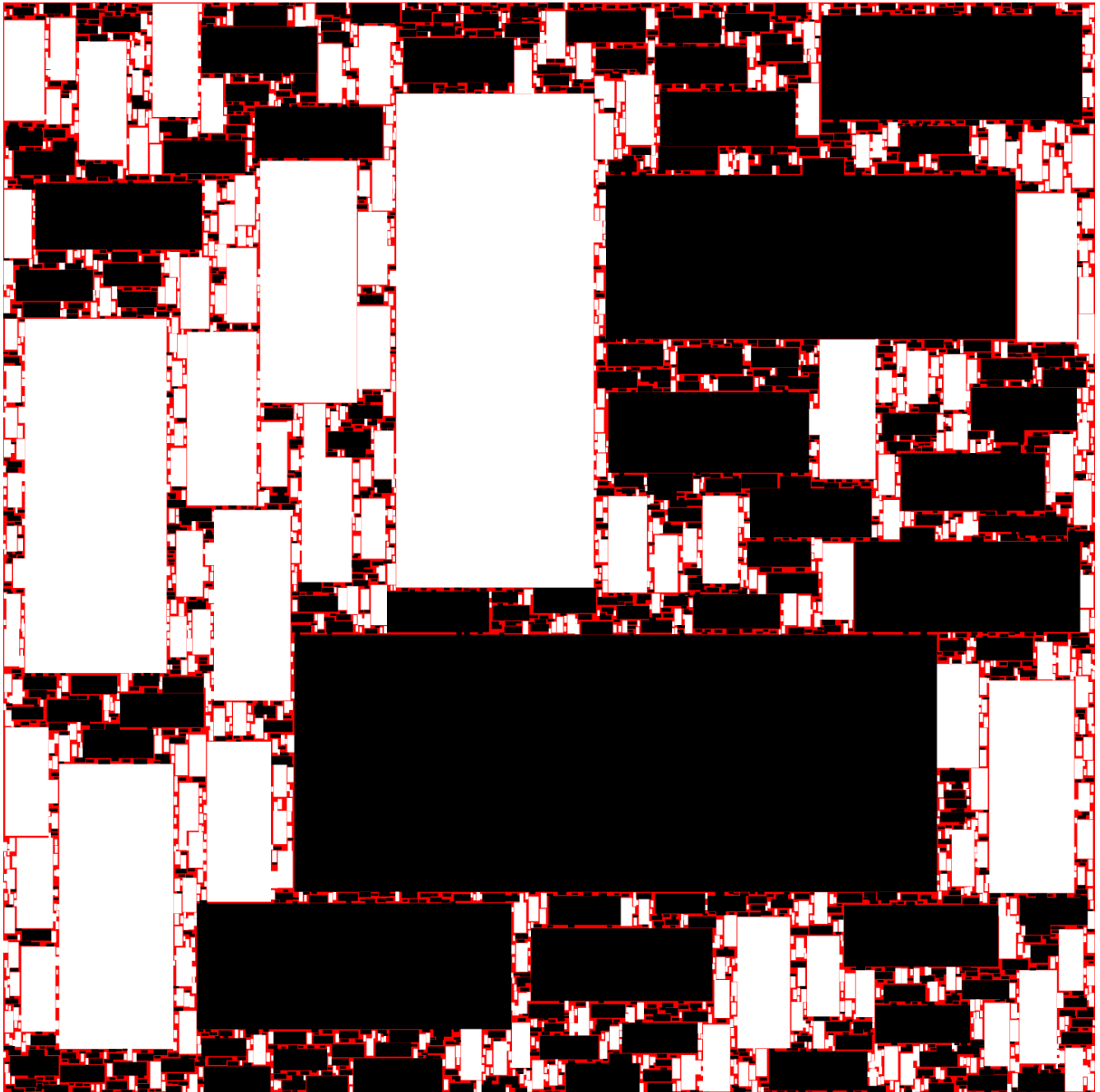




Fig. 9.8. Rectangles as flags.  $c=1.42$ ,  $N=2$ , 235 flags, fill 88%

Here there are 235 American flags, one for each year of independence (to 2012). This can, of course, be done for any flag. The smallest stars are not fully resolved here, but modern inkjet printers can define them crisply in a paper print.

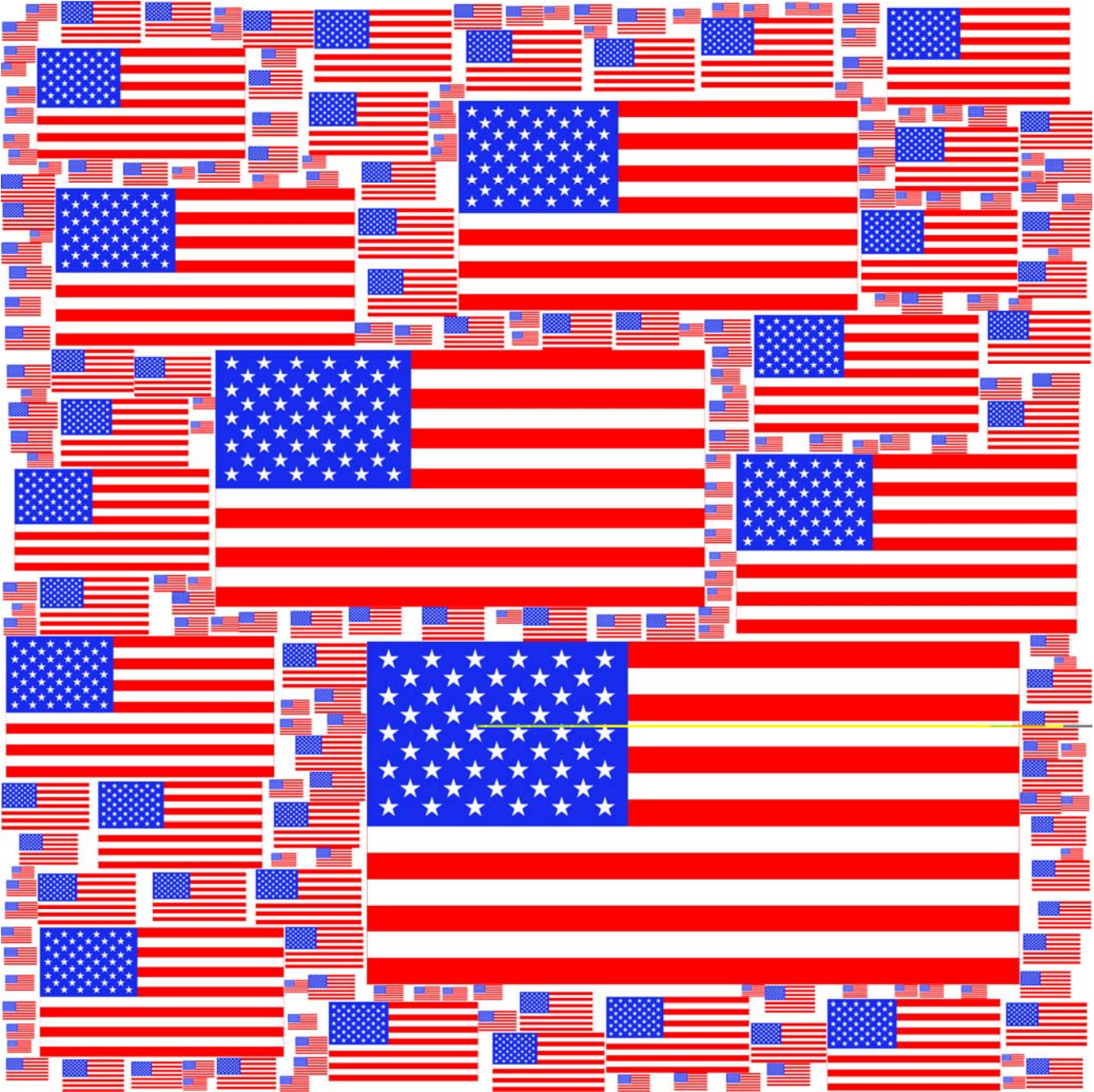


Fig. 9.9. Variable-angle squares.

Here the squares are allowed to have an orientation angle. At each trial a new random orientation angle is chosen along with random positions  $x$  and  $y$ . The color scheme is periodic in the orientation angle so that two squares with the same orientation have the same color. The viewer will see that there are "islands" of nearly-same orientation, resulting from the later placements needing to approximately line up with earlier ones. This is yet another form of correlation. This was first explored by Paul Bourke. Periodic boundaries.

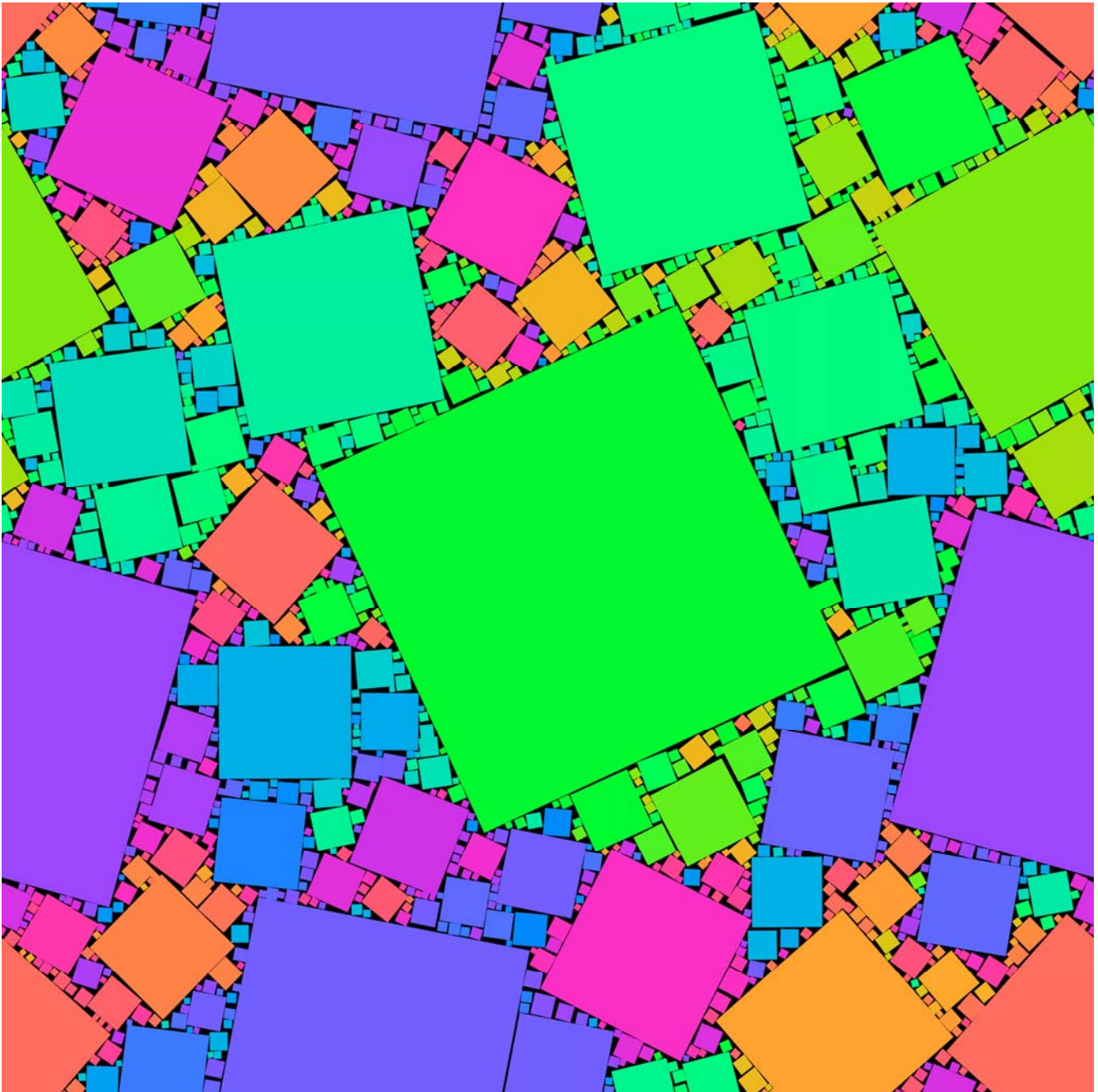


Fig. 9.10. Plusses (or crosses).  $c=1.32$ ,  $N=2$ , 1000 shapes, fill 87.4%

The arm width and length are the same. This is a somewhat more chaotic fill pattern than for squares. This  $c$  value is about the largest that can be used for this shape. Log-periodic color, white gasket. This shape is used by the Red Cross, and is on the Swiss flag.

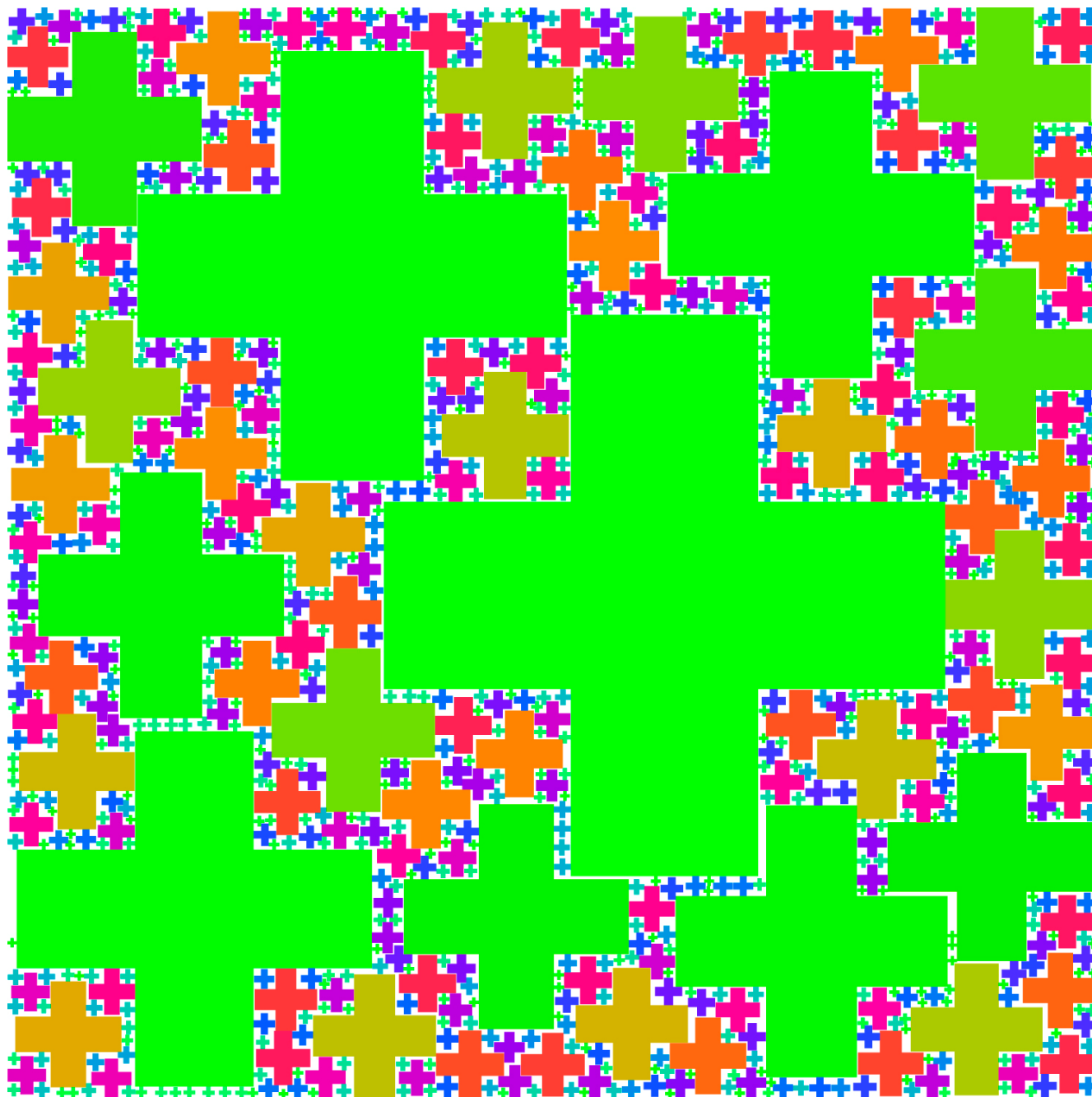


Fig. 9.11. Pi symbols.  $c=1.21$ ,  $N=2$ , 2000 shapes, fill 77.8%

This pattern has an interesting recursive-like feature. The “hollow” in the pi has a 2:1 aspect ratio and the pi symbol has a 1:1 aspect ratio. If you look at the pattern you see that in most cases the hollow has two of the next-smallest-size pis. This relationship is not exact due to the random placement. Originally created for a Pi-Day lecture (3-14-12).

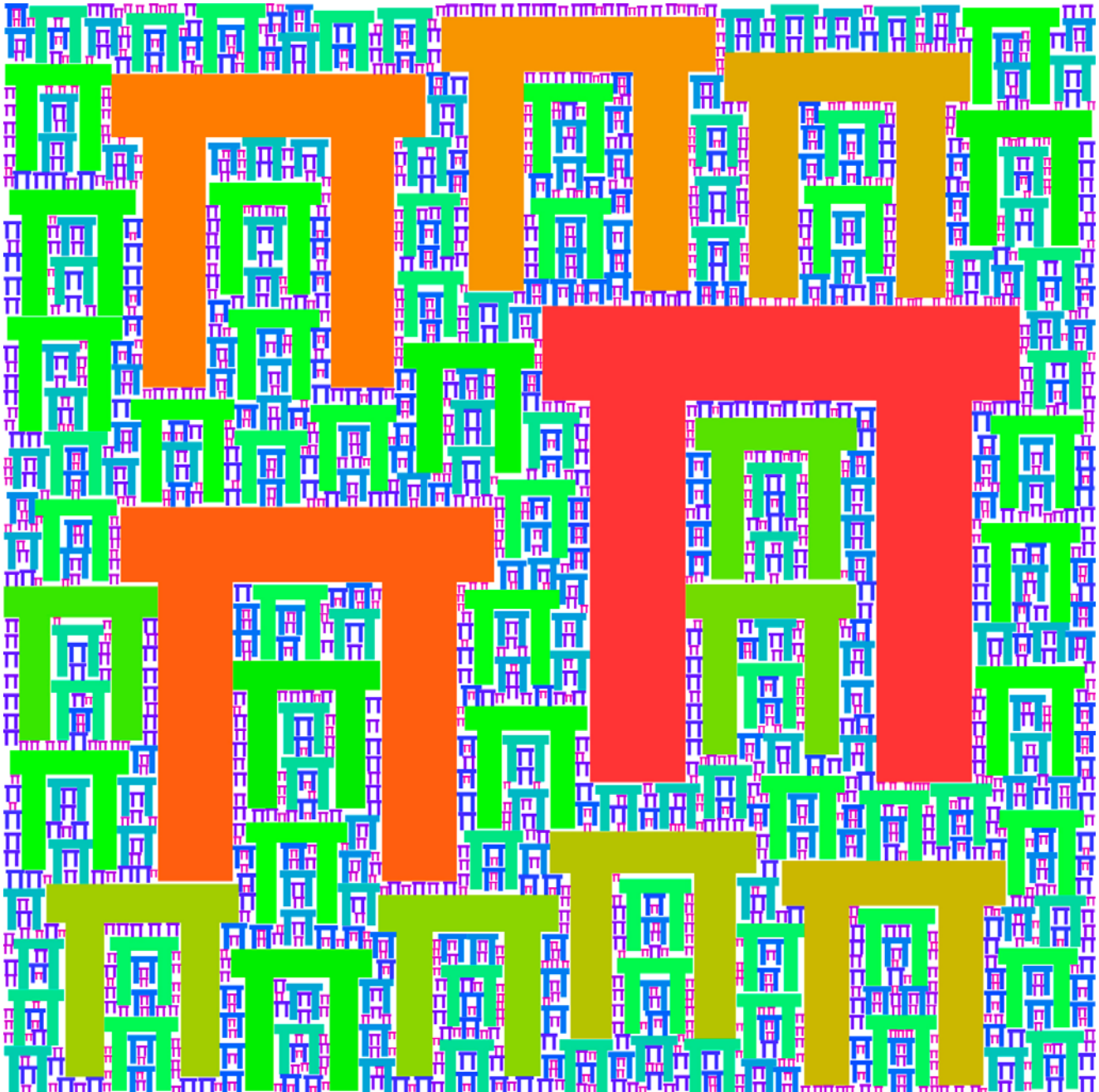


Fig. 9.12. Mixed squares and circles.

This was something of an eye-opener when I first saw it. The shapes clearly don't need to be congruent but only need to obey the area law. The placements were alternating circle-square-circle-... . Red gasket. This image has fairly high  $c$ , and one can see a strong correlation effect, with circles mostly near other circles etc. Fewer trials are needed to place a square than a circle.

One "fan" Email had an image of this kind where a heart was placed in each circle and a picture of a bride and groom in the square.

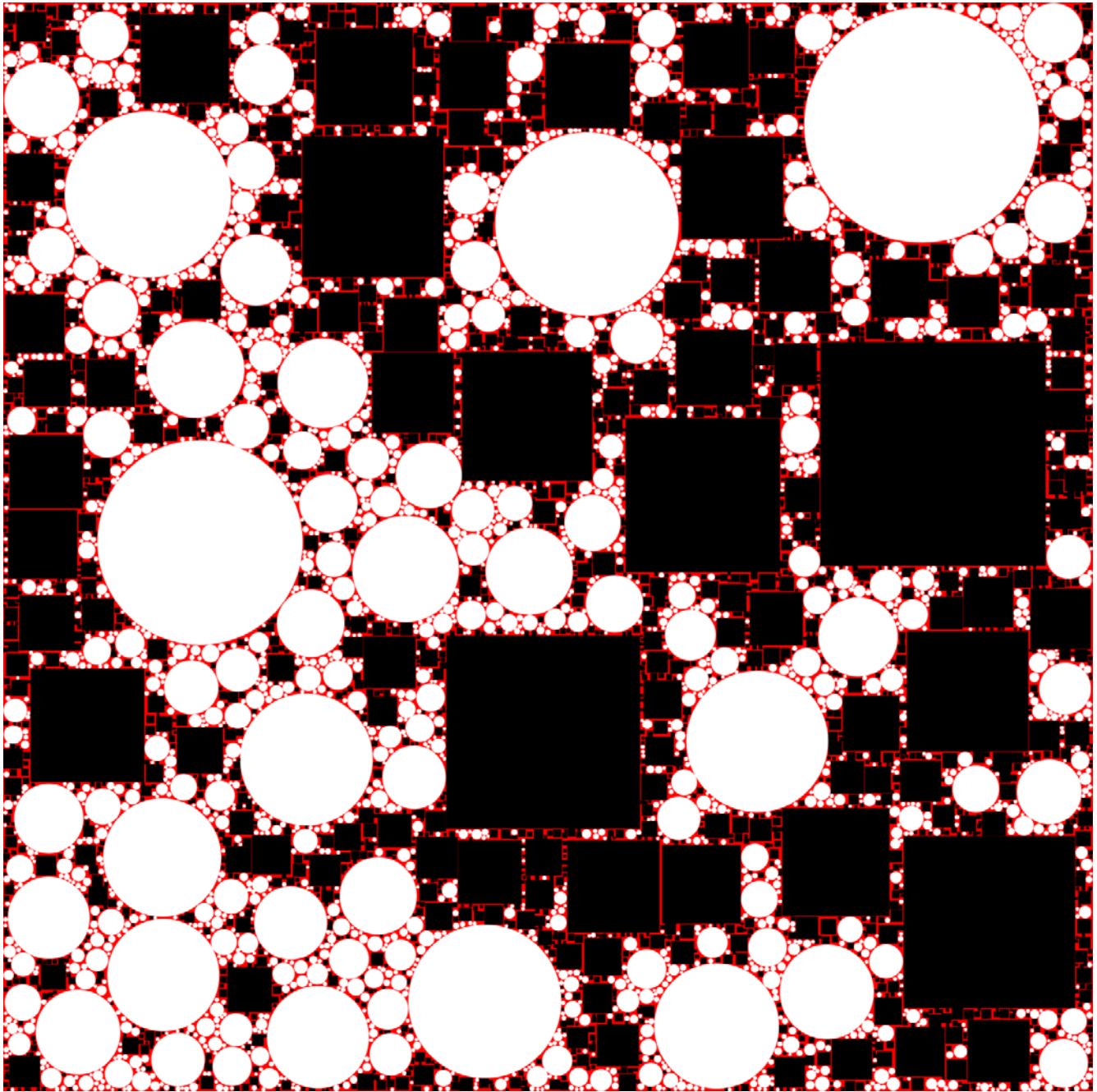


Fig. 9.13. Squares and diamonds.  $c=1.44$ ,  $N=2$ , 500 shapes.

The shapes alternate after each placement, which ensures equal numbers of both shapes. There is extremely strong correlation, amounting to segregation of the two shapes. Fine-scale interpenetration of the two shapes occurs largely at the boundaries. The correlation is weaker for lower  $c$  values. It is remarkable that a (constrained) random process produces such a highly ordered pattern. Order from chaos! Mixed cubes and octahedra in 3D show the same remarkable segregation.

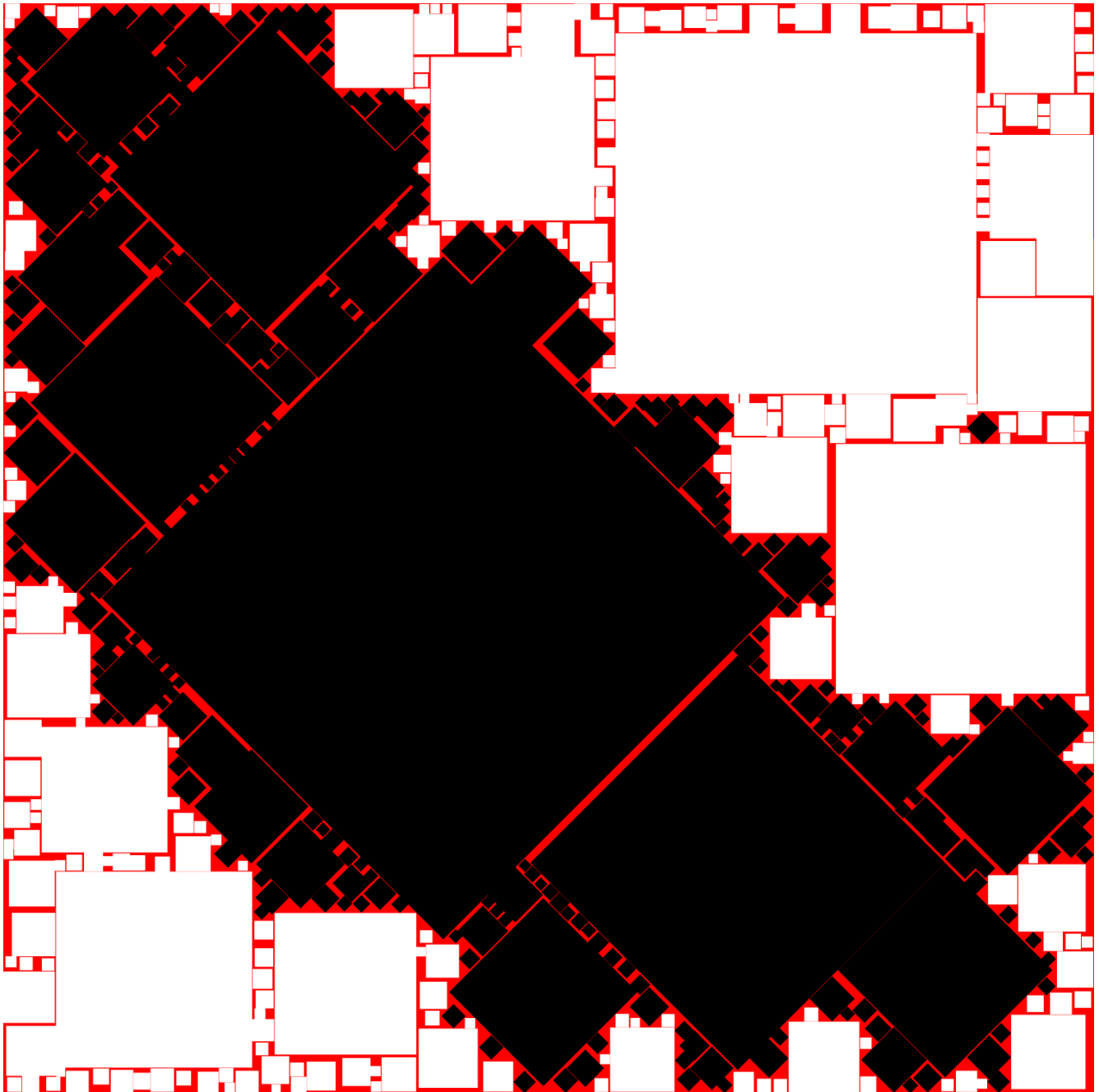


Fig. 9.14. Squares and diamonds. Order versus  $c$ .

The  $c=1.5$  case shows near-perfect segregation of the two shapes. As  $c$  decreases one can see more and more interpenetration of the two shapes on all length scales. It can be seen from this that  $c$  plays the role of a "degree of order" parameter. The very high maximum  $c$  for this mixed fractal is the same as for squares only.

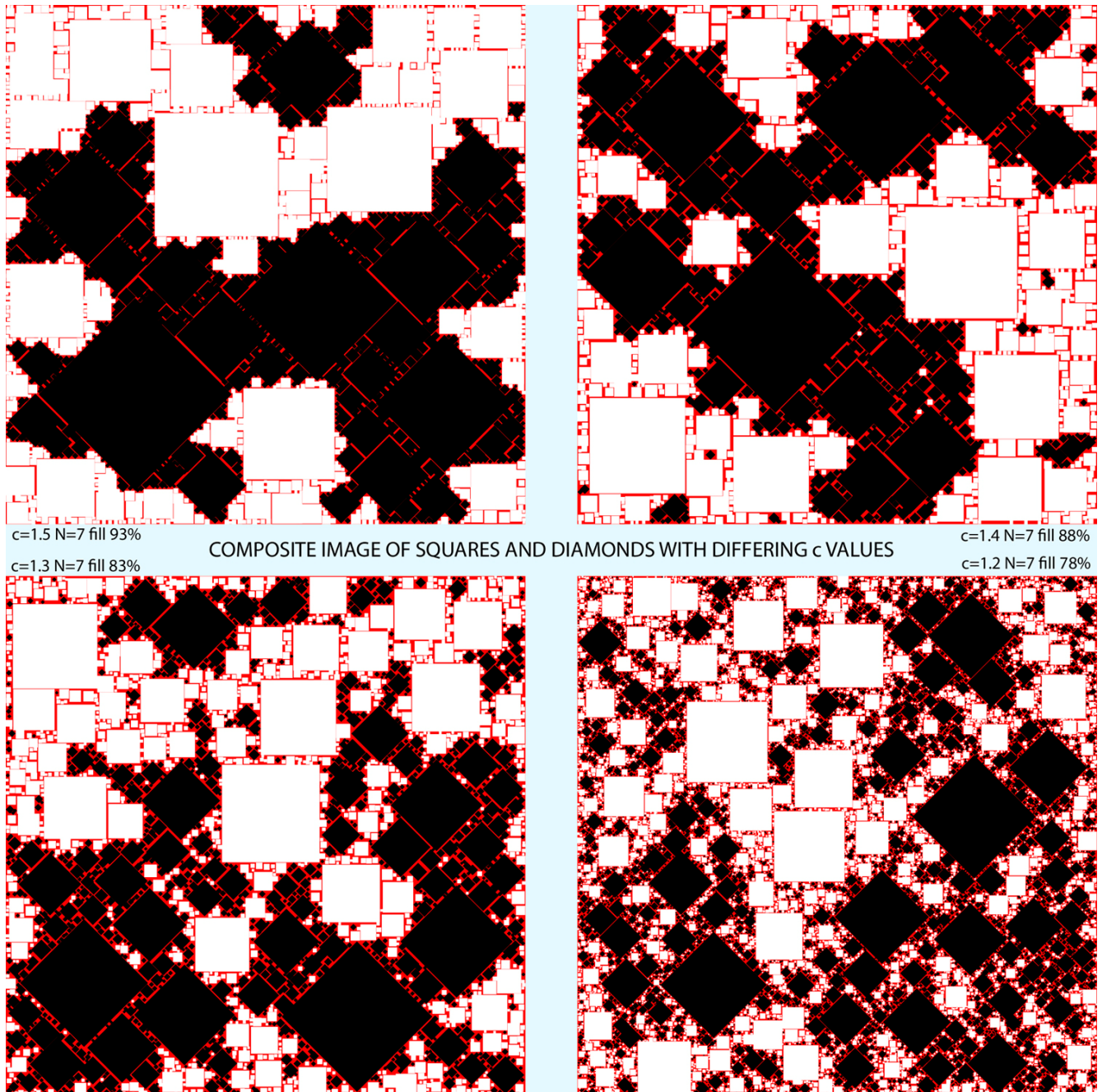


Fig. 9.15. Triangles with two orientations.

Equilateral triangles all having the same orientation fractalize slowly and only up to a fairly small  $c$  value. If you use two mirror-image triangles the fit is much better as you can see here. There are white "down arrow" triangles and black "up arrow" ones. Red gasket. Note the very strong anti-correlation. "Up" has mostly "down" neighbors and *vice versa*.

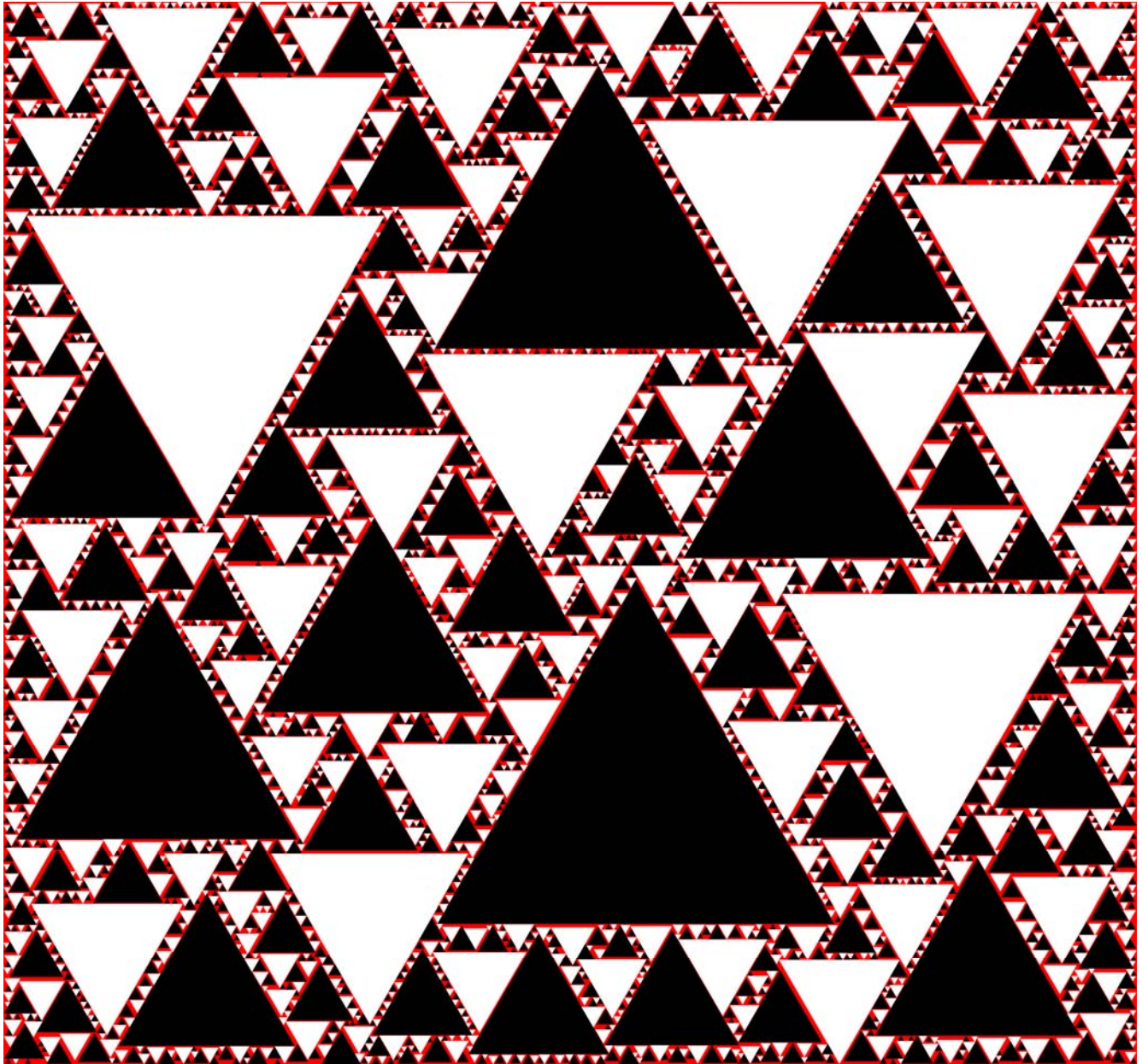




Fig. 9.16. Triangles with one orientation.  $c=1.24$ ,  $N=4$ , 1200 shapes.

Equilateral triangles all having the same orientation fractalize like this. This is about the upper limit for  $c$ . Close study will show that the smallest triangles tend to group themselves in the "Sierpinski" motif -- a big triangle with smaller ones at the 2 o'clock, 6 o'clock, and 10 o'clock positions. A cuneiform text?

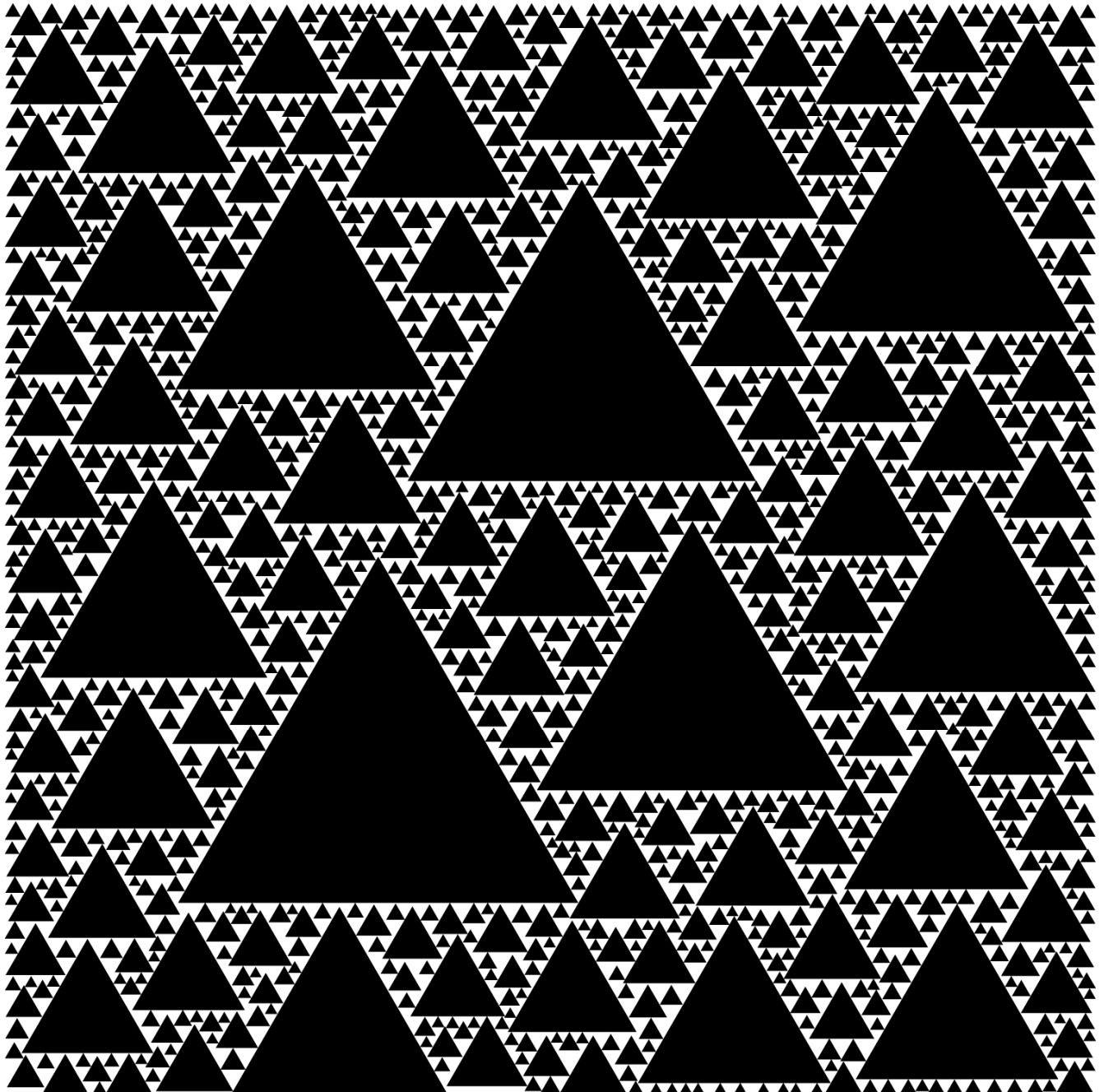


Fig. 9.17. Triangles with one orientation, fractalized in a triangle.  $c=1.24$ ,  $N=5$ .

This example is provided to show the resemblance between a random triangle fractal and the famous Sierpinski fractal construction. Log-periodic color is used so that one can see the progression of sizes. One conclusion is that as  $c$  approaches its limiting value of about 1.24, the fractal looks more and more like Sierpinski.

The fractal dimensions are interesting. When  $c=1.24$ , fractal  $D=2/1.24=1.600$  for the random case. For Sierpinski the fractal  $D$  is well known to be  $D=\log(3)/\log(2)=1.585$ . Is this near-agreement a coincidence? Based on the idea that as  $c$  increases the pattern becomes more and more ordered, could we not regard Sierpinski as the completely ordered triangle fractal -- in a sense a limiting case of the random fractal. This would explain the observed upper limit of  $c$  -- the limit would arise because the random fractal's  $D$  cannot go beyond  $D$  for the nonrandom fully-ordered case.

If one looks at the smallest triangles, they mostly either have no near-neighbor triad or a full set of three. The ones with 1 or 2 neighbors are rare to a degree which is statistically unlikely for a truly random process (explained by the nonoverlap constraint?). This feature was first noticed by Chris Innes.

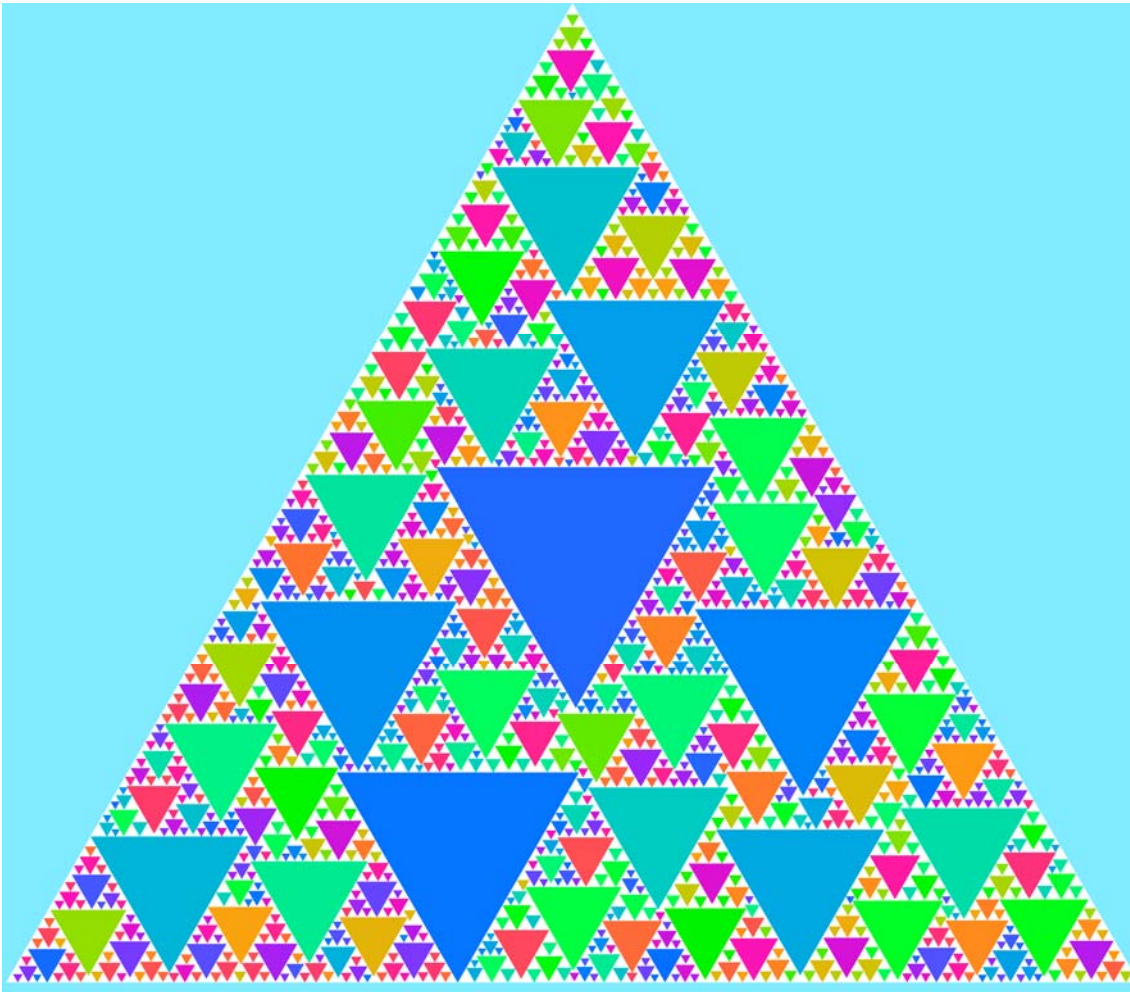


Fig. 9.18. Triangles and circles.  $c=1.30$ ,  $N=2$ , 500 shapes.

As usual the algorithm ran smoothly. Choice of shape is made at placement, with alternating shapes. This is about the highest  $c$  for the 50-50 mix.

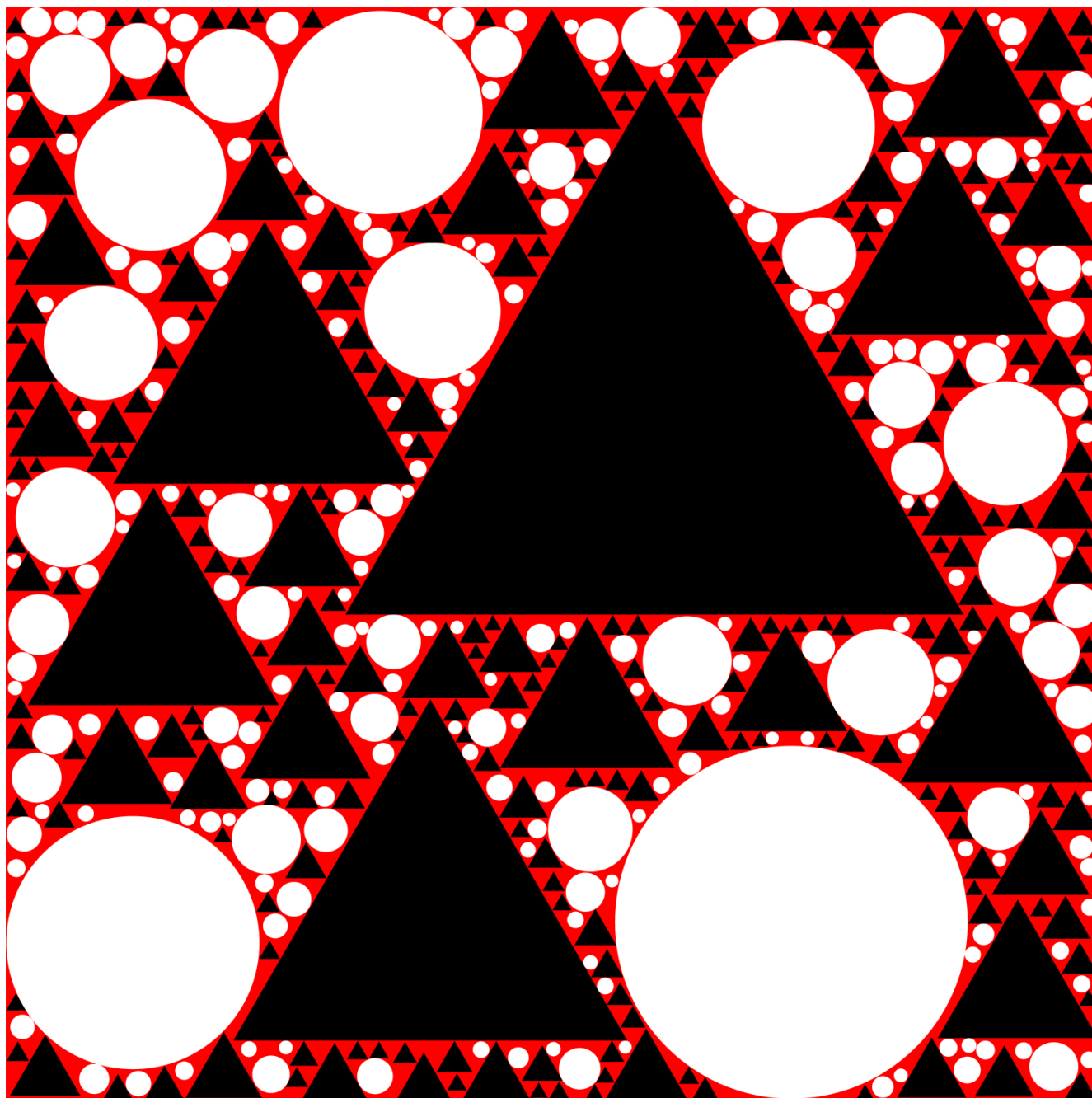


Fig. 9.19.  $45^\circ$  Triangles.  $c=1.37$   $N=2$  1200 shapes

There are 4 types of  $45^\circ$  triangle here. Two have diagonals with positive slope and two have negative slope. The 4 types are placed in a recurring sequence with each rotated 90 degrees from the previous one. The triangles with positive-slope diagonals are red and orange; those with negative slope are blue and aqua. It can be seen that there is very strong correlation -- blue-aqua and red-orange regions seldom mix. The blues are mostly adjacent to aquas, and similarly for red-orange. These shapes have some similarity to Truchet tiles.

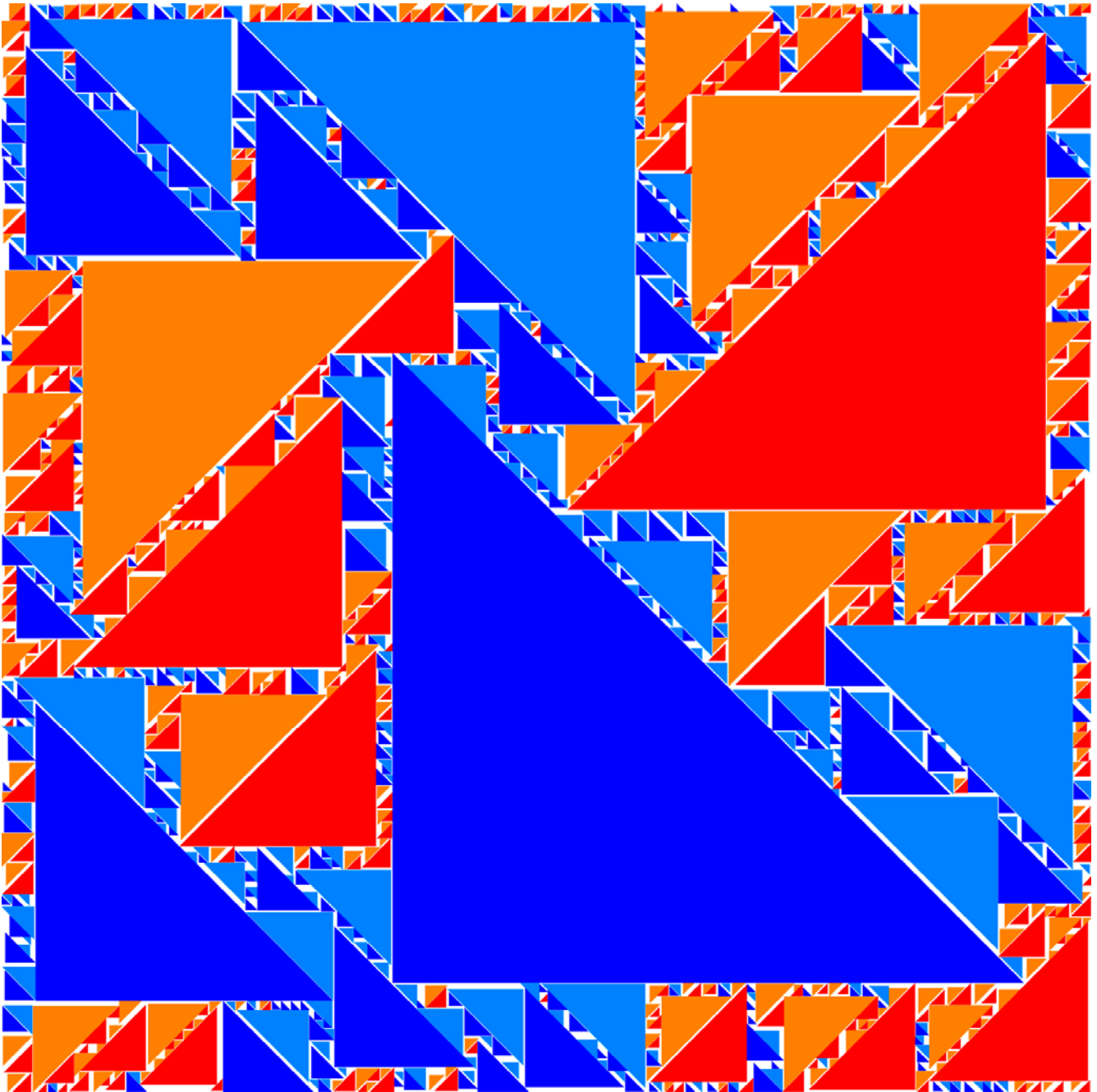


Fig. 9.20. Diamonds.  $c=1.47$   $N=5$  1000 shapes

These 3 diamonds make up a well-known tessellation which has a 3D illusion. Here they are fractalized. The very high maximum  $c$  value is something of a surprise – comparable to circles or squares. Note the very strong clustering – the 3 colors only interpenetrate to a small degree. In art, these diamonds have been used a couple of times by Escher, and many times by Vasarely.

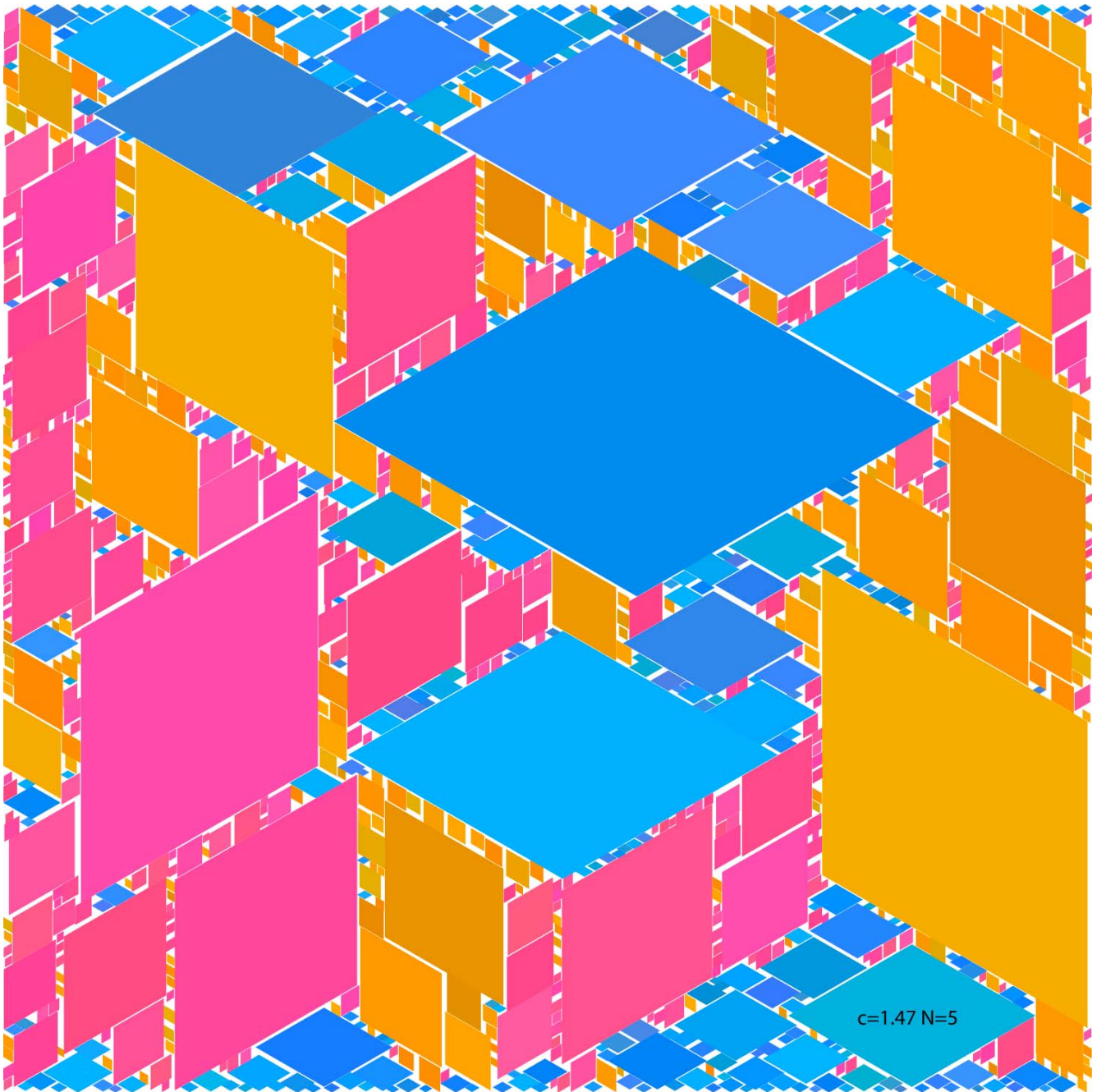


Fig. 9.21. Arrows.  $c=1.43$   $N=4$  1000 shapes

The arrows have 8 orientations, each with a unique color. The  $c$  value is surprisingly high. This can be viewed as a visual metaphor for the confusions of modern life, where you are constantly bombarded with confusing directions.

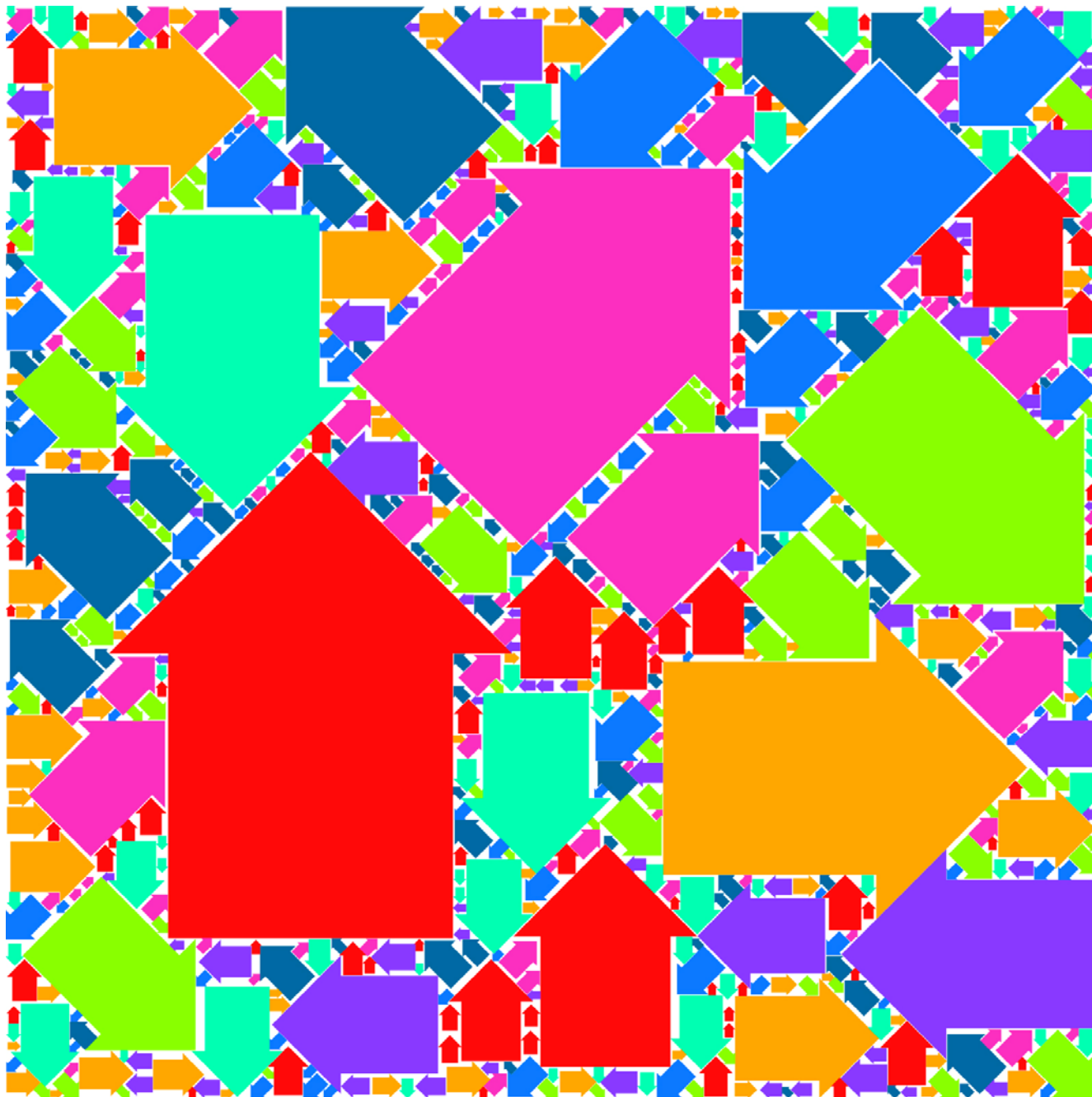


Fig. 9.22. Rings.

I doubted *a priori* if this would work, but here is the result. Log-periodic color. Black gasket. There is strong correlation in the form of nesting. The algorithm runs fast with an inner diameter much smaller than the outer diameter. As the diameters become closer it becomes much slower and the highest  $c$  value for which the algorithm succeeds becomes smaller -- but the algorithm always works at some  $c$  value.

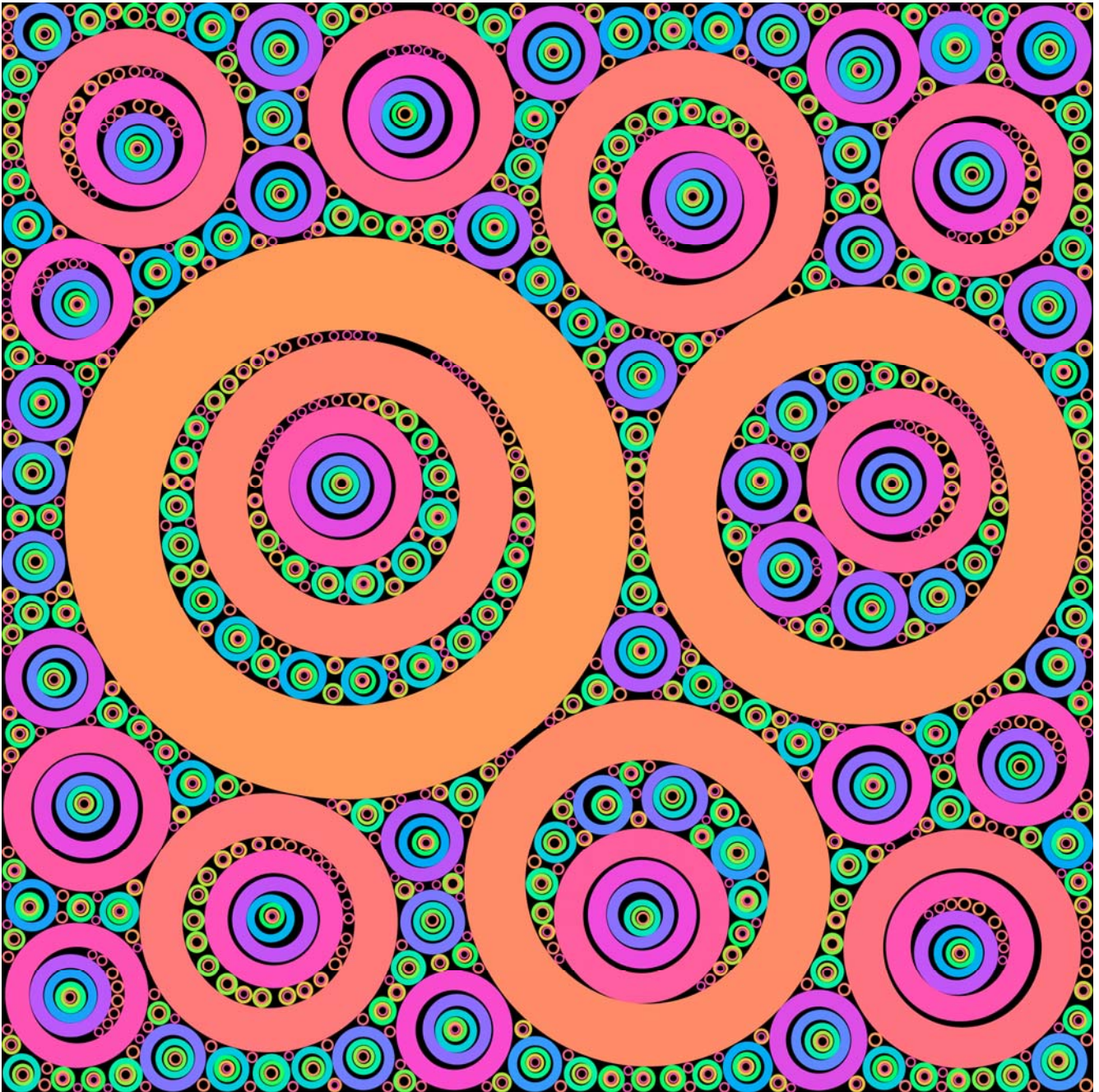


Fig. 9.23. Crescents.

The crescent is a two-circle geometric figure. With its sharp "horns" it provides a rigorous test of the algorithm. It passes the test easily, as you can see. Black crescents with white gasket. Note the very strong correlation in the form of nesting (correlation becomes stronger with higher  $c$  values and narrower "moons").

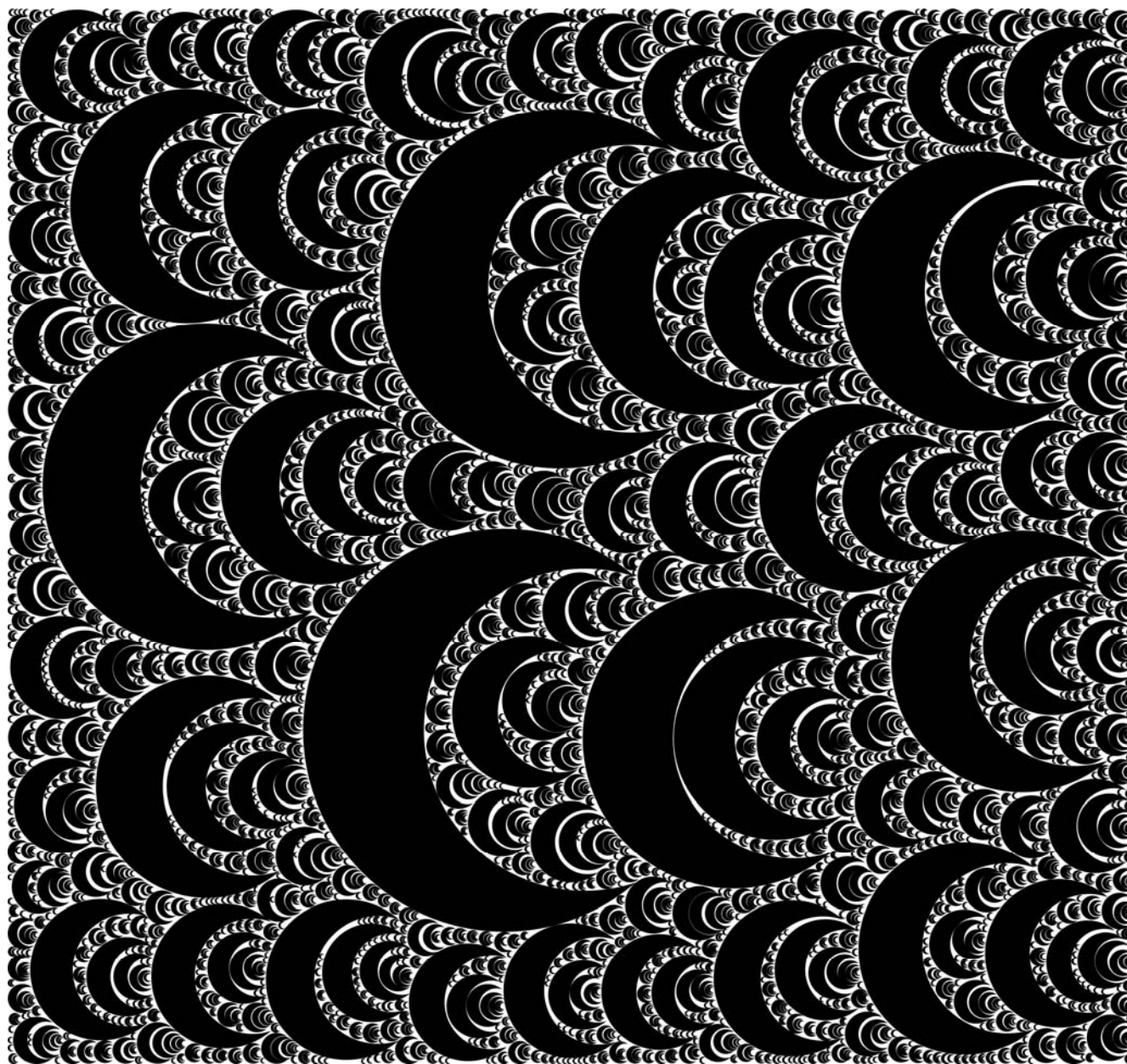




Fig. 9.24. Lens.

This is another two-circle shape. Black gasket. It fractalizes much more easily and rapidly than the crescents. I have rather whimsically placed an eye at each site as another illustration of how these fractals can be used decoratively. One could alternatively place a football at every site.

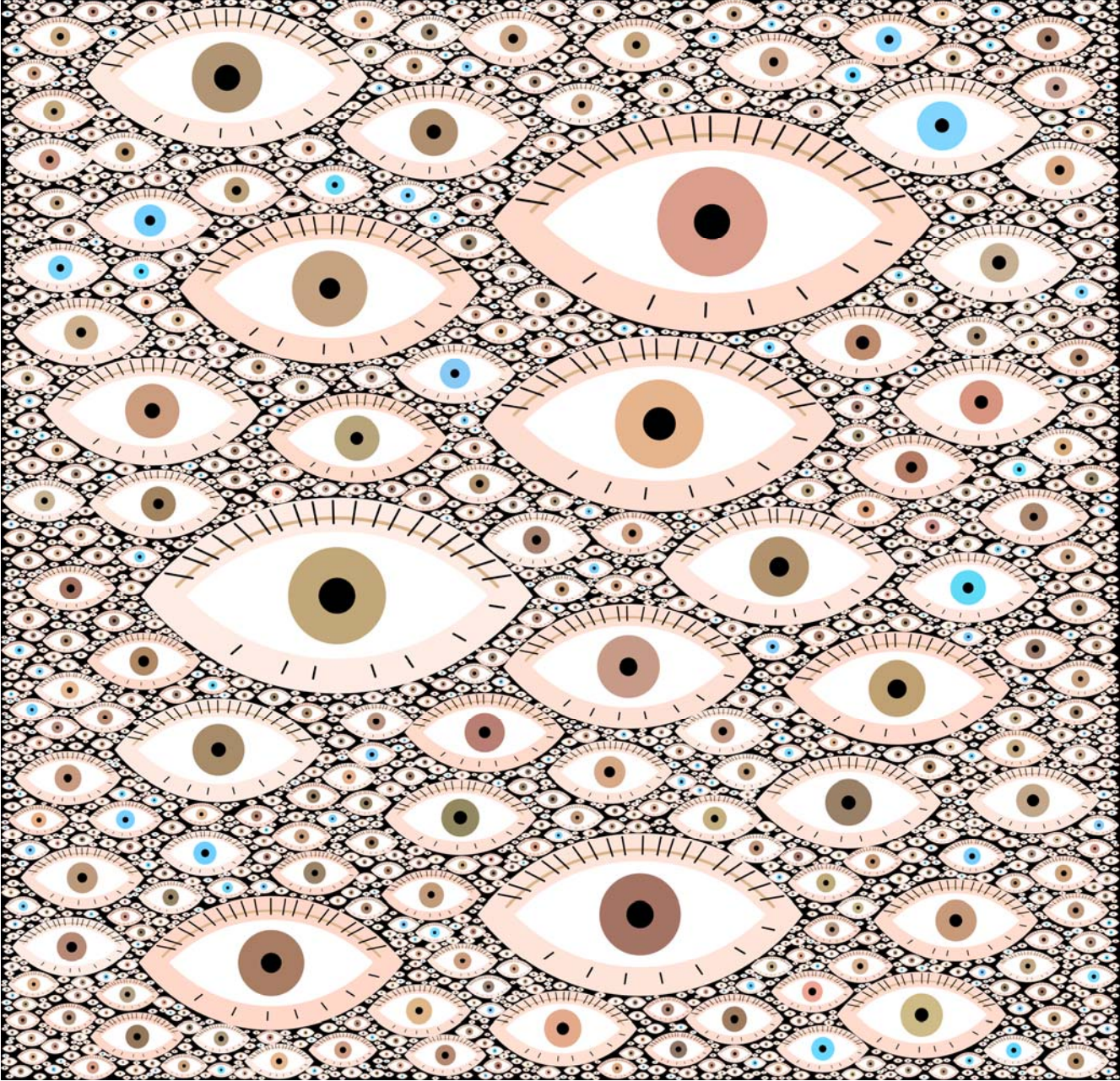


Fig. 9.25. Bicircle.  $c=1.37$ ,  $N=2$ , 1600 shapes, fill 92.3%

A two-circle shape, black gasket, log-periodic color. Not much was expected here, but the results are interesting. This  $c$  value is close to the upper limit for this shape, and the image shows strong ordering (correlation).

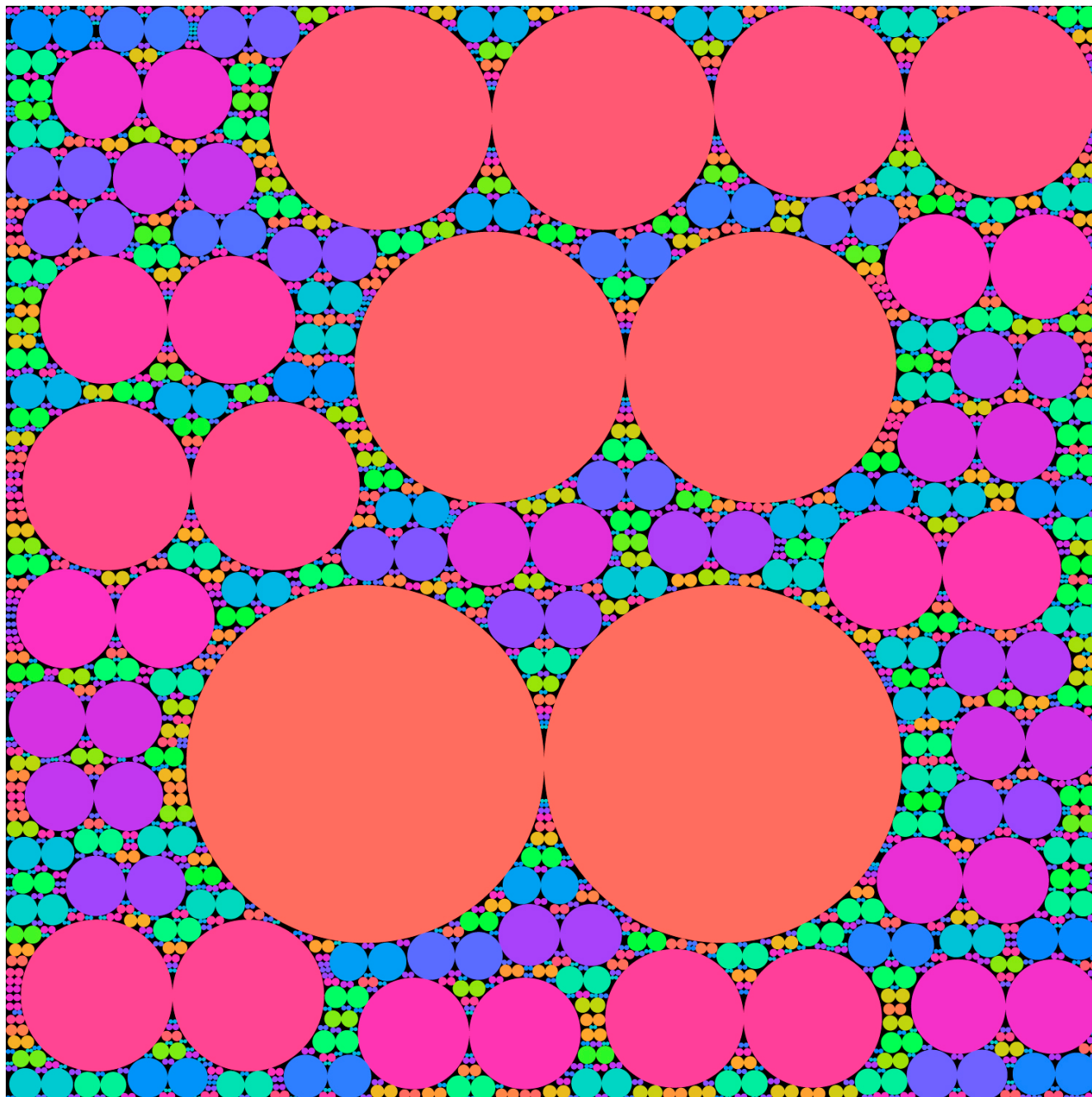


Fig. 9.26. Ancestors.  $c=1.41$ ,  $N=4$ , 300 shapes, fill 84%

This is an art usage of bicircles, with paired cartoon portraits of ancestors. This is, in effect, a "family tree". Considerable effort has been made through the use of random numbers to avoid any two faces looking alike. There is room for an infinite number of ancestors.

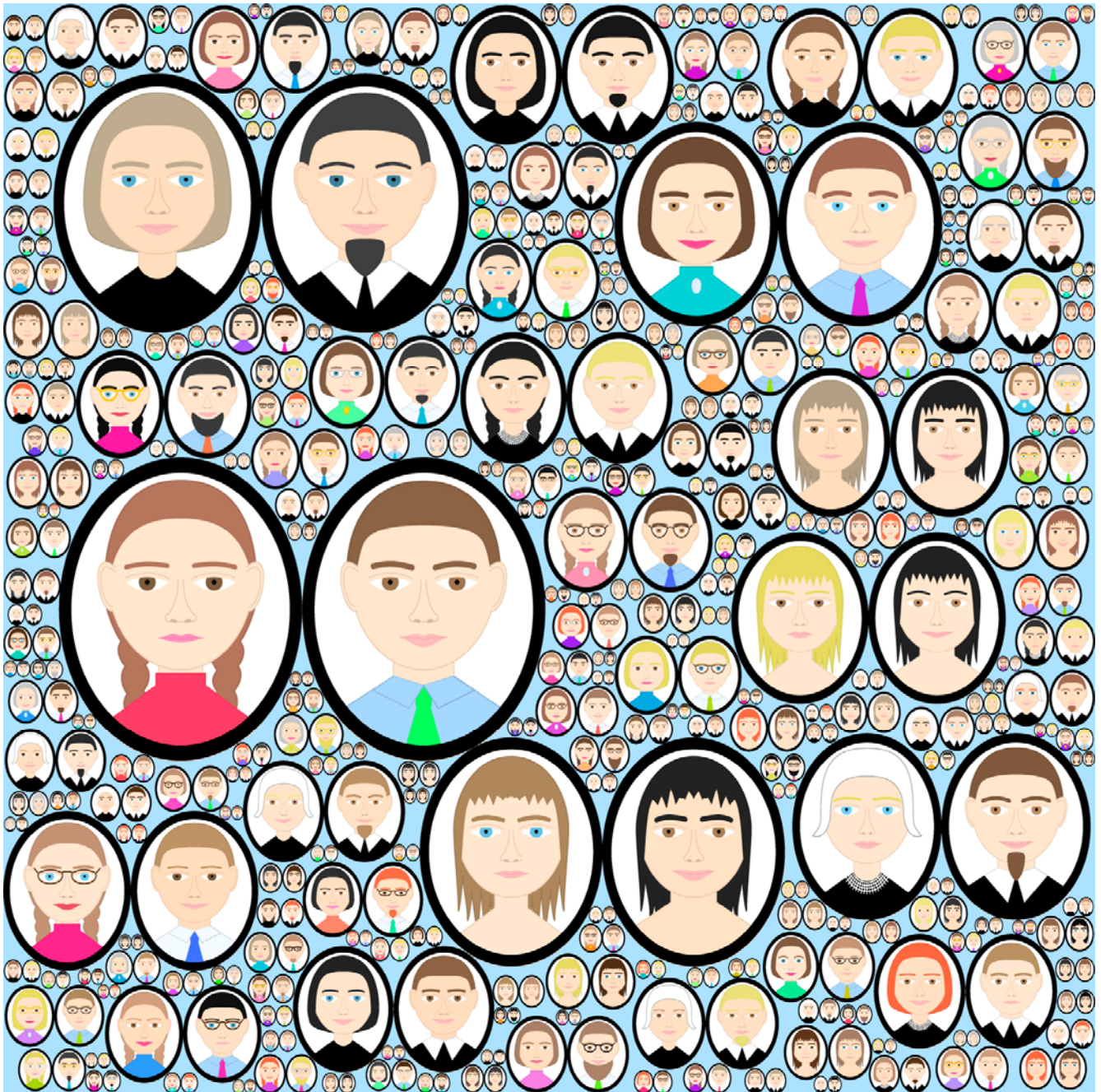


Fig. 9.27. Mouse.  $c=1.28$ ,  $N=2$ , 300 shapes, fill 77%

A three-circle shape. White gasket. It is an example of applications in decorative art. Disclaimer: Any resemblance to famous show-business mice, living or dead, is purely coincidental.

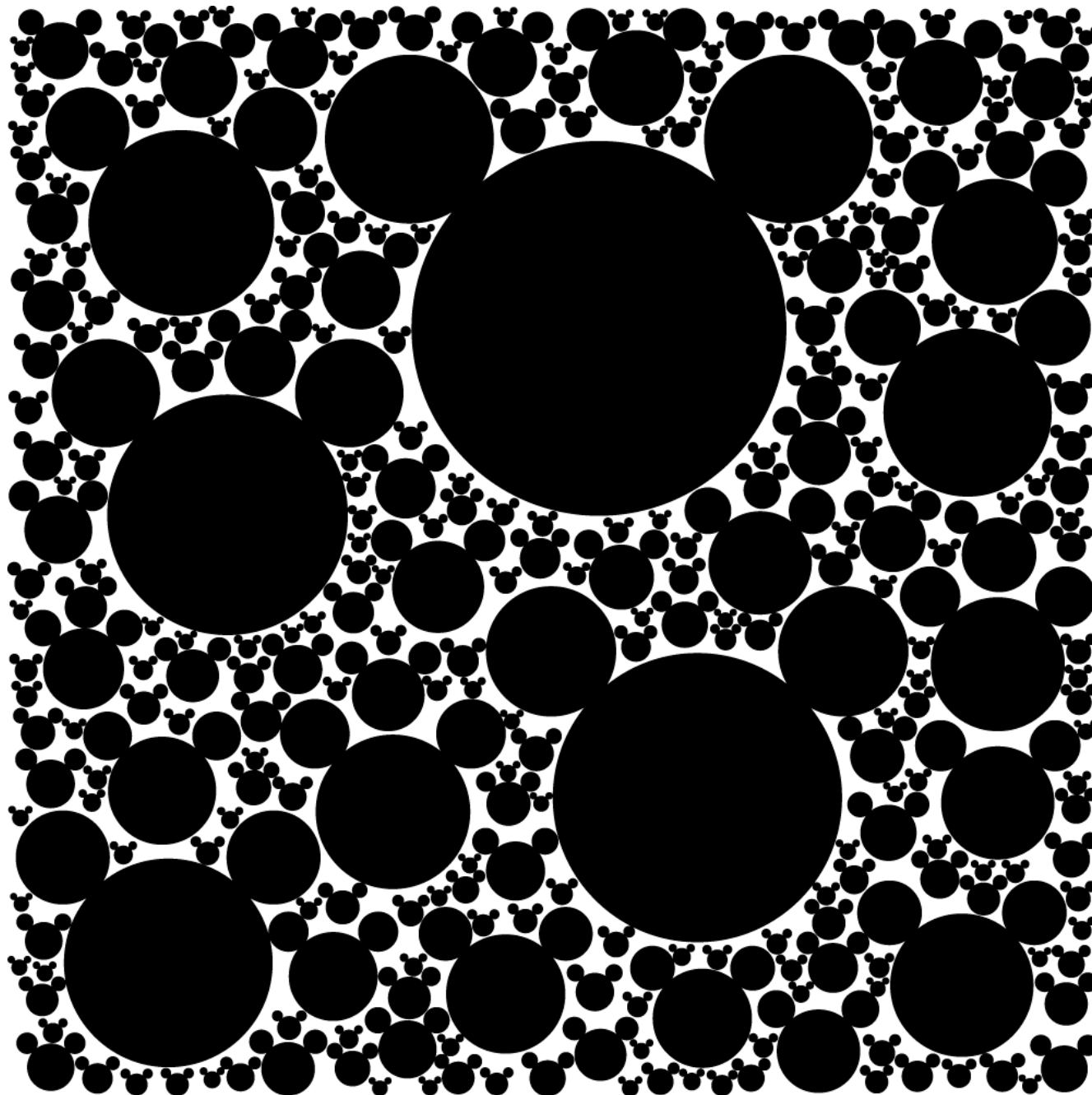


Fig. 9.28. Infinity.  $c=1.18$ ,  $N=2$ , 4000 shapes, fill 75.7%

A four-circle shape. Black with white gasket. It is a visual answer to the question "What are the possibilities?" Close study will show that the shapes are strongly correlated. Some people see faces here. This is one of the most elaborate shapes thus far studied. Rotated  $90^\circ$  it is, of course, an 8.

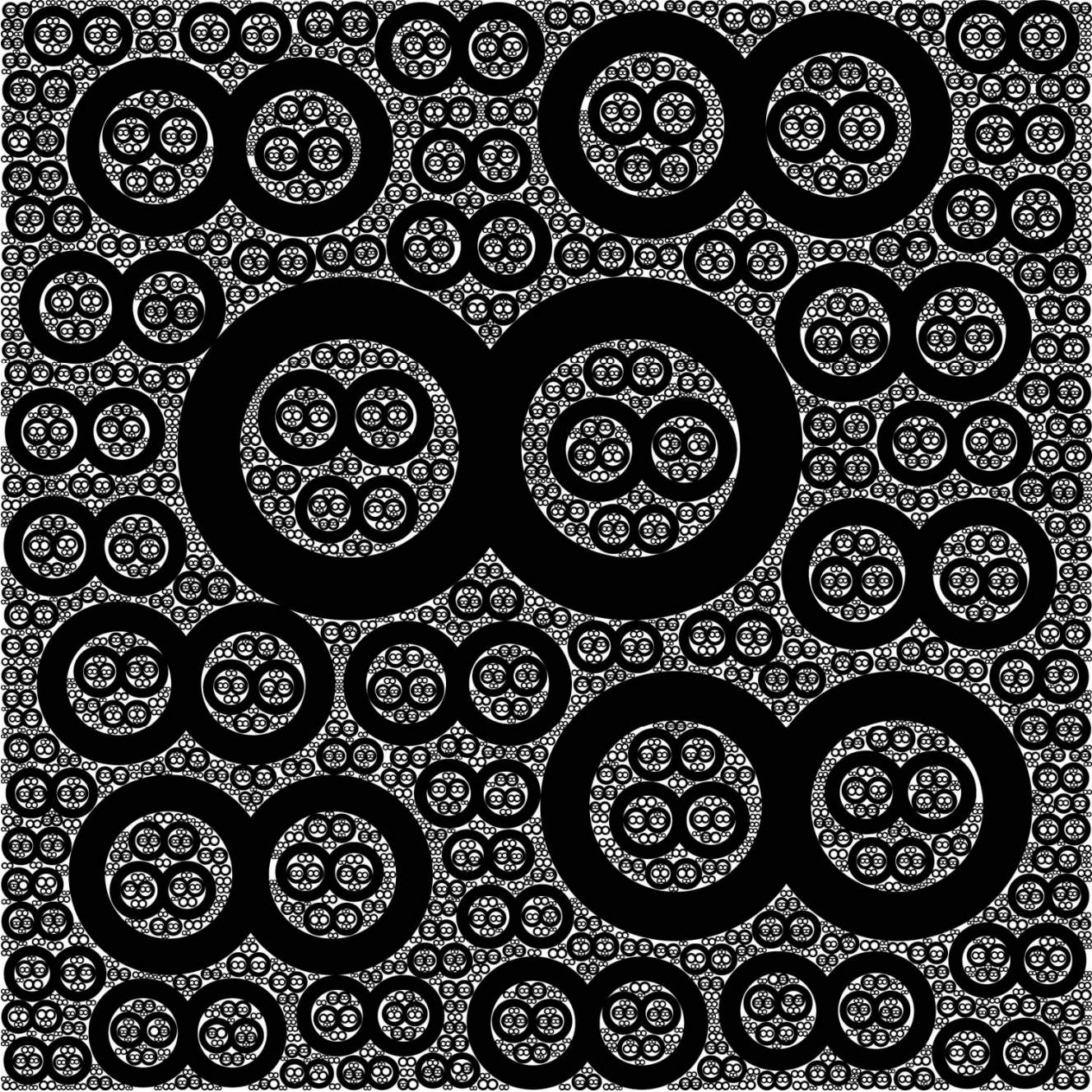


Fig. 9.29. Hearts.

The heart is a complicated shape. Here, for ease of computation, it is made up of a diamond and two semicircles. It provides another illustration of the use of these fractals in decorative art. It is space-filling in the limit, as with the other examples here.

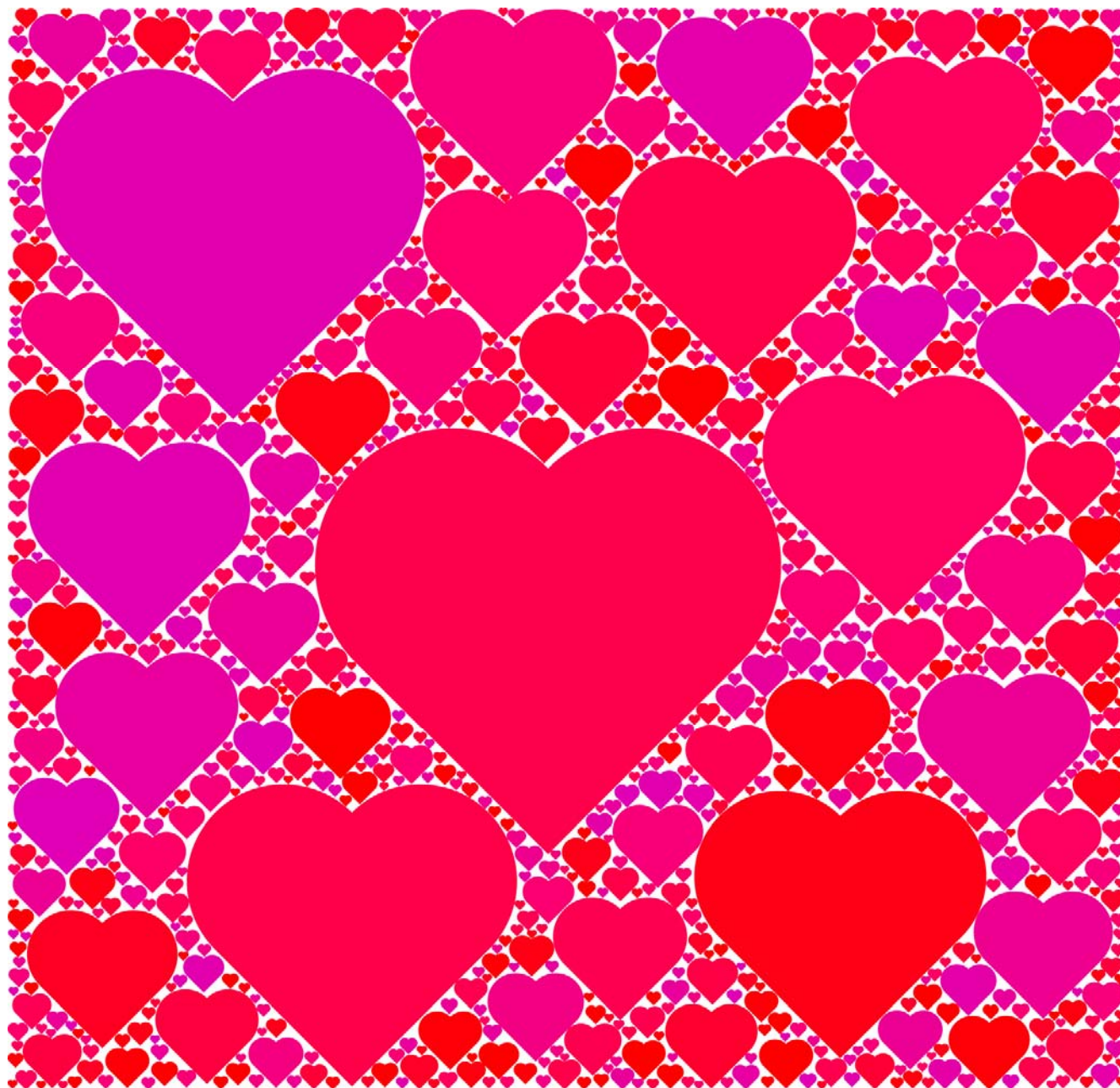


Fig. 9.30. Vans.  $c=1.39$ ,  $N=2$ , 1000 shapes, fill 92%

A rectangle plus two semicircles makes a shape resembling some mini-vans. This "parking lot" can accommodate an infinite number of such vehicles. Popular with small boys. A nostalgia item for some boomers.



Fig. 9.31. Gears.

This shape can be thought of as a circle with a sine wave (in the radius coordinate) running around its edge, with arbitrary random orientation of the 7 gear lobes (any number of lobes can be used). Log-periodic color, black gasket. This shape fractalizes very slowly (it is an interesting test object). Fractalization time depends very strongly on the depth of the teeth. Local polar coordinates are used in the computations. Periodic boundaries.

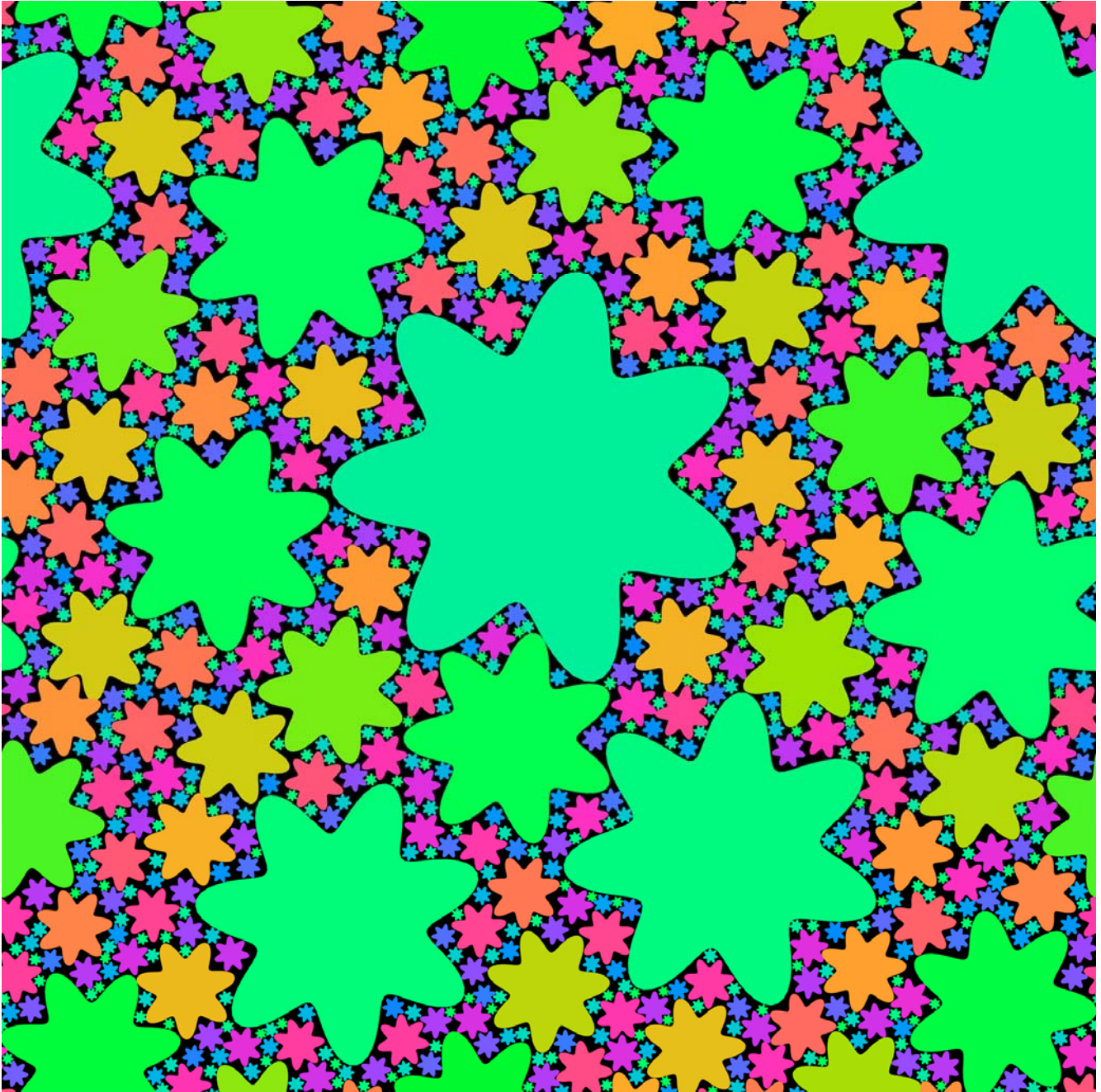




Fig. 9.32. Multishapes (aka blobs).

This is another shape specified in polar coordinates. You can think of it as a circle with three random-phase sine waves running around the edge; kind of blobby. None of the resulting shapes is congruent with any other, yet if the usual area sequence is followed the algorithm runs flawlessly. *Congruent or similar shapes is evidently not a requirement.* An interesting test object. It uses five random variables.

The color scheme needs explanation. The color coordinates R, G, and B are each proportional to one of the phases, so that each shape has a unique color, and shapes with nearly-same colors are nearly the same shape. It is not clear whether there is correlation (similar colors adjacent). Black gasket. Periodic boundaries.

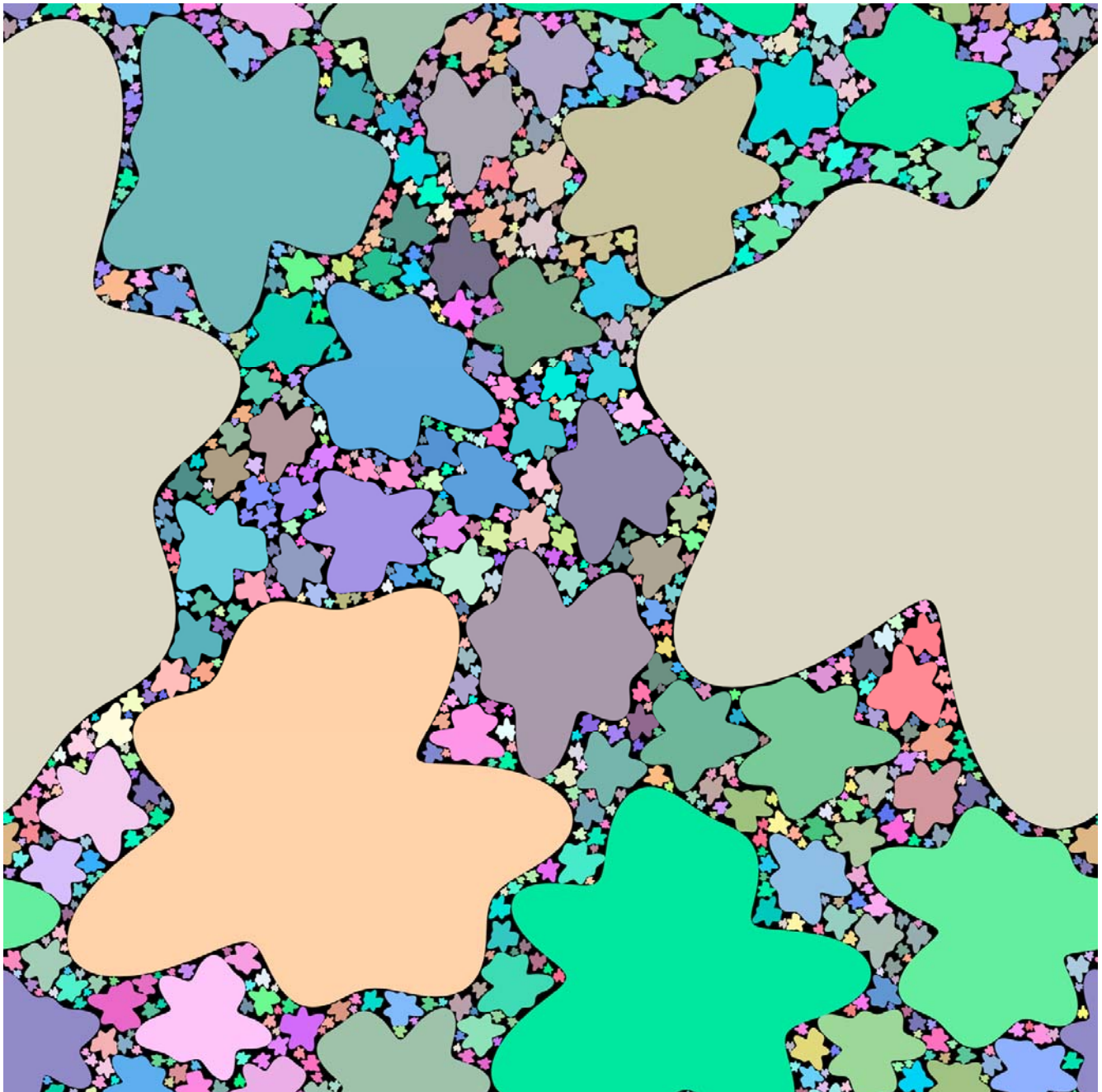


Fig. 9.33. Flowers.  $c=1.30$ ,  $N=3$ , 2000 shapes, fill 86.5%

This is another shape which uses polar coordinates. One can imagine a single sine wave running around the edge of a circle, but taken as the absolute value. (EEs would call it a full-wave-rectified sine wave.) Here there are 5 petals, but any number could be used. Black gasket, periodic boundaries. Log-periodic color, with the flower centers having a different log-periodic color sequence. This is another illustration of decorative art possibilities.

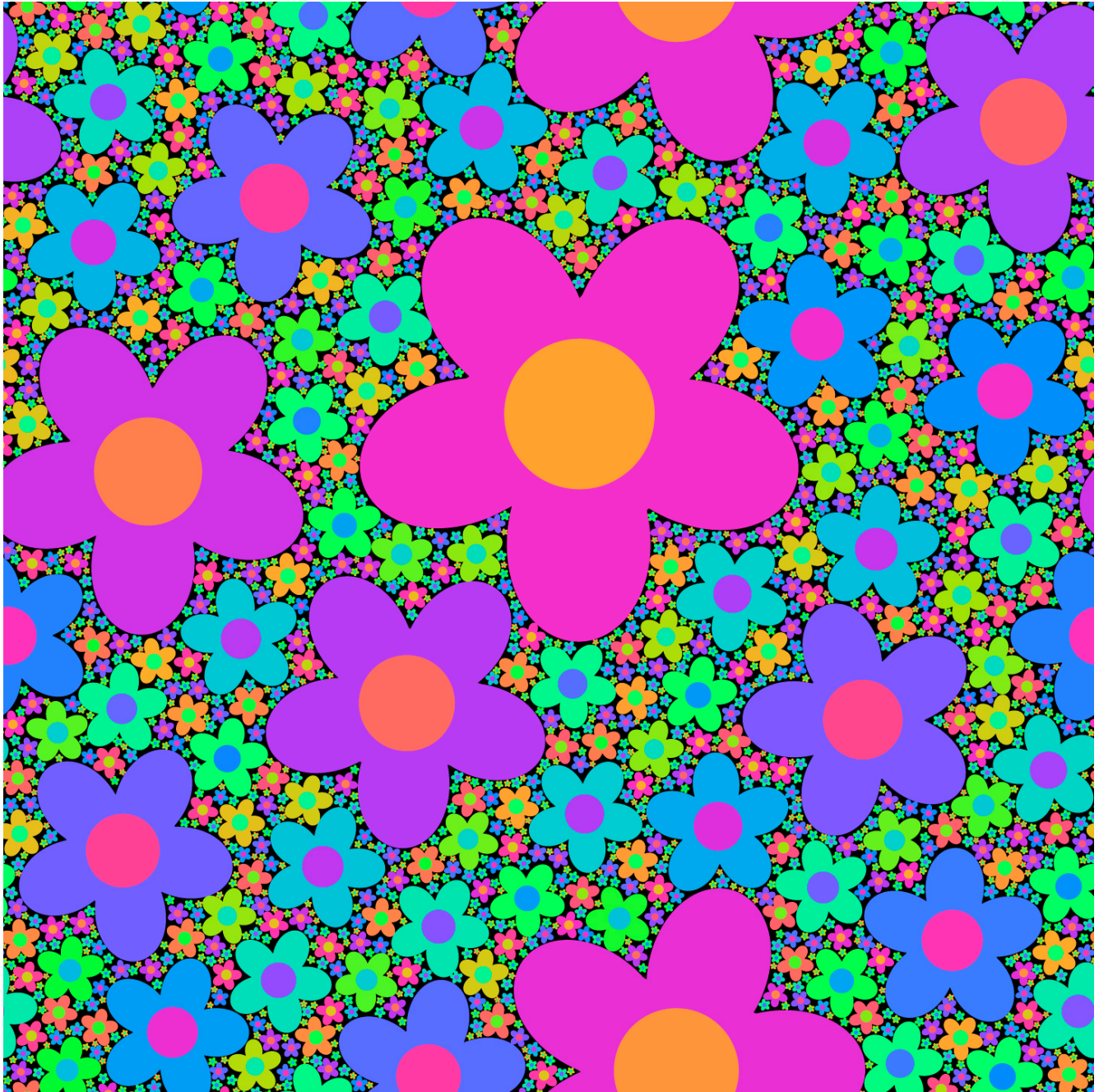


Fig. 9.34. Starfish.  $c=1.20$ ,  $N=4$ , 1945 shapes, fill 71.7%

This is another shape defined (by a Fourier series) in polar coordinates. Because of this definition, the points are rounded, hence "starfish" rather than star. Log-periodic color, black gasket. An immense variety of shapes can be defined by suitable variation of Fourier series coefficients. Randomly varied orientation angle. Periodic boundaries. This shape is hard to fractalize and has a fairly low maximum  $c$  value.

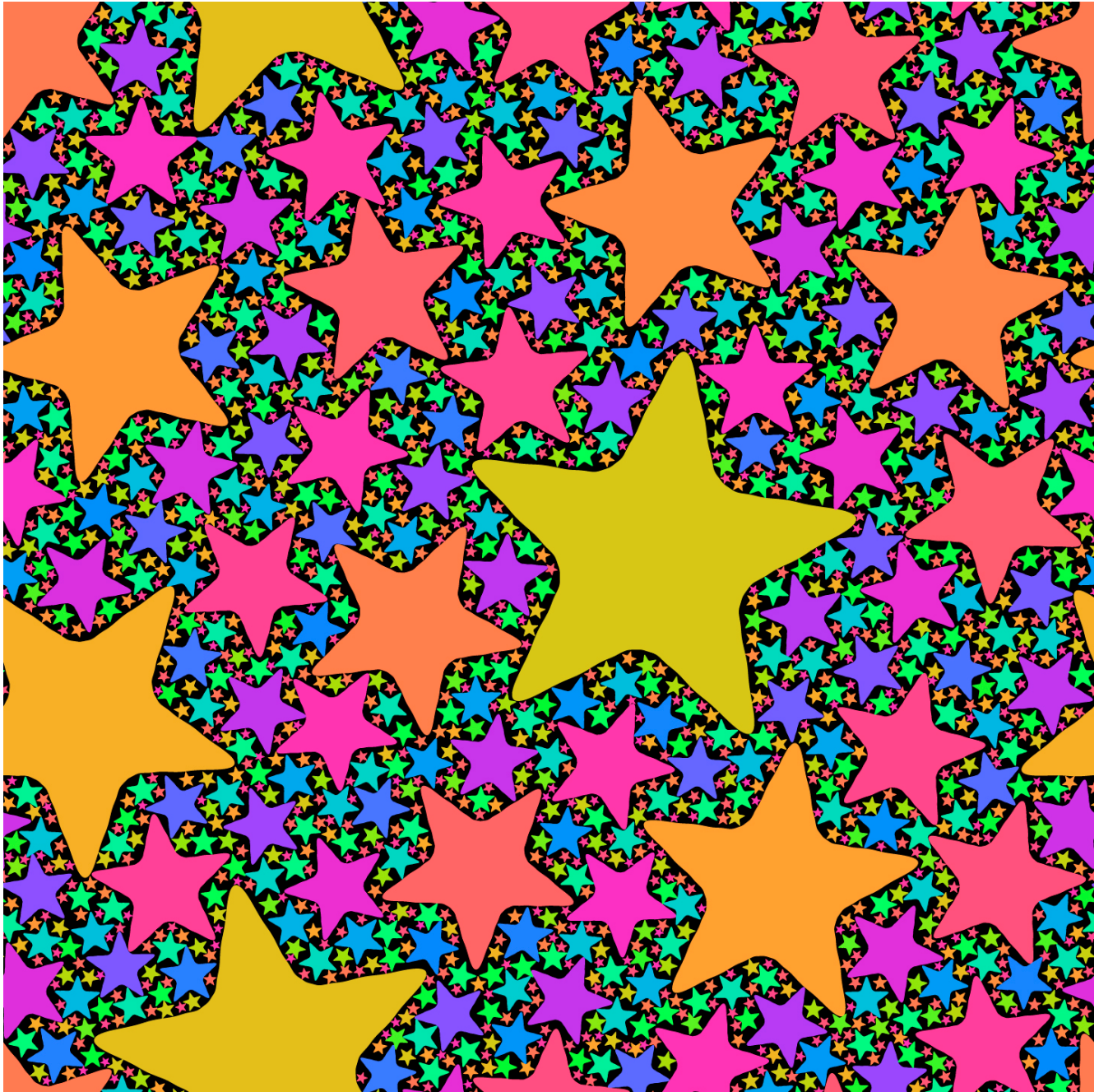


Fig. 9.35. Sailboats.  $c=1.26$ ,  $N=2$ , 600 shapes, fill 78.8%

This shape can be viewed as a kind of irregular pentagon -- or as a triangle with two corners clipped. The sailboats inscribed in the shape create a "fractal regatta". This example is more decorative art than unique mathematics. There is very little space between boats, and they have the same "triplet" motif as the triangles of Figs. 9.16 and 9.17.

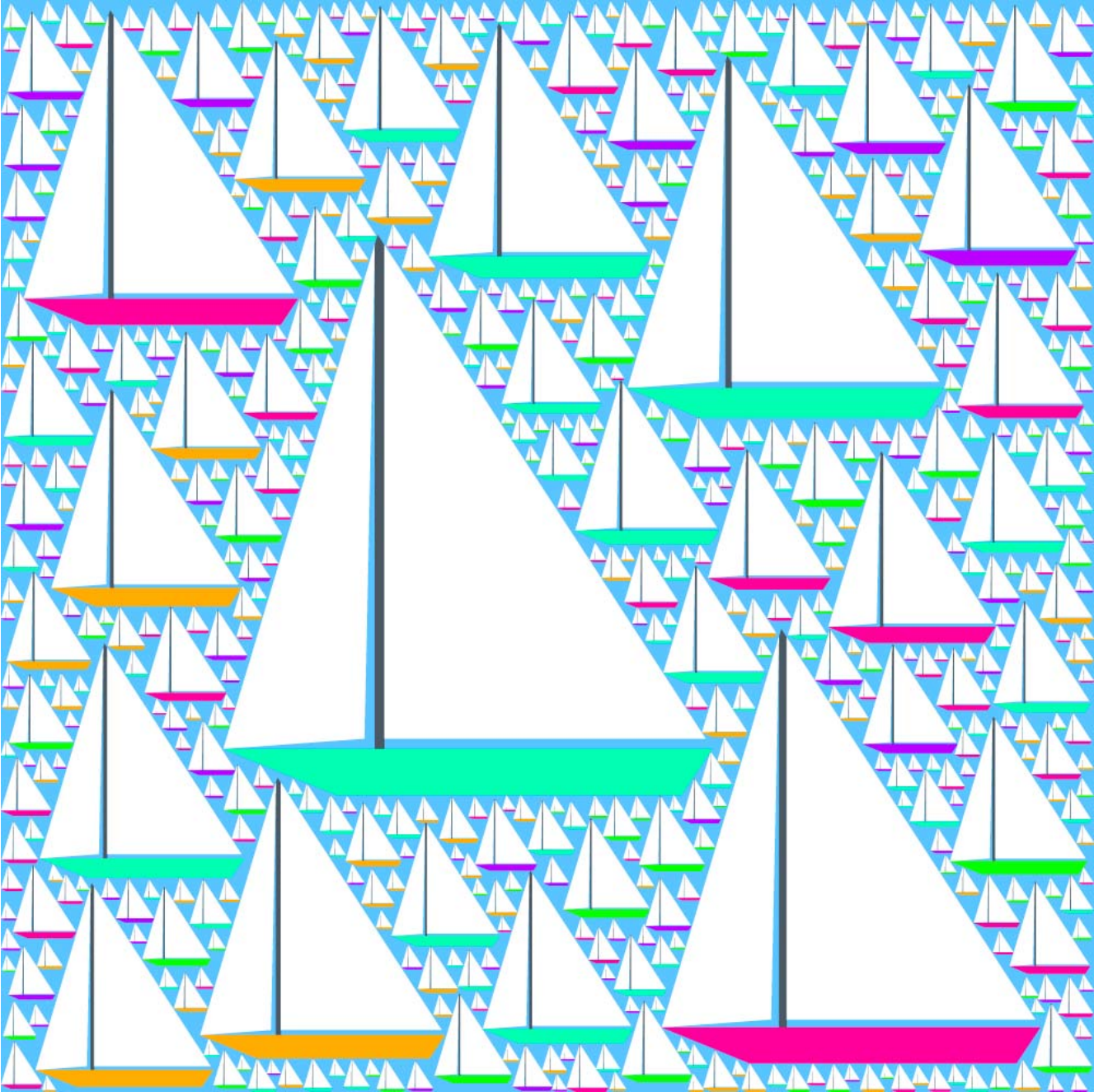


Fig. 9.36. Polygonal butterflies.  $c=1.34$ ,  $N=5$ , 600 shapes

Another illustration of the decorative uses of statistical geometry. This is not a specific butterfly species but a "designer butterfly". John has been a volunteer butterfly counter for Dakota County Parks.

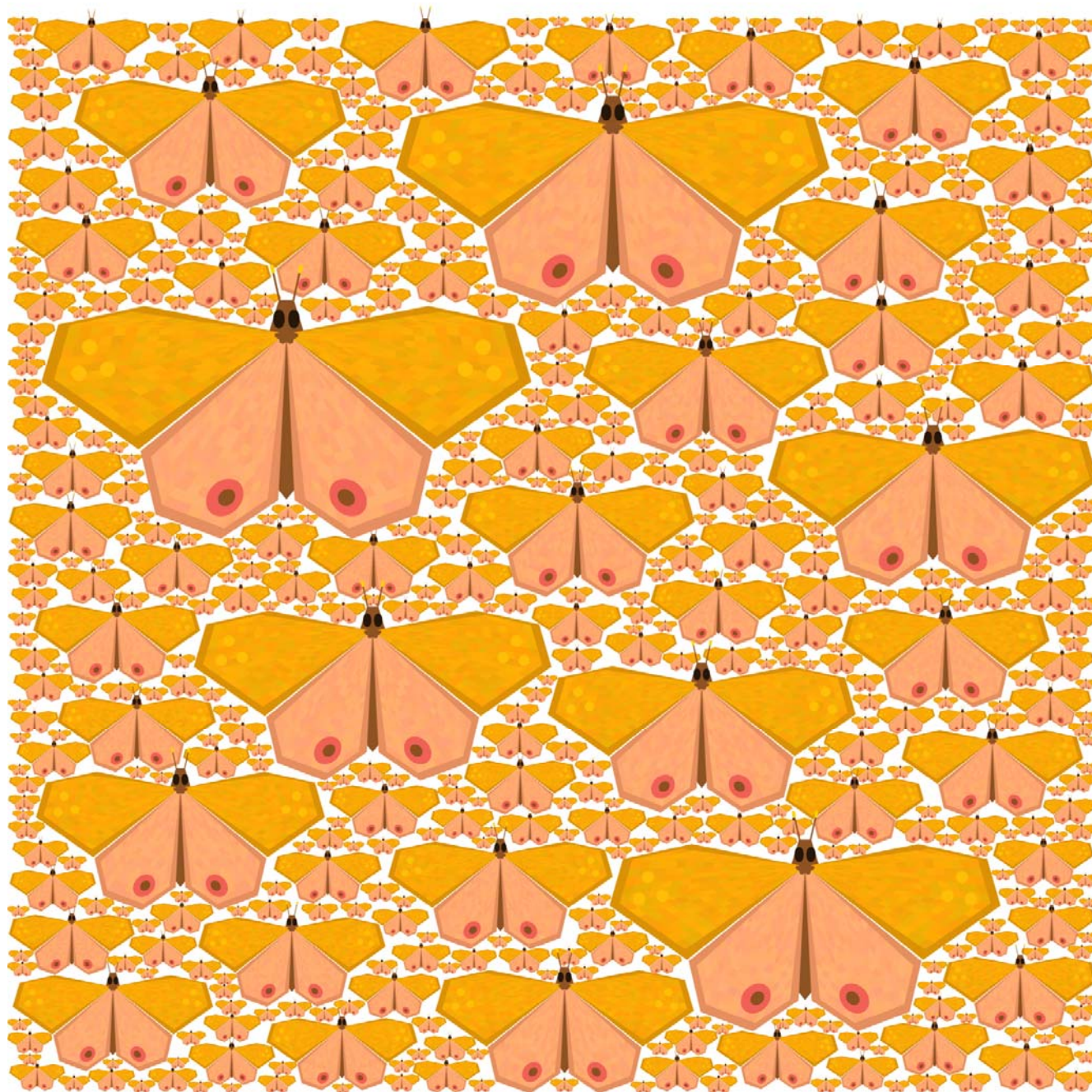


Fig. 9.37. Quadsquares.  $c=1.16$ ,  $N=2$ , 2834 shapes, fill 70%

The basic shape is seen to be a set of four squares. This rather sparse and disconnected shape challenges fractalization. Log-periodic color with grouped colors, white gasket. It is of interest more from the technical point of view than as art I think. This  $c$  value may be close to the upper limit of what works for this shape. It runs fairly fast because square-square overlap tests are fast.

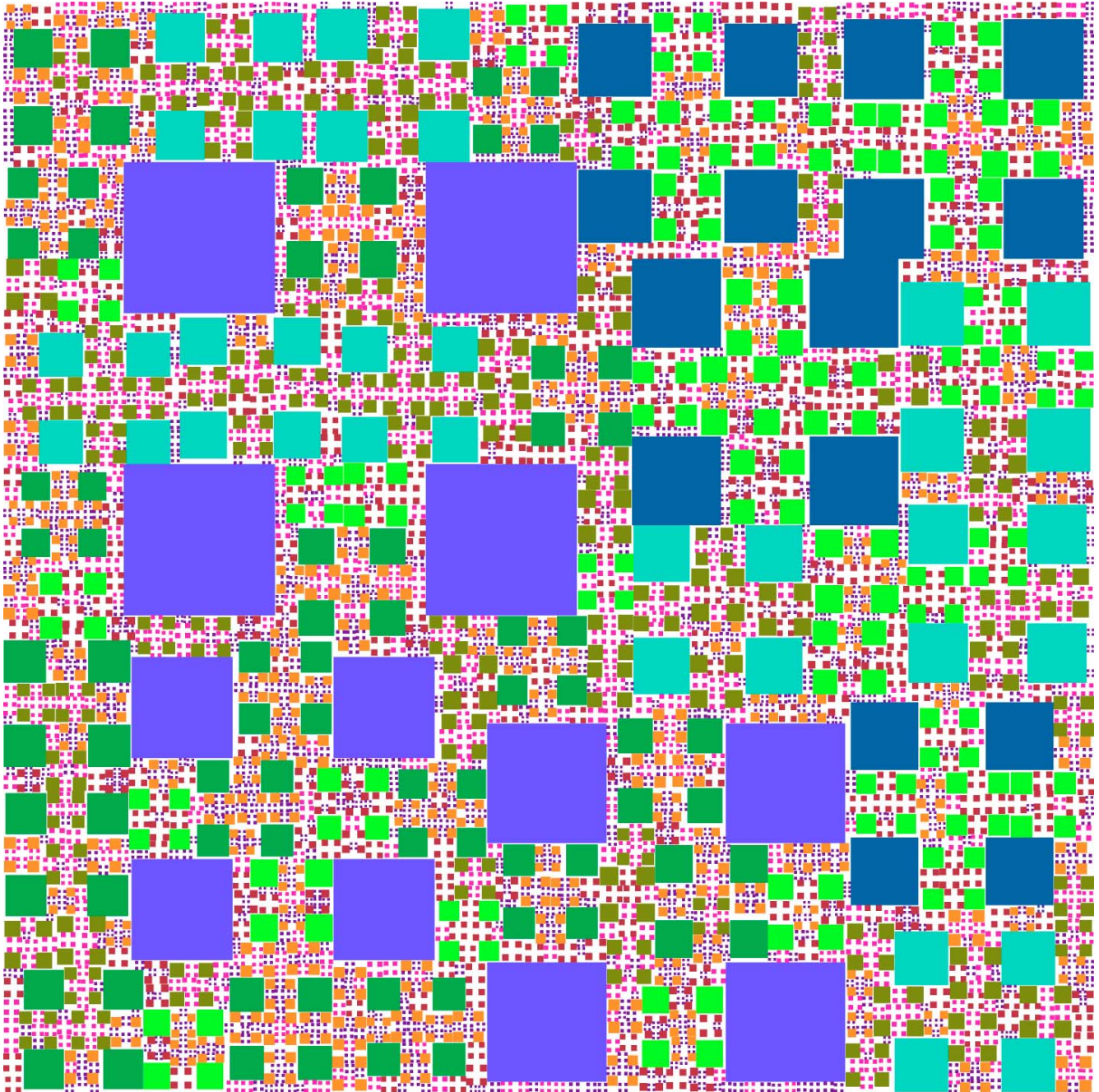


Fig. 9.38. Quadcircles.  $c=1.15$ ,  $N=2$ , 1000 shapes, fill 62%

Like quadsquares but with circles. The comparison is much the same as that for single circles and squares -- the squares have a slightly higher maximum  $c$  (i.e., are more "packable"). Log-periodic color. Fairly strong nesting correlation if you look closely. To see nesting look at the biggest shape -- it has 4 smaller shape quads centered at about the same location.

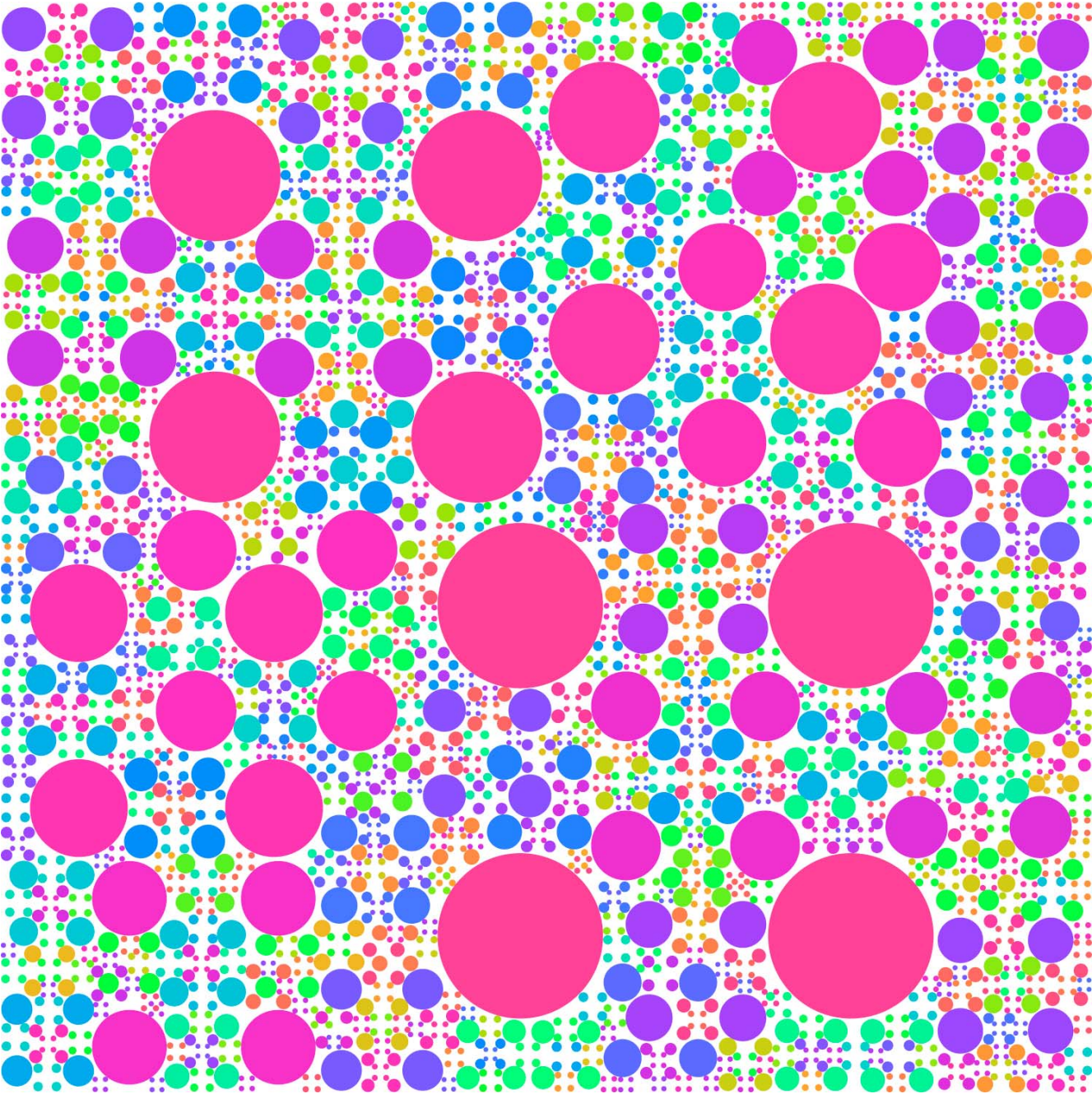


Fig. 9.39. "Beetle" cars.  $c=1.32$ ,  $N=2$ , 800 shapes, fill 86.5%

These vehicles are composed of two semicircles and two circles and are among the more complicated shapes studied to date. They look a bit like an imported car which was quite popular with college students in the 50s and 60s. Random orbital color.

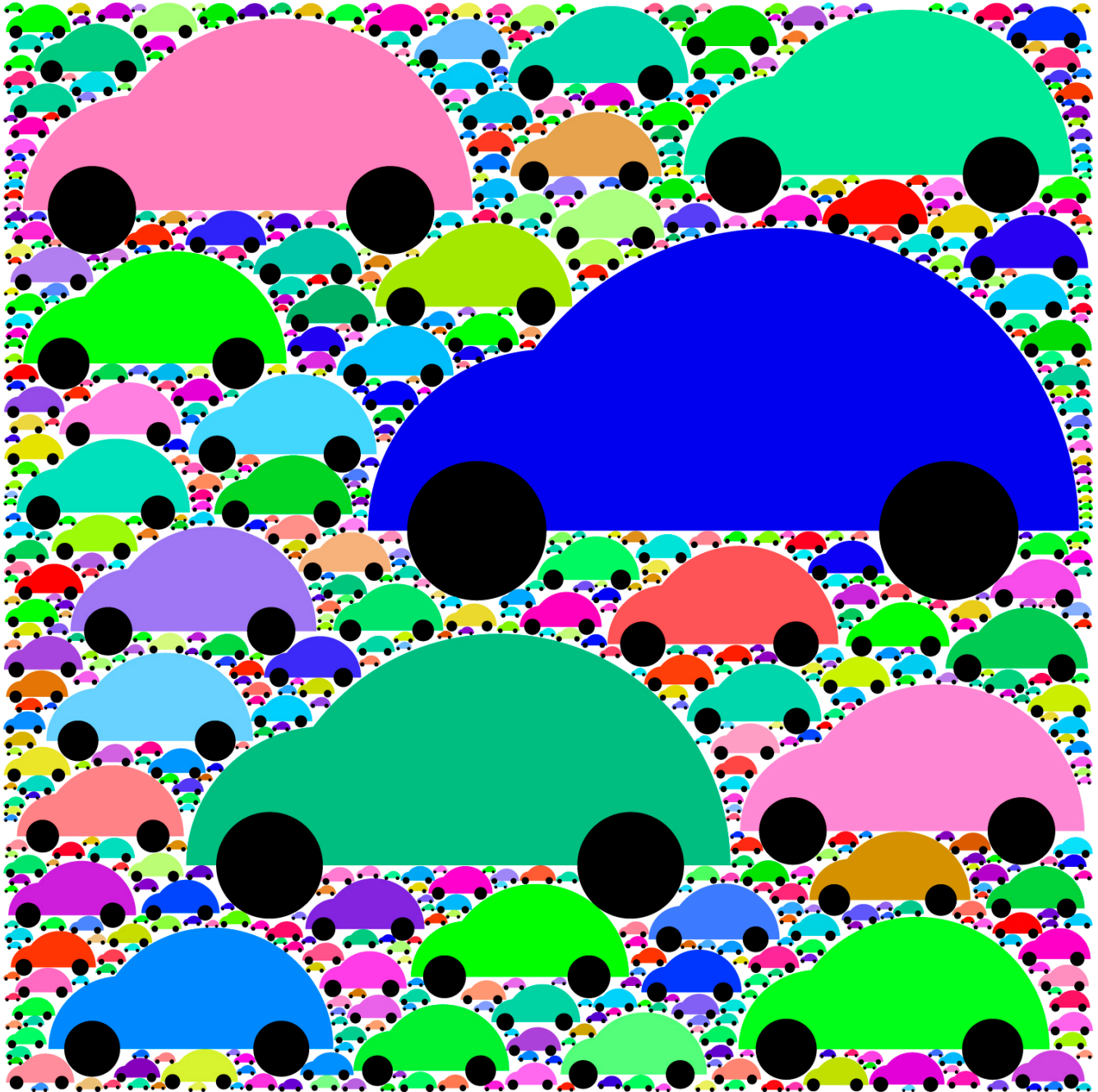




Fig. 9.40. Fractal rain.  $c=1.15$ ,  $N=25$ , fill 50%

Fractalized raindrops are used to create an impressionistic image of rain falling on a garden. This is an illustration of the possibilities for the use of this technique in abstract geometric art. The drops have a rather sparse 50% fill factor by design.

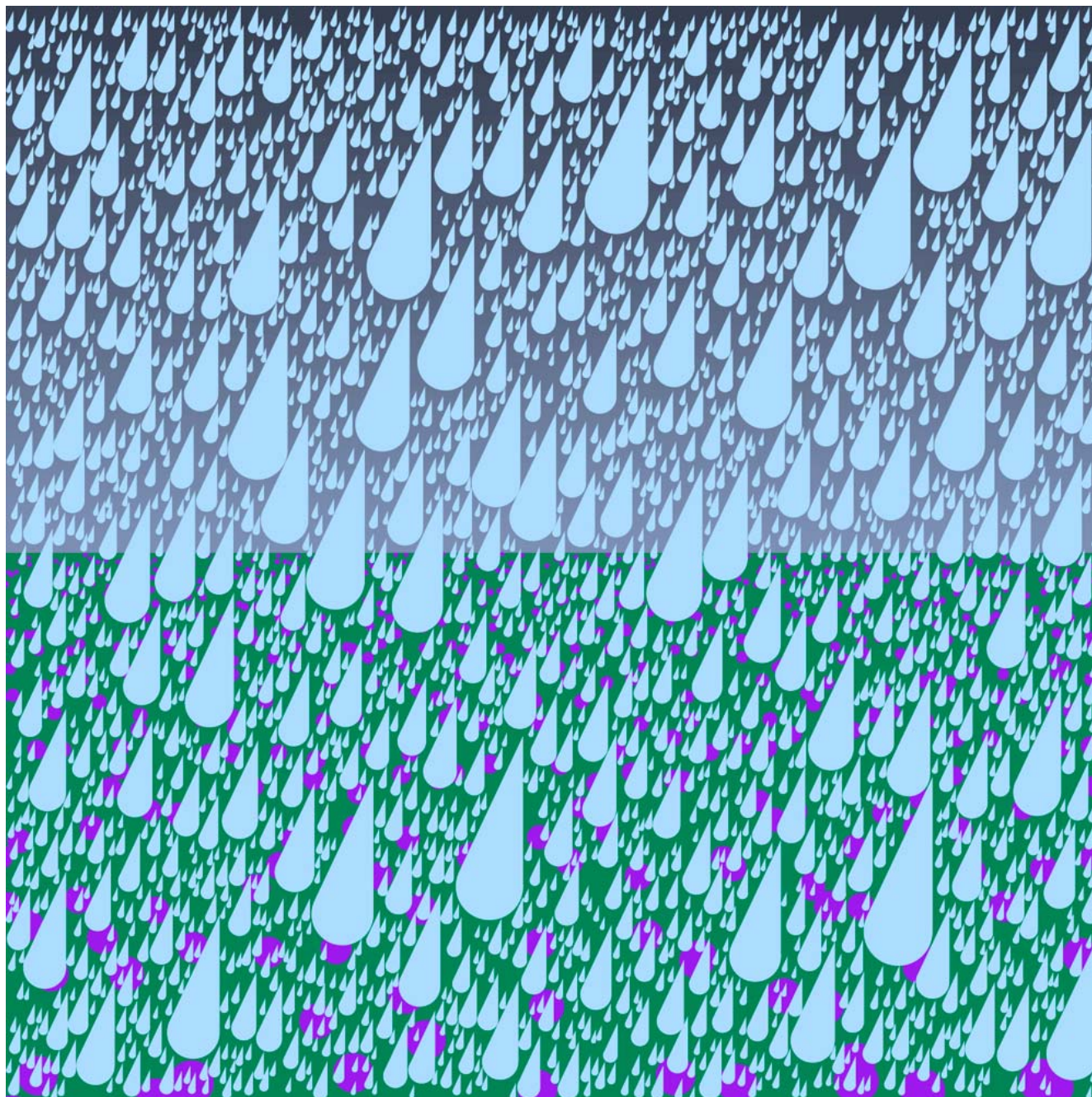


Fig. 9.41. Fish.  $c=1.32$ ,  $N=6$ , fill 50%.

More art than science here. The graded background gives the illusion of an underwater view with light coming from above. The fill factor has been deliberately kept low so that one can see both fish and background. Each fish is a different color.

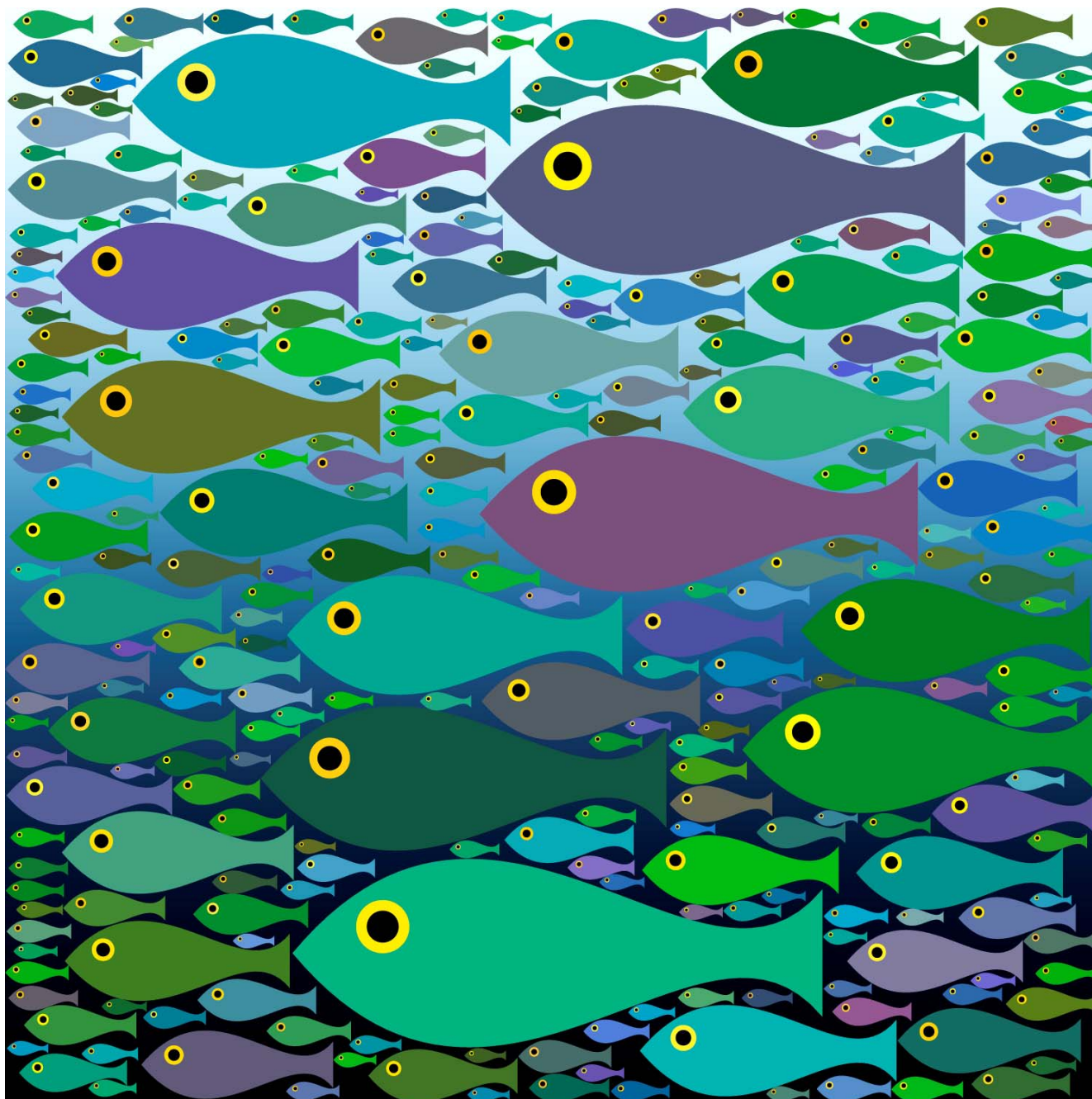


Fig. 9.42. Apple cores.  $c=1.34$ ,  $N=2$ , fill 87%.

This shape could perhaps also be thought of as a "spool" or "bobbin" or an "axe head". It is constructed from four circular arcs, each of the same radius. The green and red apples are rotated  $90^\circ$  from each other, and the image shows some clustering.

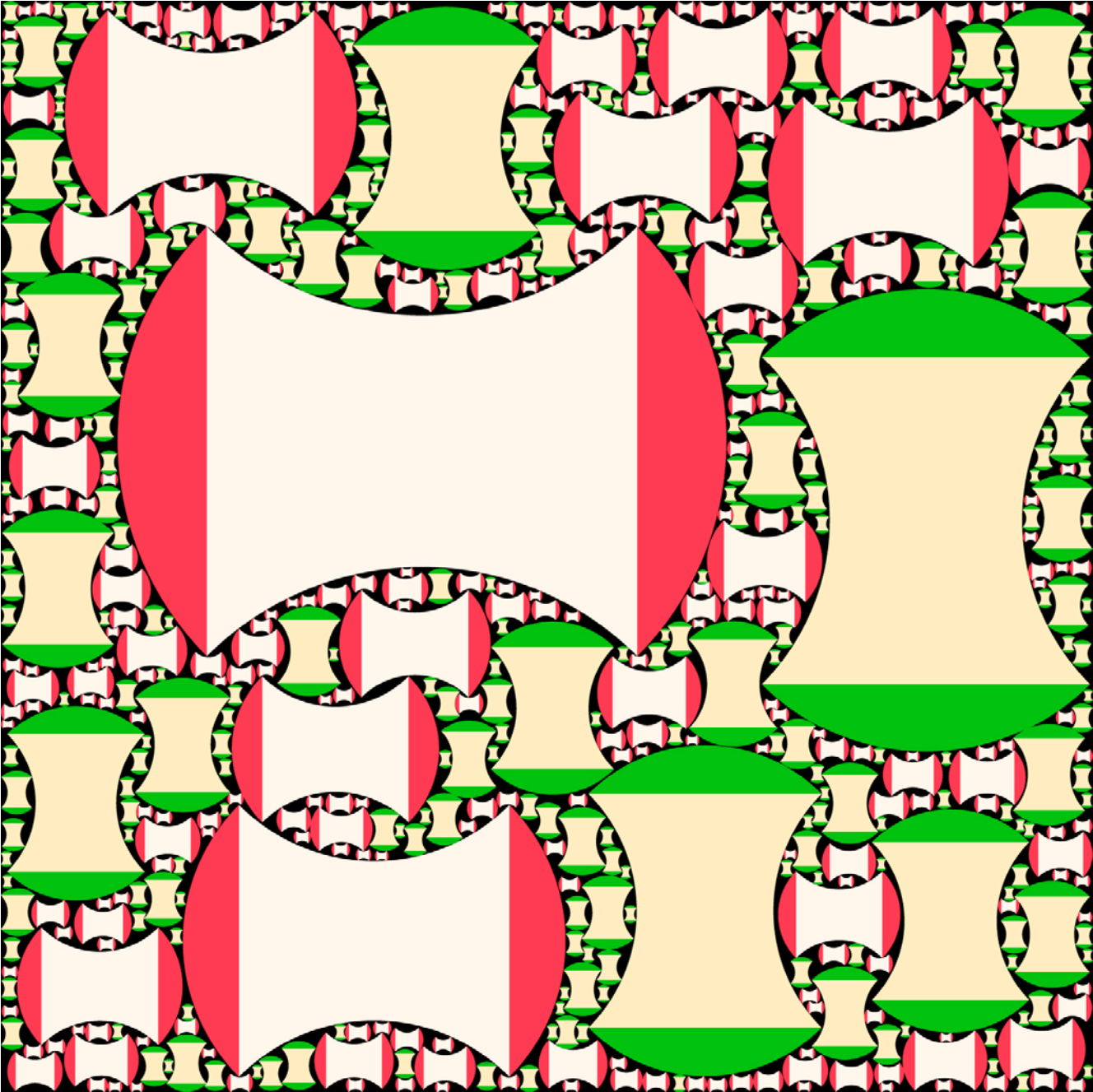


Fig. 9.43. Kisses.

This is yet another example of decorative art. There are in fact 1000 kisses here -- perhaps what the Roman poet Catullus had in mind when he wrote *da mi basia mille*. One could have a million or a billion kisses, but real physical images couldn't show them. The shaded line between lips doesn't survive the image compression process in all instances. I have tried (and failed) to include all of the lipstick colors available at the cosmetics counter. The background is a skin tone.

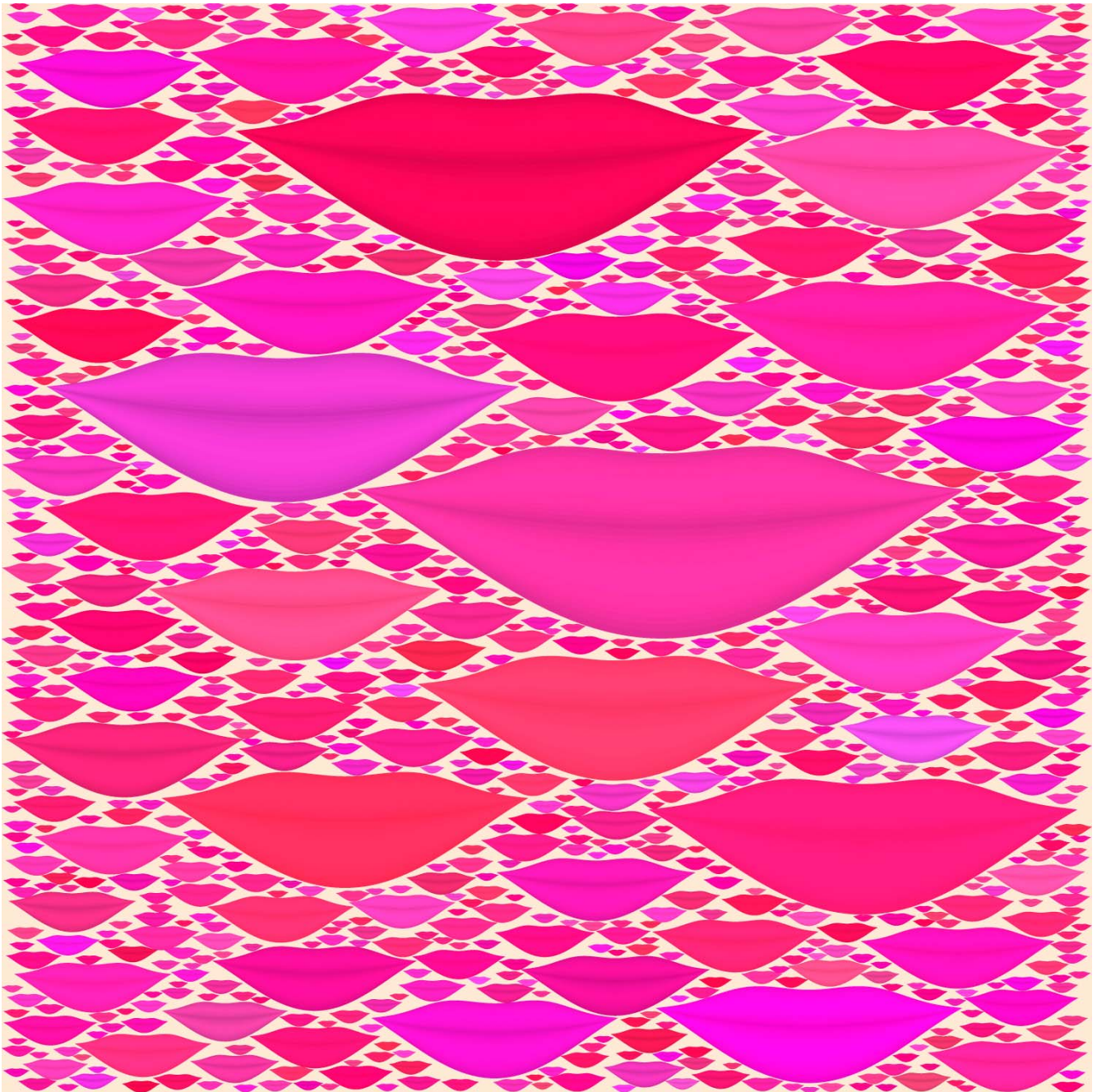


Fig. 9.44. Dunes.  $c=1.31$ ,  $N=4$ , 400 shapes.

The basic shape is bounded above and below by parabolic arcs. This makes overlap computations easy. The resulting lenticular shape is shaded from sandy yellow at the bottom to a brown tone at the top, giving a 3D illusion. A very simple color scheme -- less is more? I think of these as dunes, but there are plenty of other impressions. Some, for example, think of bubbles.

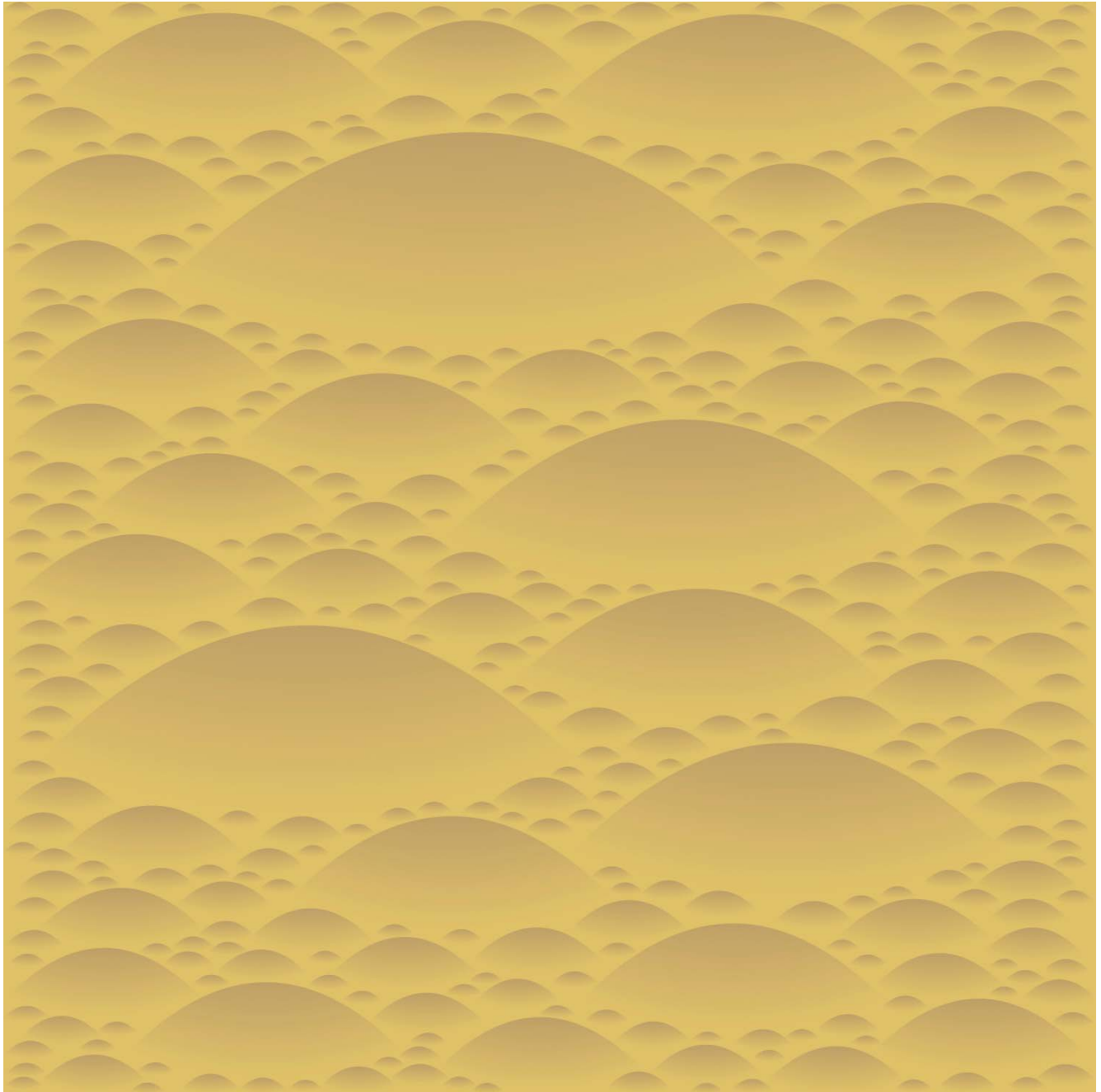


Fig. 9.45. Serpents.  $c=1.16$ ,  $N=2$ , 350 shapes, fill 58%

This is one of the most elaborate shapes thus far studied, and the  $c$  value of 1.16 is fairly close to the upper limit. One can see the smaller shapes nesting into the bends of earlier, larger shapes. As one can see from the eyes, these are Egyptian asps. One of them is the one which bit Cleopatra.

The shape is what EEs would call a sinusoidally phase-modulated sinusoid. Rotated  $90^\circ$  and colored differently these shapes would look like corkscrews. The algorithm ran smoothly (but slowly).



Fig. 9.46. Blackbirds.  $c=1.27$ ,  $N=3$ , 1500 shapes, fill 82%.

These are rather stylized birds -- a flock of birds "so dense that it darkens the sun". They are all flying up from a roost at the same time, beating their wings in unison. The maximum  $c$  for this shape appears to be about 1.31. This is more art than mathematics.

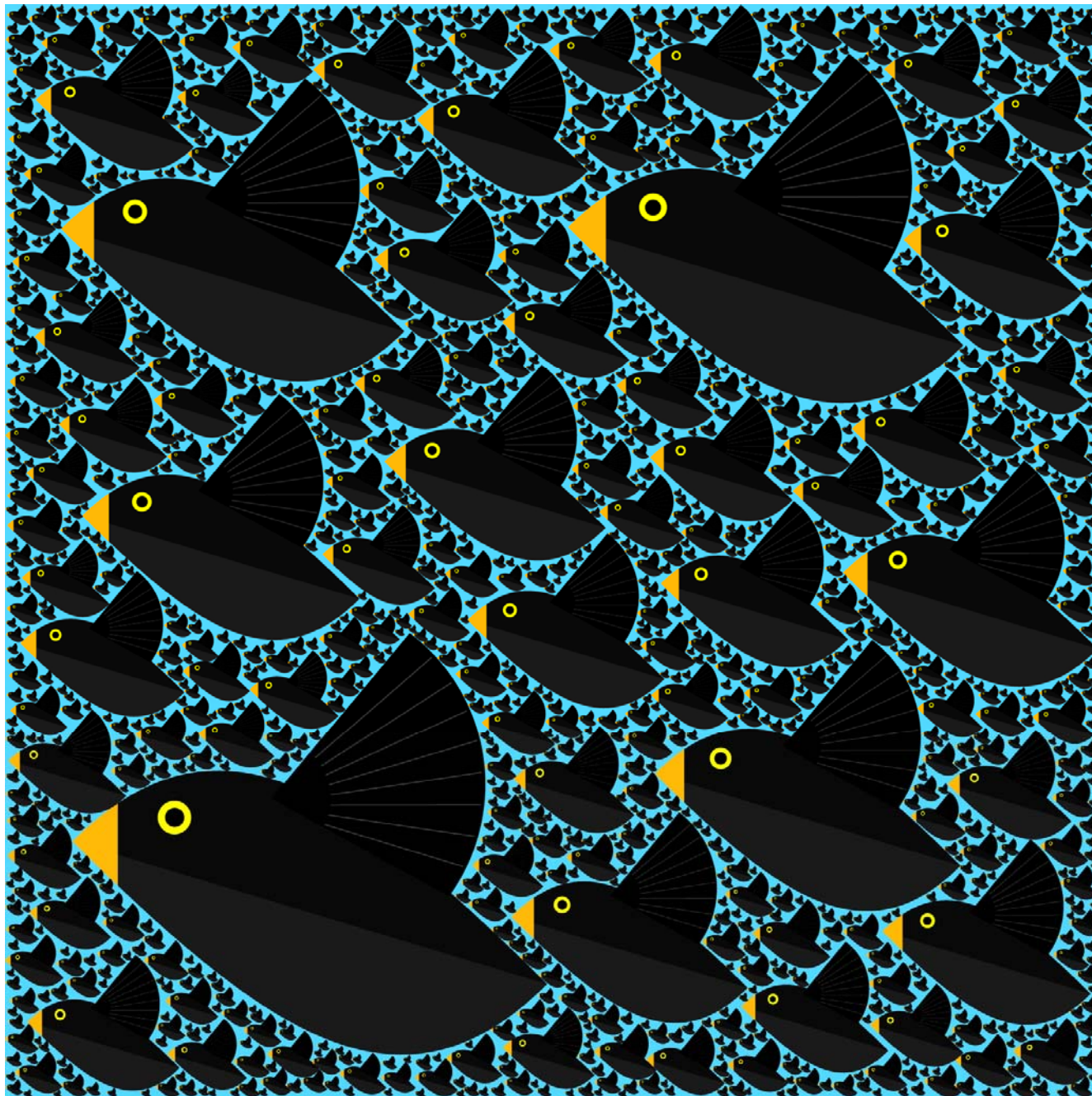


Fig. 9.47. Cardinals.  $c=1.27$ ,  $N=3$ , 600 shapes, fill 77%.

This can be viewed as a variation on the blackbird fractal. Additional code was required for the crest. The background is white below and blue above, suggesting a sunny winter day. This bird is a frequent winter visitor to back yard bird feeders -- a flash of color in winter white.

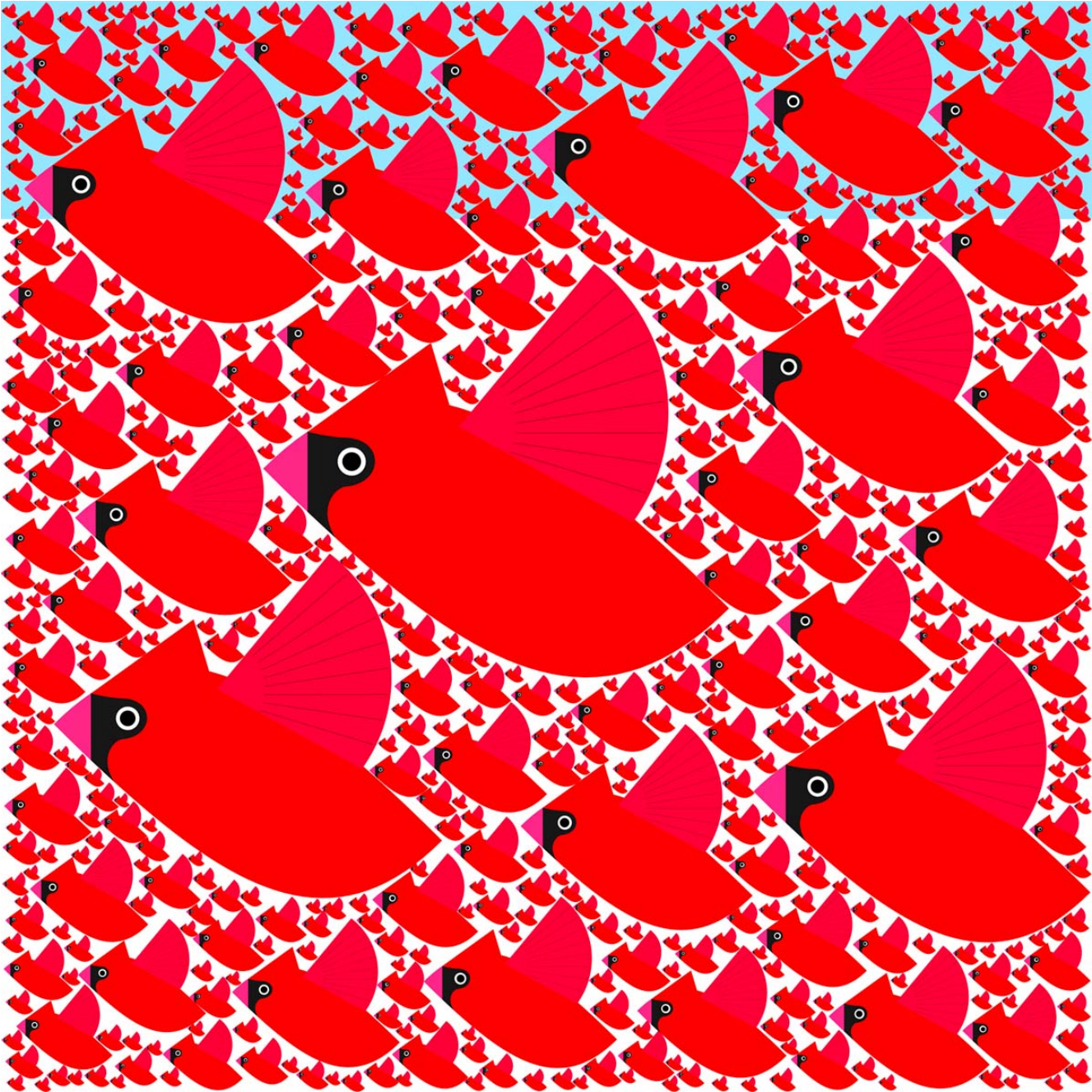




Fig. 9.48. Hot-air balloons.

This is a fairly sparse two-piece shape, but fractalizes quite nicely. Art teachers say that a picture should not be "too busy". This could be used as a classroom example of what "too busy" means -- but if you go to a real hot-air balloon festival you see a kaleidoscopic range of colors and patterns. Pale sky-blue gasket. The suspension ropes and rider are not part of the basic shape, and overlie the smaller shapes.



Fig. 9.49. Candles.  $c=1.31$ ,  $N=3$ , 940 shapes.

This two-piece shape fractalizes easily. It uses all the basic shapes -- a circle, a triangle, and a rectangle. A black gasket and dark candles emphasize the bright flames. The count of candles is about right for Methuselah's birthday cake.

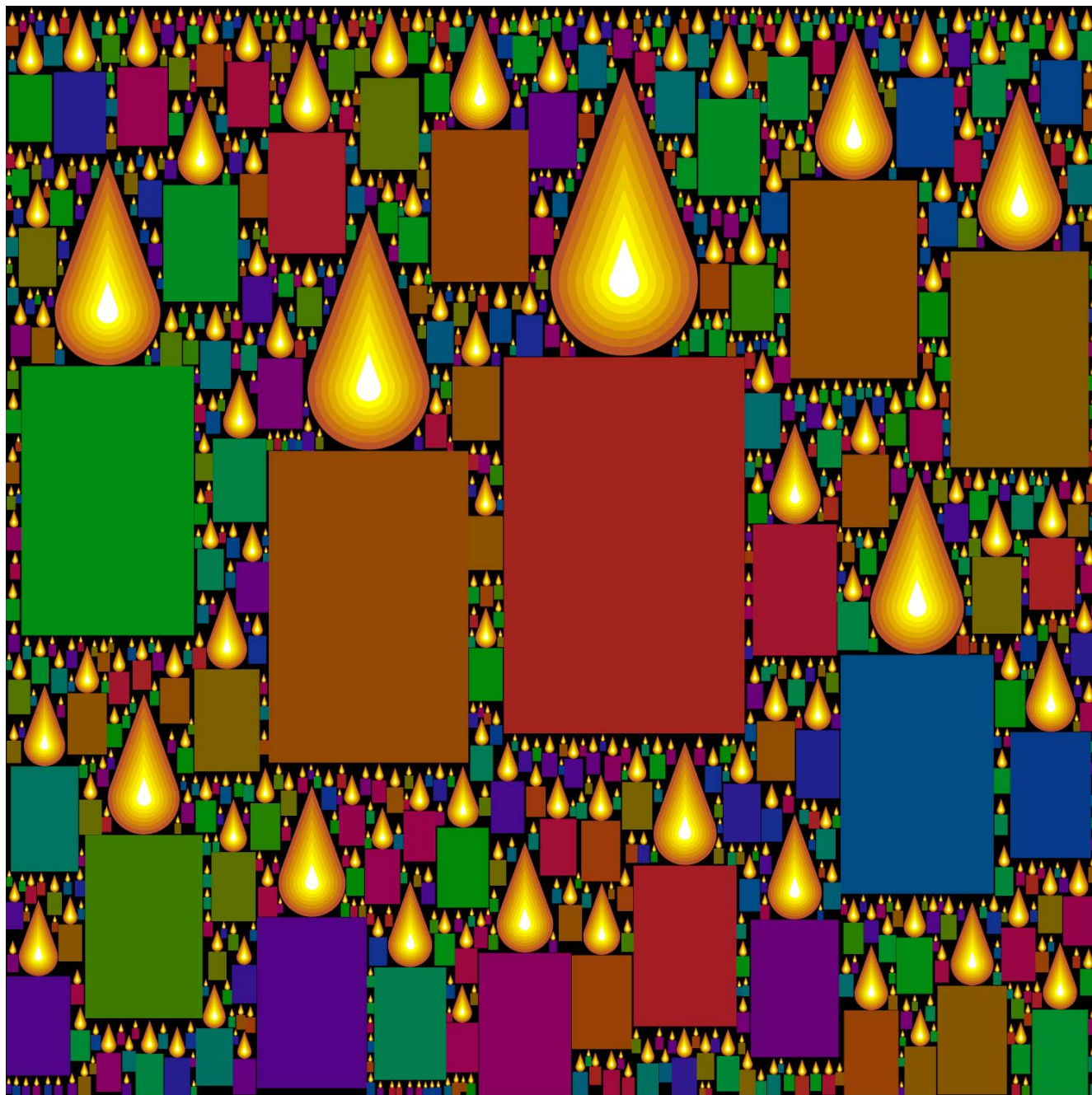


Fig. 9.50. Smiles.  $c=1.26$ ,  $N=2$ , 1000 shapes.

This was begun as a visual joke -- a satire on all those yellow "smiley faces" that you see. It turns out to be more interesting than originally expected, in that the "face in the mouth" motif shows the "statistical self-similarity" property rather well, with each mouth hierarchically containing more faces. The nesting is similar to that seen with annular rings. Here  $c$  is close to the upper limit, so there is strong correlation. Yellow was abandoned as a color because of its low contrast with white -- so ... voila! ... a Halloween scene!

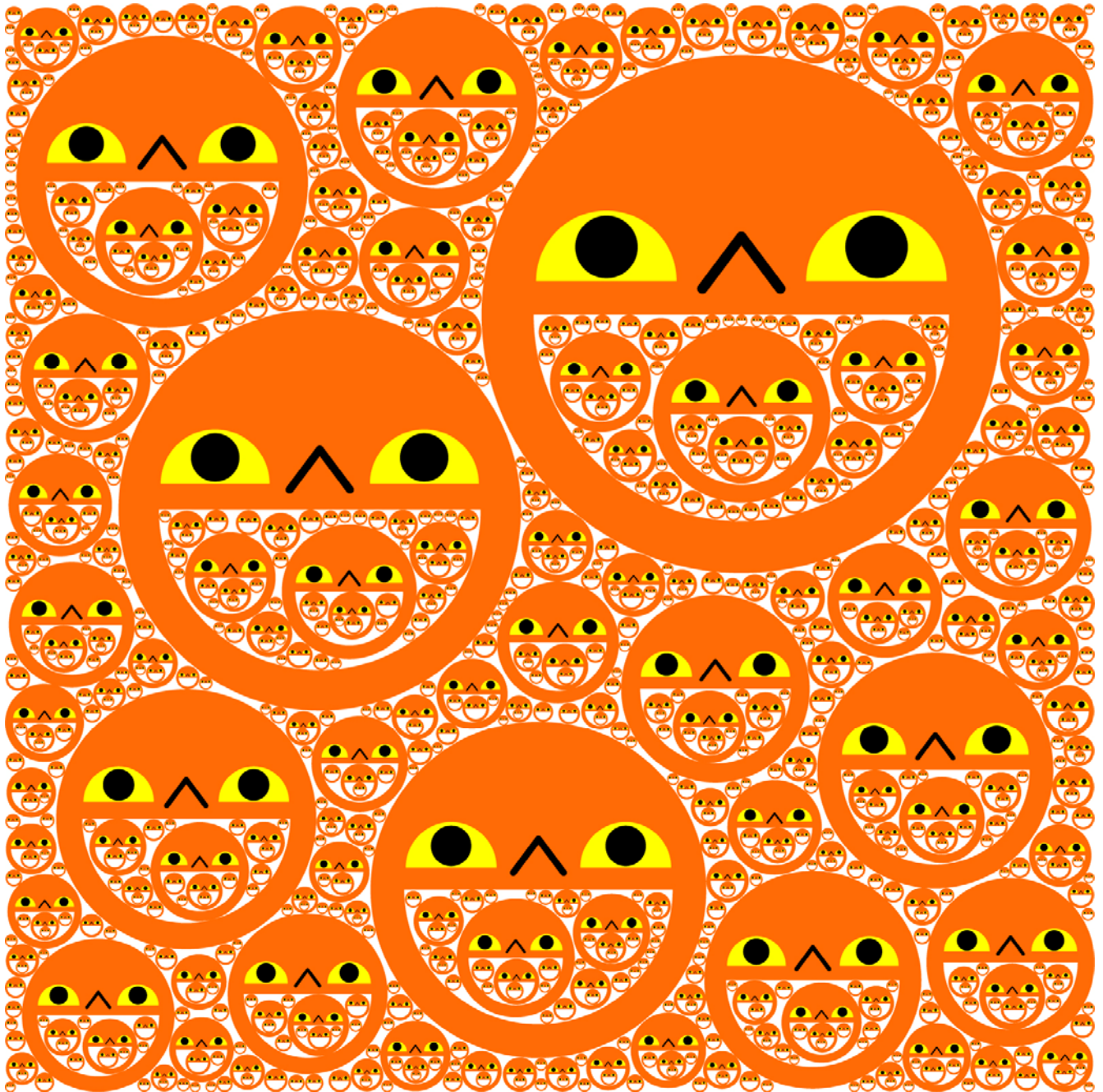


Fig. 9.51. Fish II.  $c=1.22$ ,  $N=2$ , 3000 shapes.

A satirical view of big fish eating little ones. I have seen several cartoons on this theme, but none of them had 3000 fish. This provides a nice illustration of the hierarchical nature of random fractals. Each fish has an opportunity to be both dinner and diner. Geometric -- the fish is somewhat distorted to have a large mouth, and is made with 4 circles and 2 triangles. The smallest fish are only marginally resolved. I hope this revision of Jonathan Swift will be forgiven:

Big fish eat little fish, and think 'em gastronomic.  
And little fish eat smaller fish, and so to size atomic.

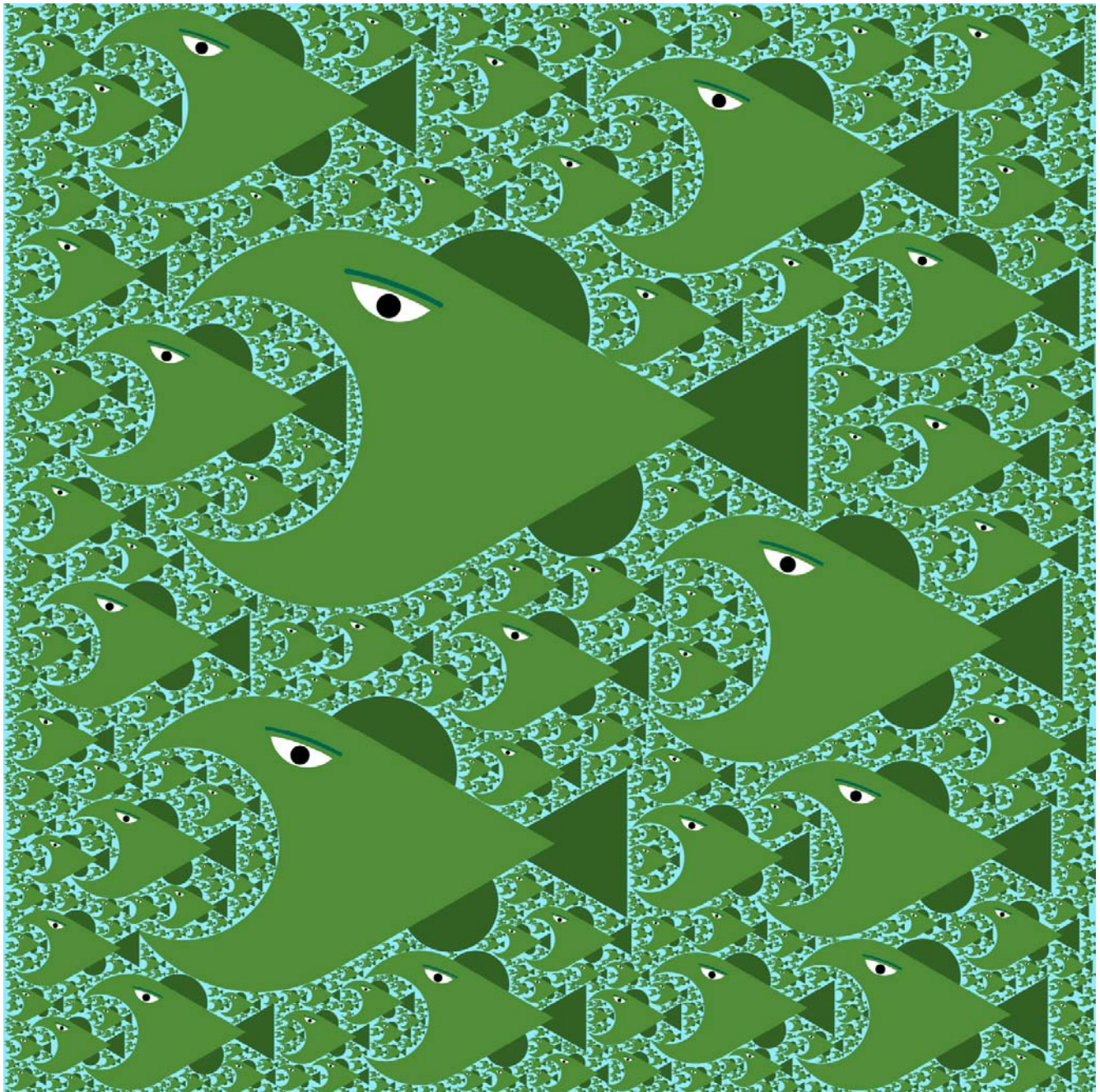


Fig. 9.53. Eyes.  $c=1.20$ ,  $N=3$ , 300 shapes.

This is a 3-circle pattern, with an "eye" defined by two circular arcs within a larger circle which can be thought of as an eye "surround" (skin color, folds, eyelashes). It is a hollow eye, as in the nested rings. The "outer" gasket is black, while the "inner" gasket is white. Both white and black regions are available for further placements. The last-generation eyes (ones which do not have any other eyes nested within them) have a further set of eye features (uvea, pupil). This is my first image to make use of the nesting generation information. Six instances of 4th generation eyes. Surreal.

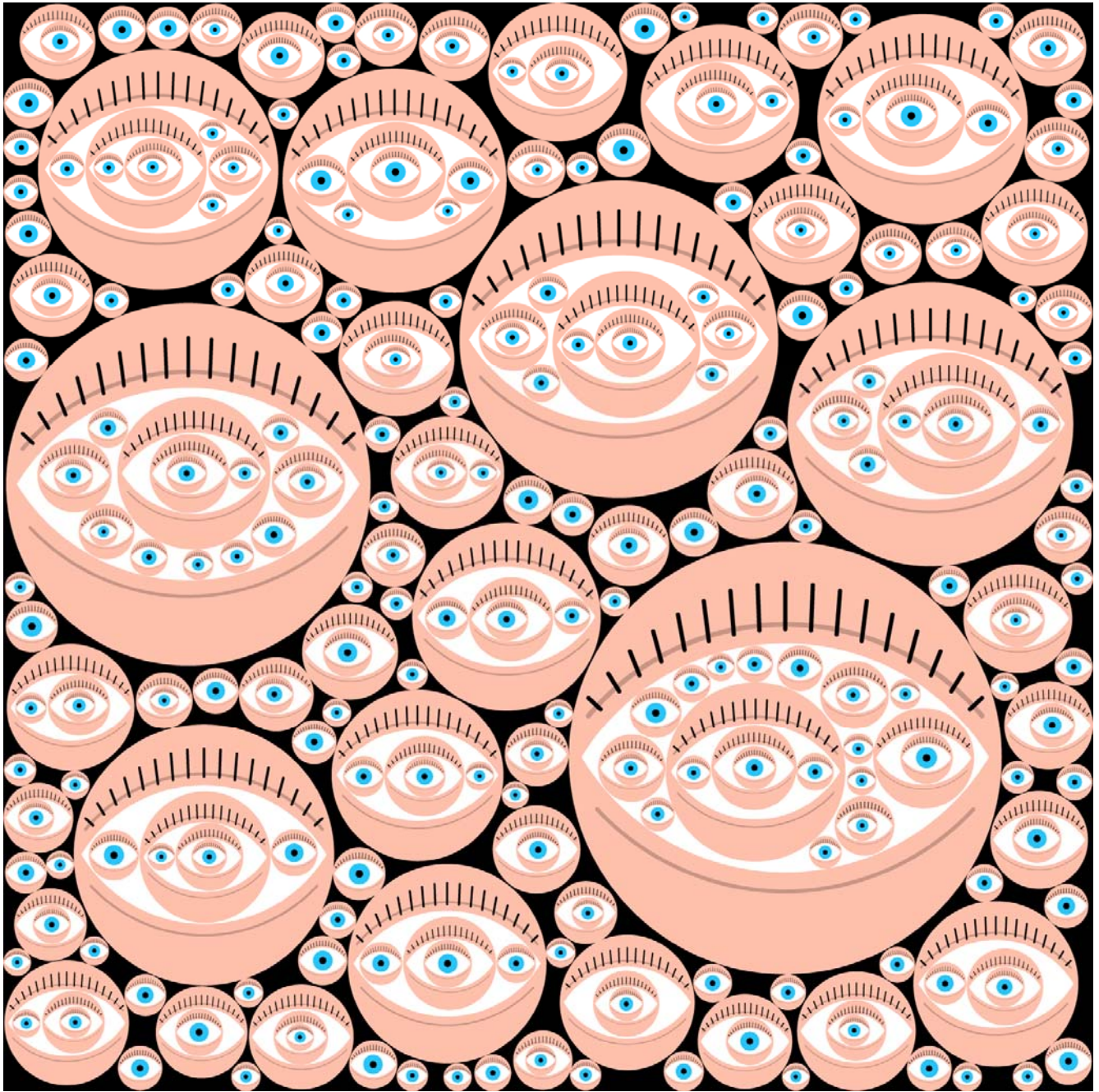


Fig. 9.54. Lips by rank.  $c=1.20$ ,  $N=3$ , 151 shapes.

This is the same shape as the previous eyes example, but without the special features for eyes. They look like lips to many people. Here the shapes have been colored by rank, an interesting concept which applies to "hollow" shapes. Shapes without anything in them are rank 1; those with only rank 1 objects inside are rank 2, etc. It can be seen that rank tracks closely with size. There is 1 shape of rank 4, 13 of rank 3, 36 of rank 2, and 101 of rank 1. Rank tracks closely with size, and changes at size boundaries. The hierarchy in this random fractal is well illustrated here.

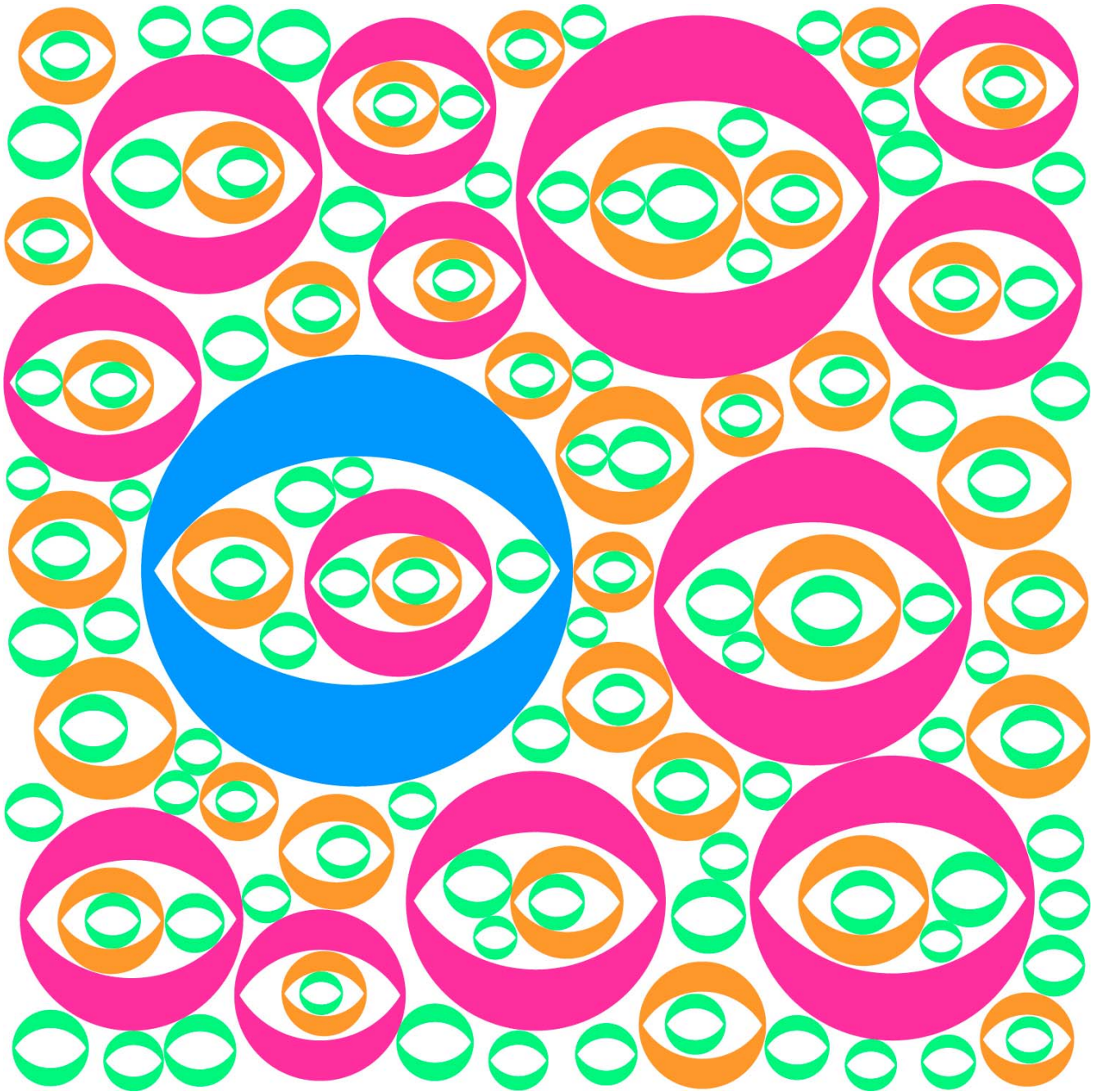


Fig. 9.55. X and Y.  $c=1.17$ ,  $N=4$ , 1500 shapes.

The style that is used throughout this work is symbols filling an area. Here the symbols are X and Y, alternating. Random color. These rather sprawling shapes allow only a low  $c$  value. The resulting white space makes it easier to see the shapes. This might be the (bad) dream of a reluctant algebra student. If we interpret X and Y as sex-linked chromosomes, we could color the Ys blue and the Xs pink, for a nice baby-shower wrapping paper. Or if we interpret X as an x-spouse, one could have a punning title such as "Y I have an X", perhaps with the X red-hot and the Y cool black.



Fig. 9.56. Y.  $c=1.14$ ,  $N=1$ , 8000 shapes, fill 74%.

Ys do not pack very well. This image illustrates what you get when you operate with low  $c$  and modest fill. Log-periodic color. With low  $c$  the white gasket is still visible even with this profusion of shapes. The smallest shapes seem to fade into the background as a sort of texture. The title might be "the Ys guy".

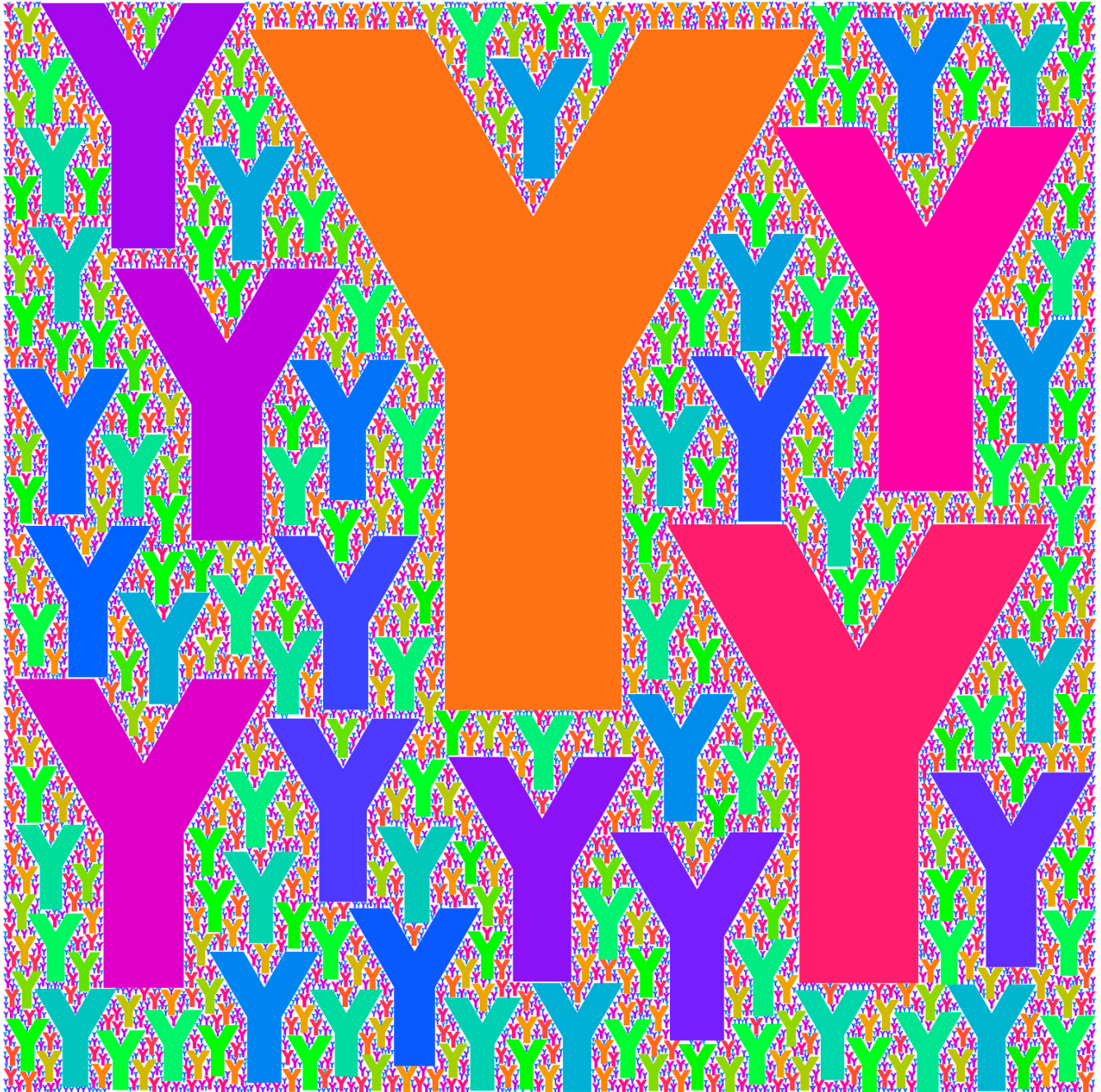




Fig. 9.57. Cones.  $c=1.28$ ,  $N=1$ , 117 shapes, fill 77%.

A triangle with a semi-ellipse on the bottom gives the illusion of a 3D cone. Here the illusion has been helped along by shading. This is Coneland, a remote region of Earth with many temporarily extinct volcanoes. It is a desert country, with the only green things growing on the tall peaks. The natives hold the tallest peak to be sacred.

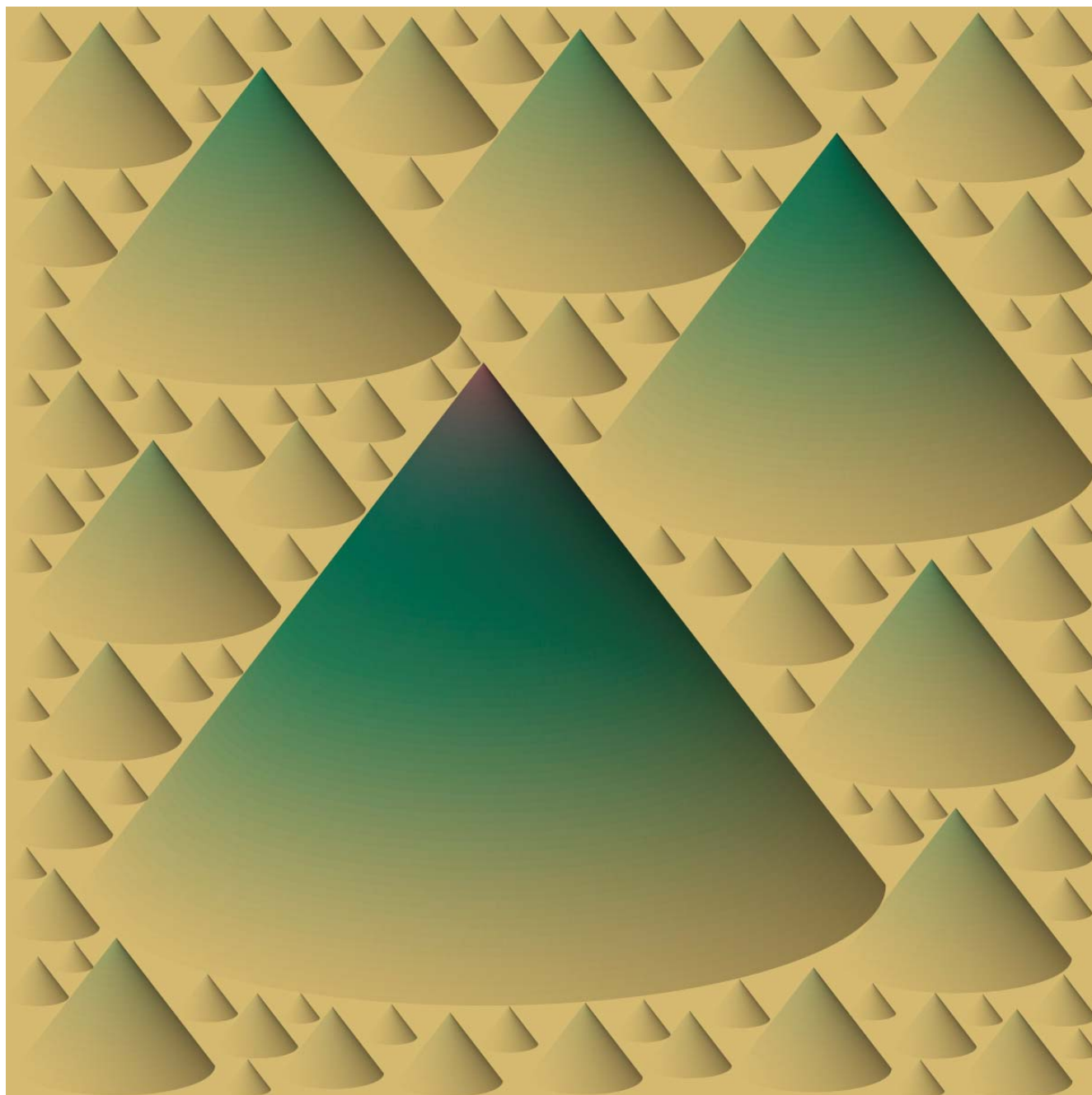


Fig. 9.58. Horns.  $c=1.24$ ,  $N=4$ , 5000 shapes, fill 82%.

A great variety of names have been suggested for this 3-circle shape -- comma, chili pepper, porpoise, dagger, paisley, cow horn, sickle, brush writing, etc. The basic shape has random 360 deg rotations at each trial, i.e., 3 "degrees of freedom". Here the shapes are colored in a way that has 180 deg periodicity in the position angle (opposite-pointing shapes have the same color). One can see regions of similar color, which brings out the ordering property (correlation). Black gasket, periodic boundaries.

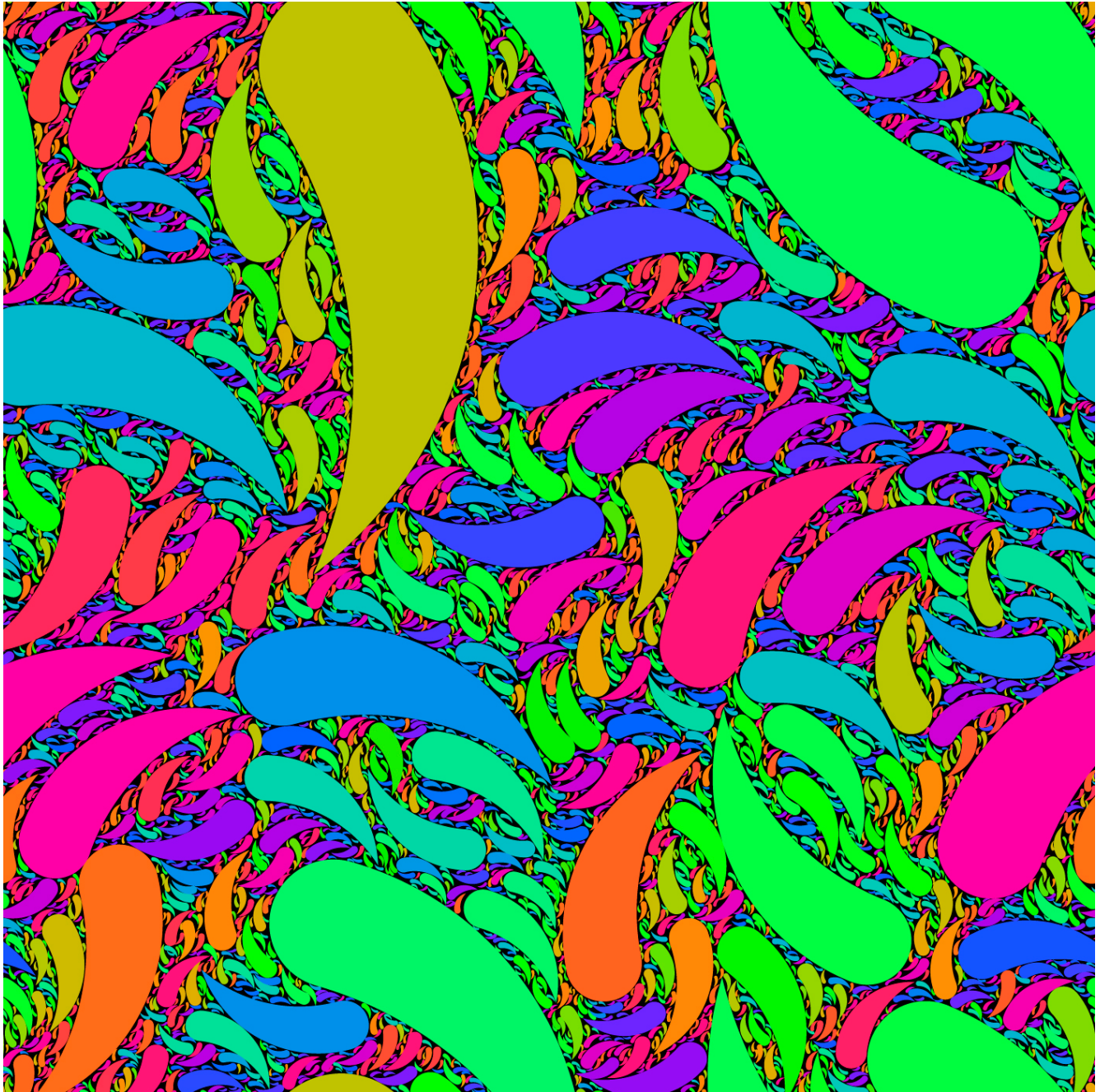


Fig. 9.59. Lenses.  $c=1.33$ ,  $N=2$ , 1200 shapes, fill 89%.

Unlike earlier work with this shape, here they have random orientation, varied at each trial. The colors are periodic in the orientation angle with period 180 deg. There is quite strong correlation in angle; each big shape influences the nearby small shapes to have a similar orientation -- just as the big shapes in human society are surrounded by crowds of imitators. Black gasket; periodic boundaries. I sometimes think of magnetic domains when I look at this.

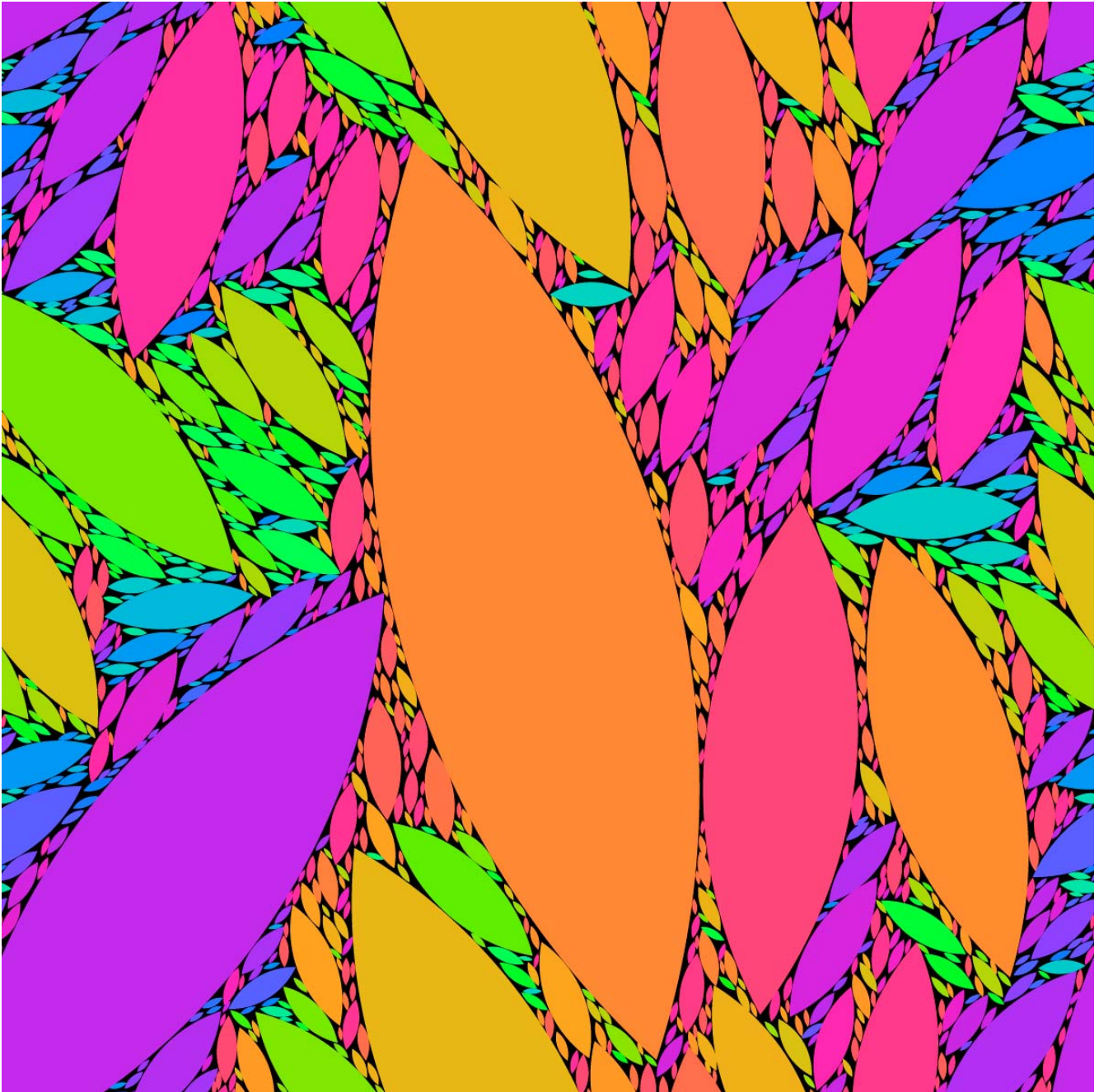


Fig. 9.60. Yang and Yin.  $c=1.32$ ,  $N=3$ , 500 shapes, fill 82%.

Here "yang" and "yin" are fractalized as separate shapes. The object was to look at correlation. It can be seen that there is correlation of the kind commonly seen with other pairs of shapes -- the "comma" and the "anticomma" tend to keep to themselves. This shape has an extremely sharp cusp.

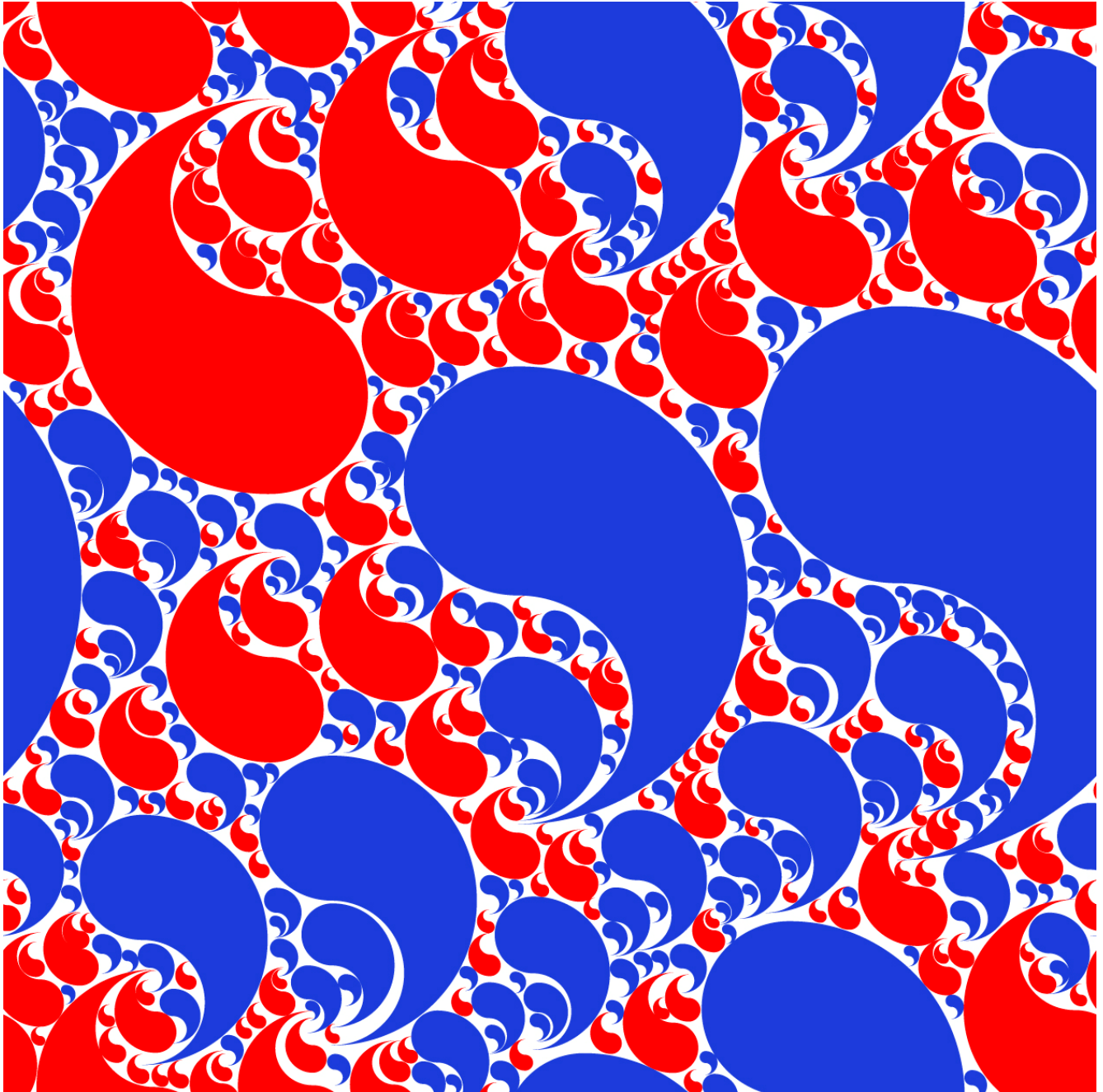


Fig. 9.61. Stars.  $c=1.22$ ,  $N=4$ , 3300 shapes, fill 82%.

These are not the rounded "starfish" of a previous figure, but precise 5-point geometric stars of the traditional kind. All stars have the same orientation. They are a rather sprawly and noncompact shape, and the relatively low value of  $c$  agrees with this. Log-periodic color, black gasket.

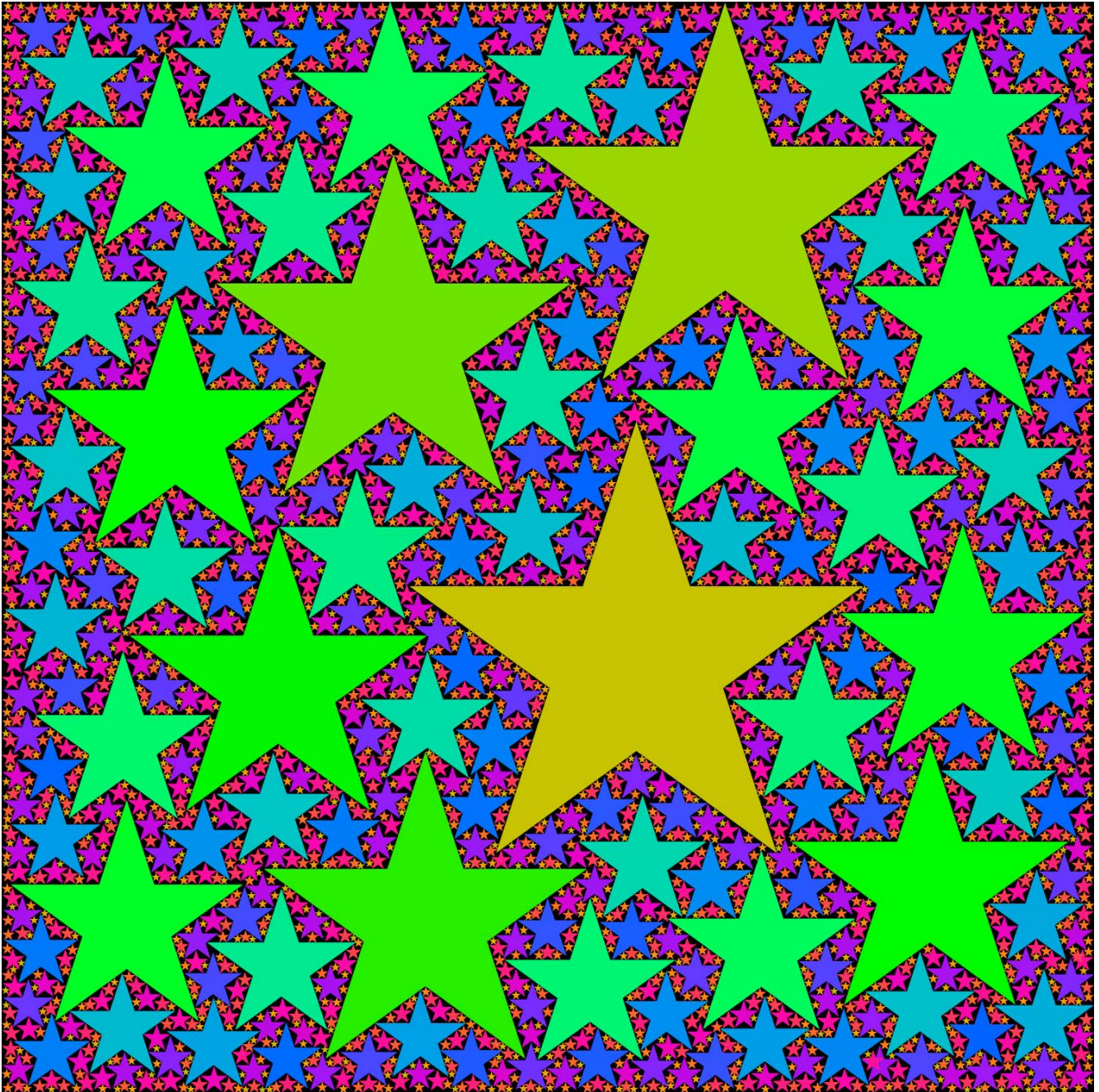


Fig. 9.62. The argument.

The basic shape is two circles with circular cut-outs. They are drawn in a way that resembles two men in an argument.

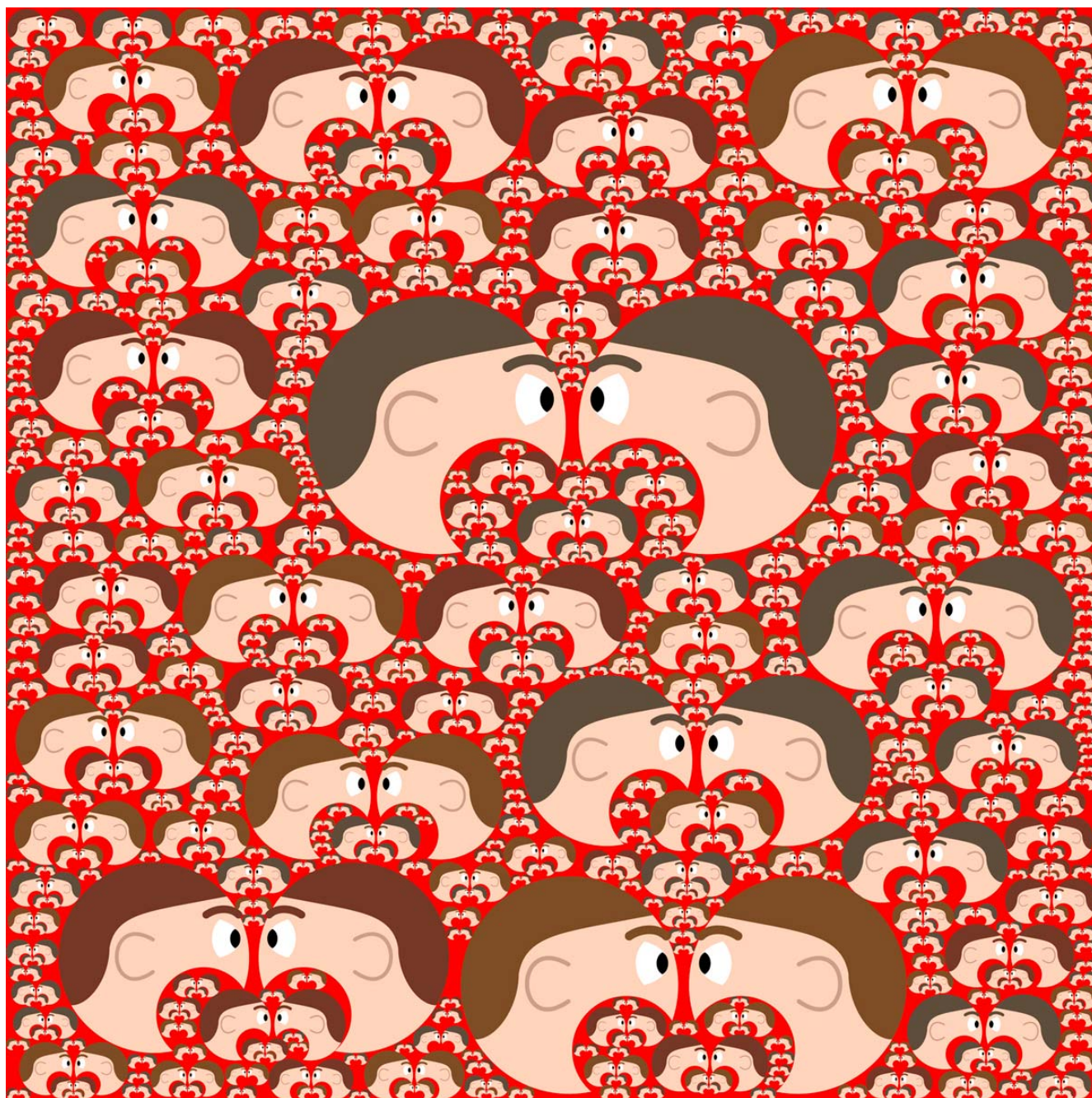


Fig. 9.63. Butterflies.  $c=1.22$ ,  $N=3$ , 500 shapes.

This differs from the other butterfly pattern in that it uses polar coordinates and gives a smooth, rounded shape. All angles, periodic boundaries, two butterfly color schemes.

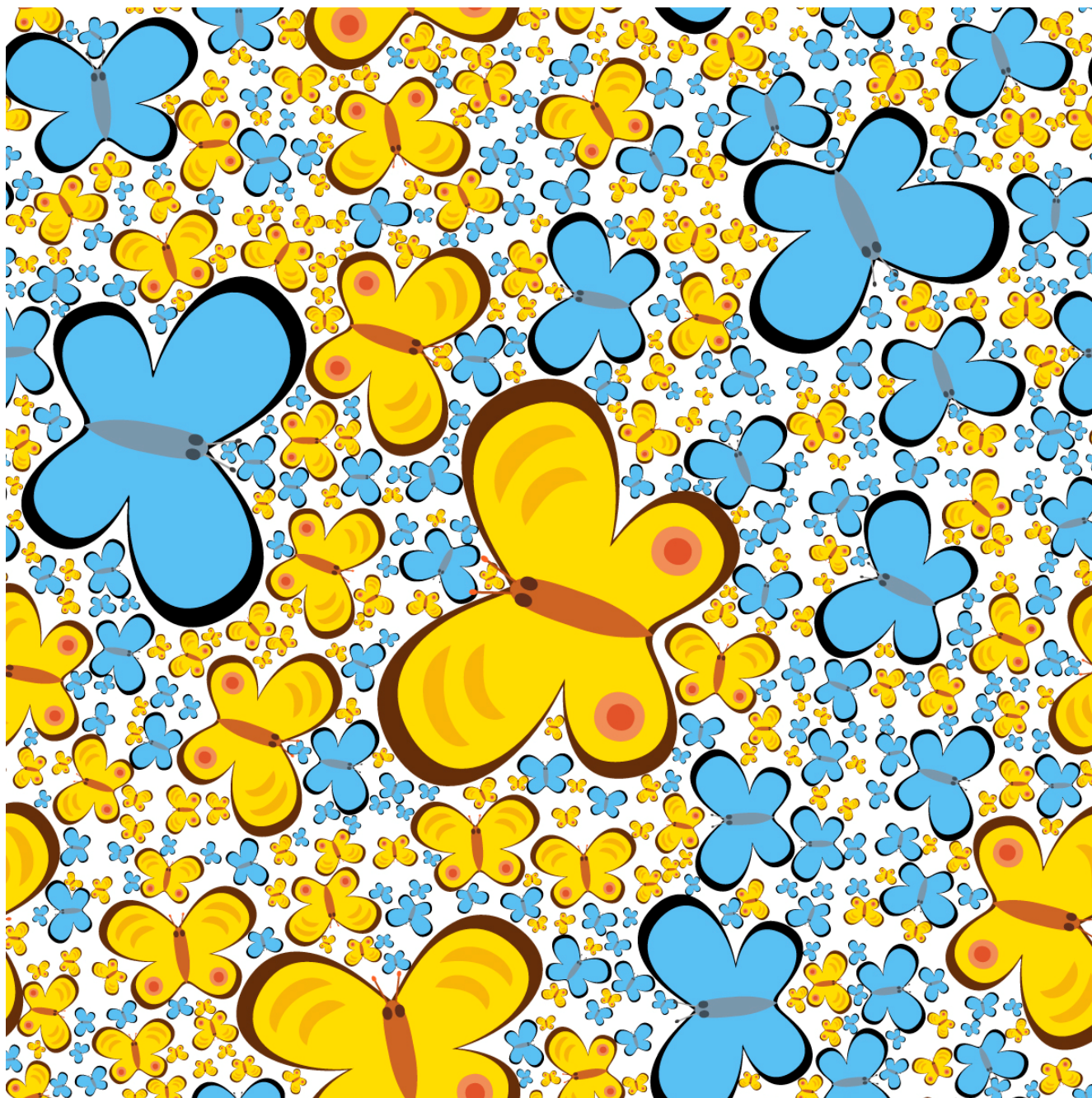


Fig. 9.64. Hearts.  $c=1.21$ ,  $N=1$ , 1200 shapes, fill 80%.

This differs from the other heart in that it has a more complicated shape and variable orientation angles. Periodic boundaries.

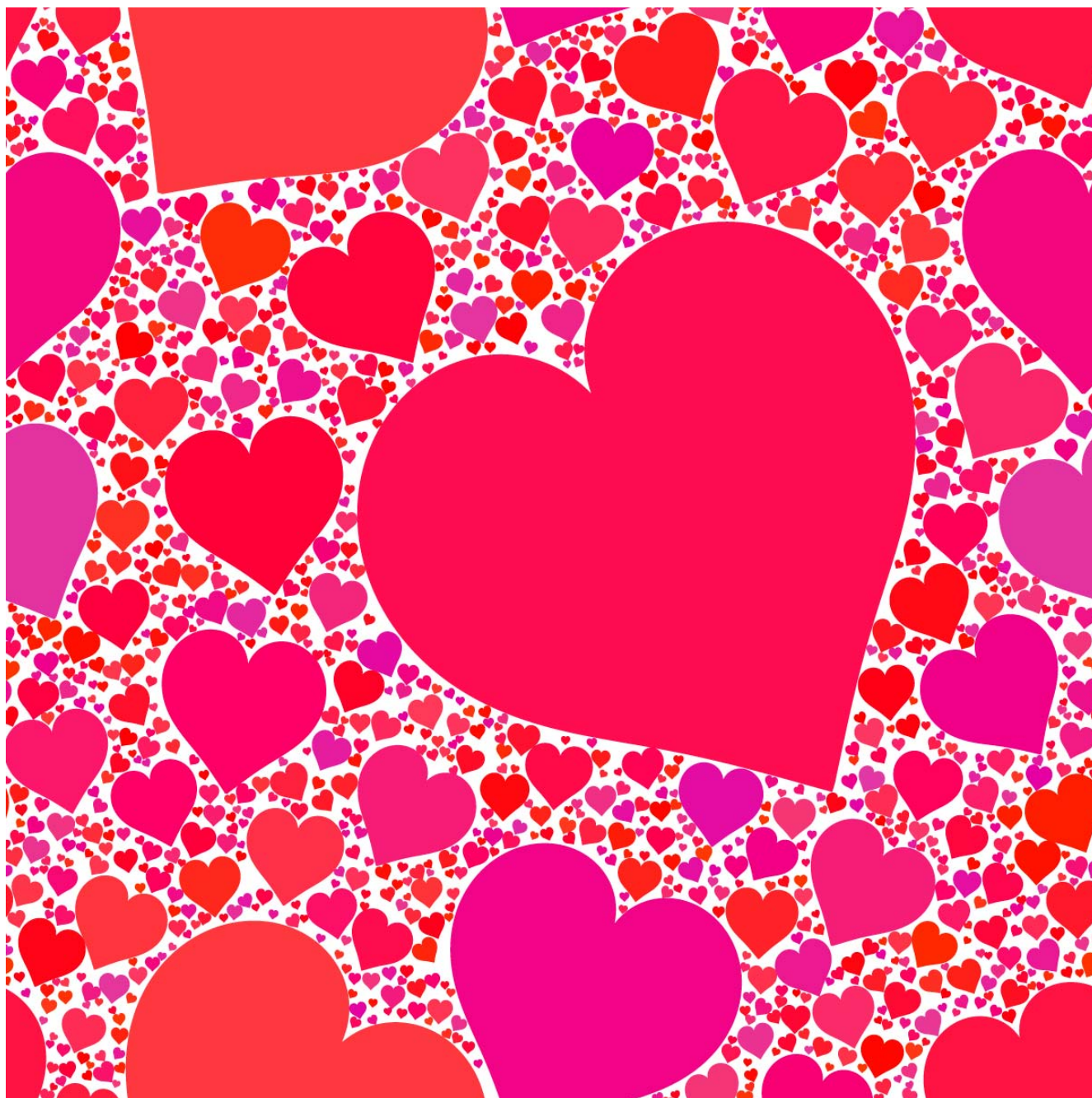




Fig. 9.65. Waves.

This sinuous shape is colored in a way that it resembles ocean waves.

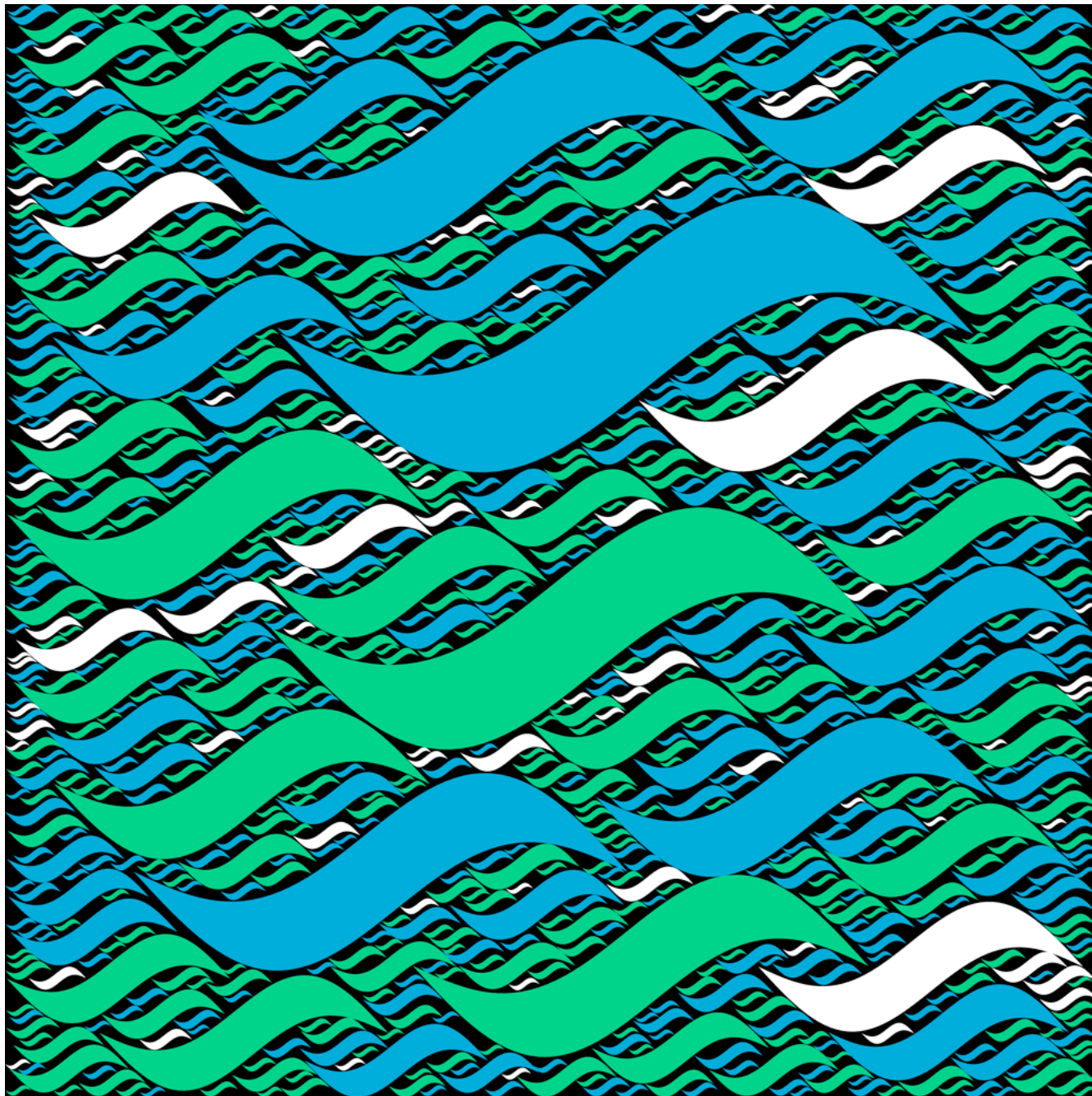


Fig. 9.66. Double triangles (bow ties).  $c=1.21$ ,  $N=6$ , 1200 shapes.

Paired triangles with log-periodic color. Inclusive boundaries.

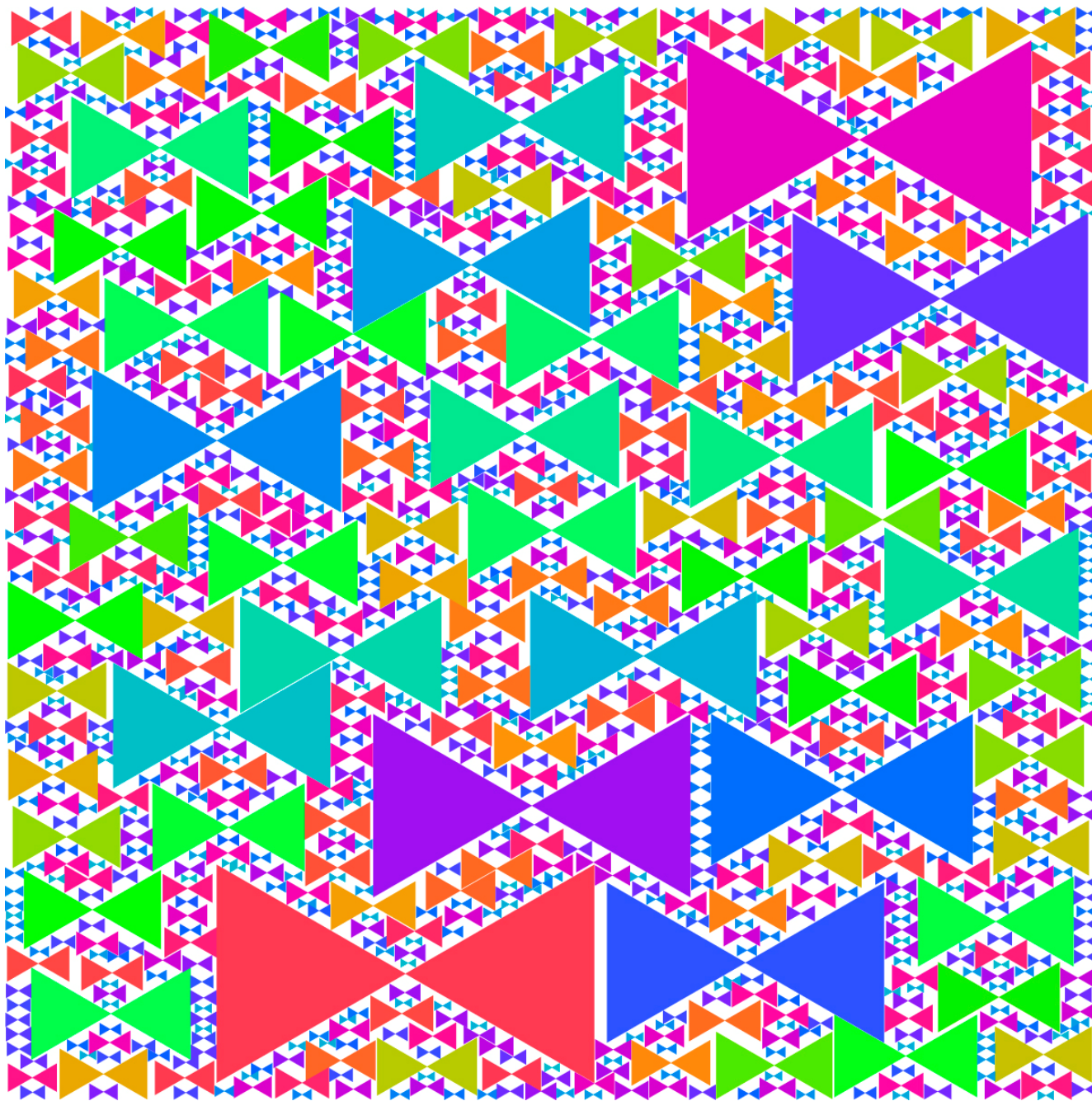


Fig. 9.67. Triple triangles.  $c=1.16$ ,  $N=4$ , 1000 shapes, fill 59.3%.

Triangle triplet with log-periodic color. This is basically the Sierpinski motif, fractalized two recursions at a time. Note the high degree of ordering.

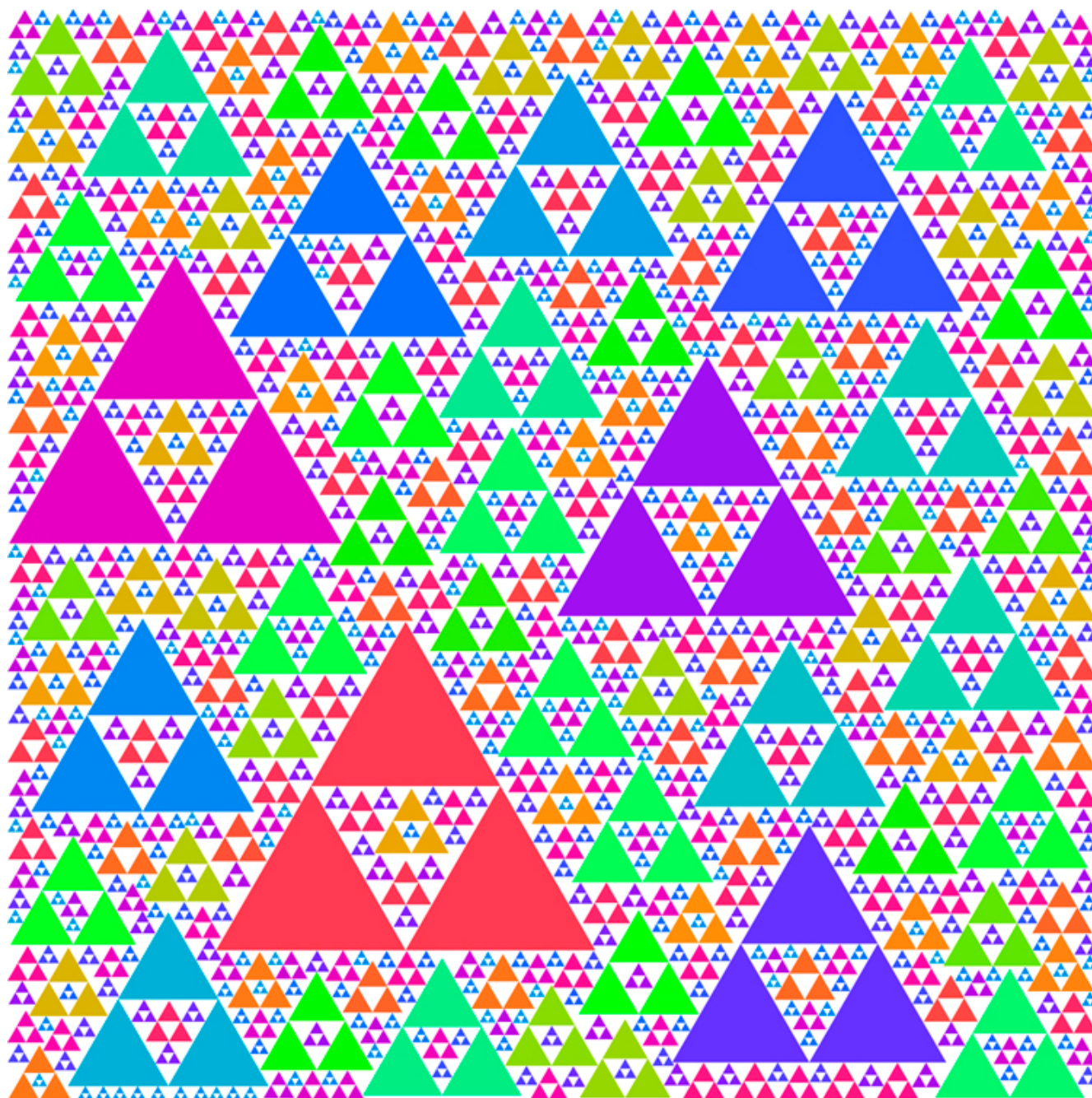


Fig. 9.68. Snowflakes.  $c=1.15$ ,  $N=2$ , 5000 shapes, fill 70%.

This rather stylized form of snowflake has a fairly low maximum  $c$  due to its sparse form. All angles, inclusive boundaries.

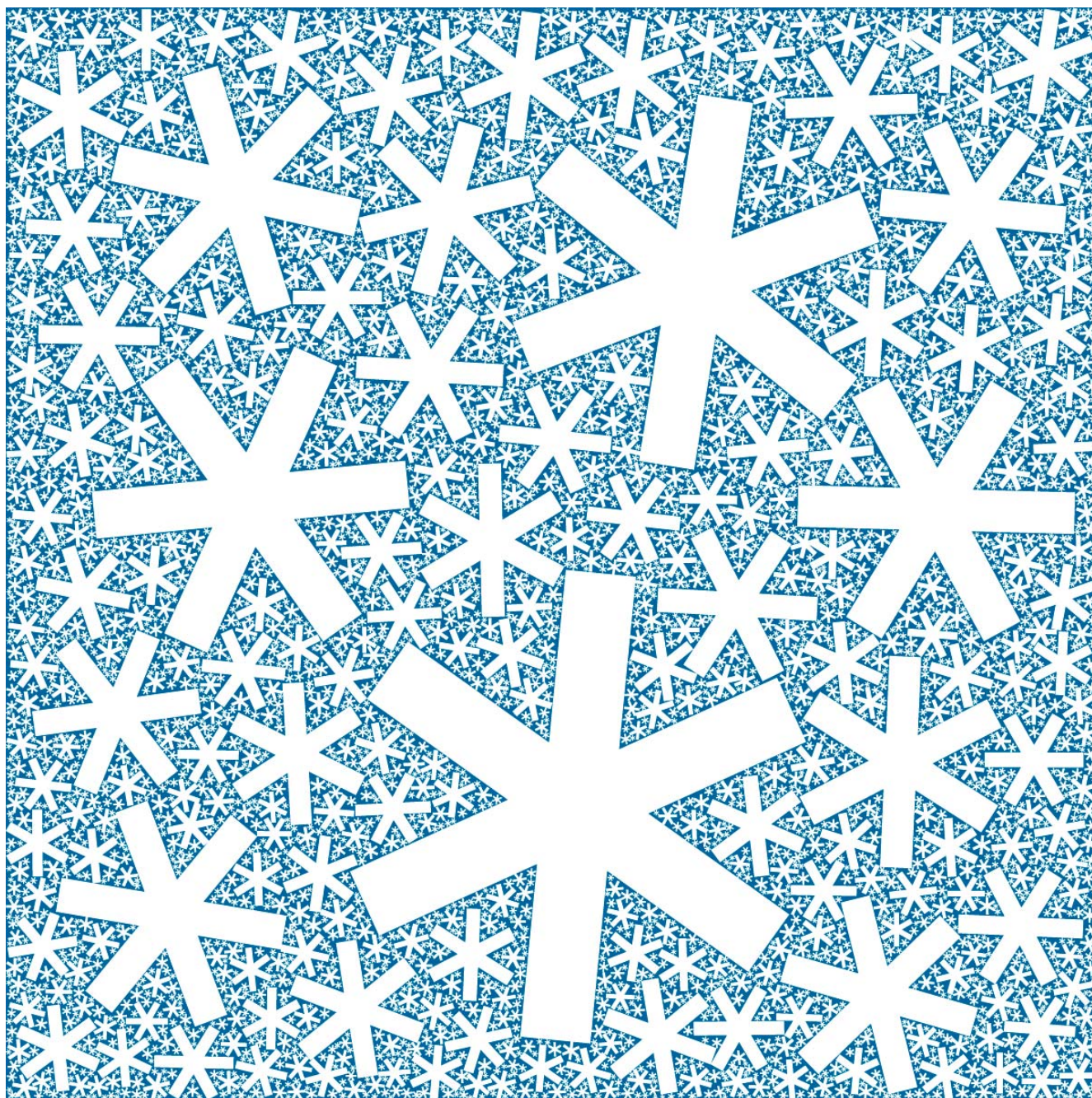


Fig. 9.69. Squares, probability gradient.

Ordinarily all positions  $x,y$  are equally probable in trials. Here the probability has been made to have a Gaussian distribution so that  $x,y$  values near the center occur much more often. The result is dense packing of the largest shapes near the center and sparse packing of small shapes near the edges. It was not set up to have 100% limiting fill (as in the other examples here). The color scheme runs from bright near the center to gray at the edge.

This is another example of variations which can be used in decorative art.

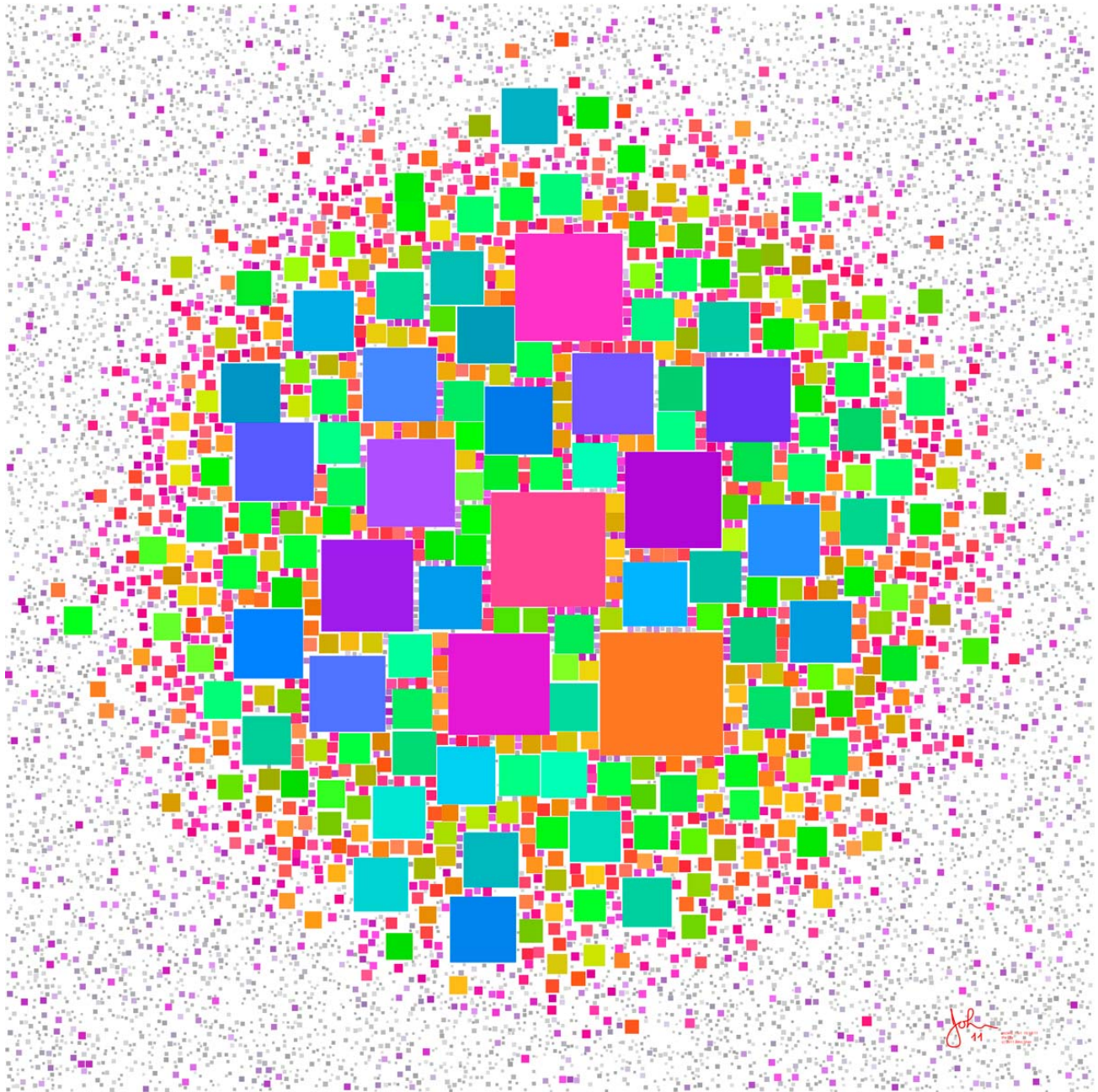


Fig. 9.70. Circles, grouped.

This is a variation in which the total areas of groups of circles obey a power law. The sizes of the circles are all the same for a given group and are (arbitrarily) made to obey a decreasing exponential law (in group number  $n$ ), with the numbers of them chosen to give the correct total area for the group. Here  $c=2.8$ ,  $N=5$  for the *groups*. Much larger exponents  $c$  can be used compared to the non-grouped case. It is set up to be space-filling. Each group has a unique color. White gasket.

This scheme has a much larger set of parameters and does not always run. Details are given elsewhere on the site.

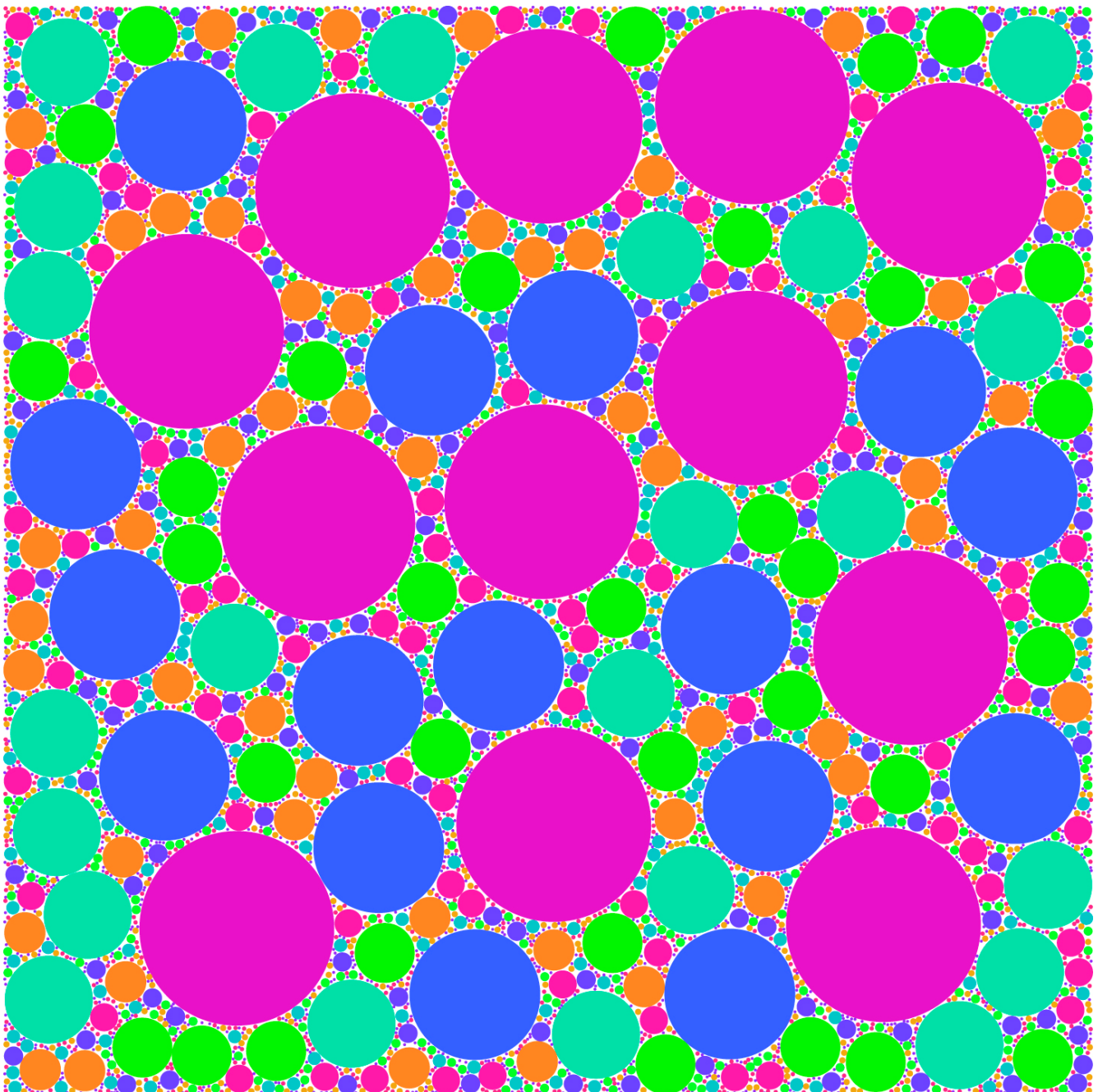
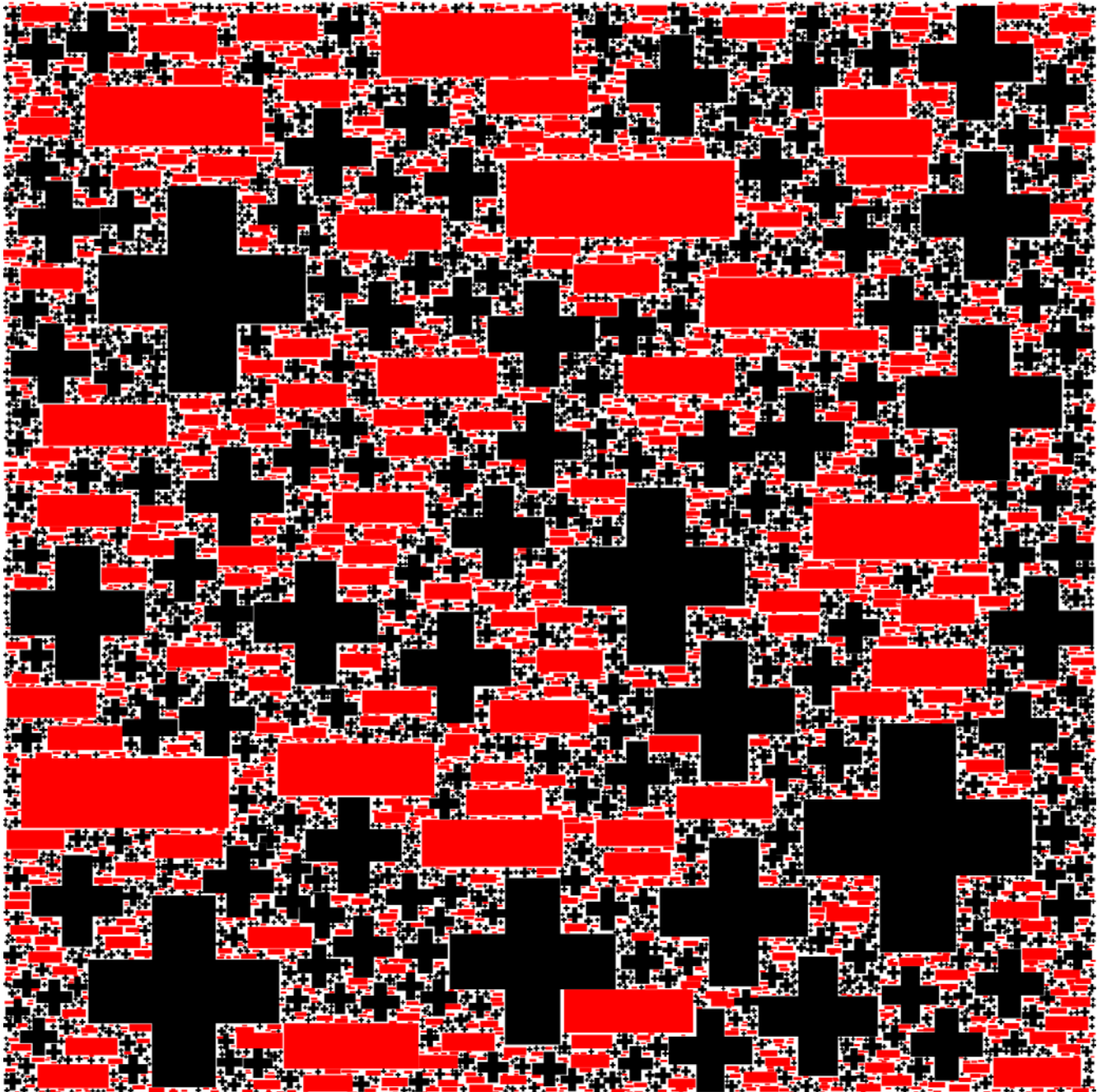


Fig. 9.71. Plus and minus, paired.  $c=1.25$ ,  $N=5$ , 8000 shapes, fill 77%

This is a variation in which the total areas of pairs of shapes obey a power law. White gasket, inclusive boundaries. Pairing was adopted because it is difficult to create + and - symbols with the same stroke width and same area, as the usual procedure would call for. The black symbols occupy 5/8 of the filled area; the red 3/8. There is significant clustering of the shapes into predominantly red and black areas. In pre-computer accounting practice red ink was for minus quantities and black for plusses.



## Rules of Construction for Two Physical Dimensions (the math-heavy page)

The object is to construct a sequence of areas  $A_i$  ( $i = 1, 2, 3, \dots$ ) which will completely fill an area  $A$ .

1. Construct a sequence of areas

$$\frac{1}{(N)^c}, \frac{1}{(N+1)^c}, \frac{1}{(N+2)^c}, \dots$$

With parameters  $N$  and  $c$ . It will be seen that  $c$  is a power-law exponent, i.e., the area sequence follows a power law.

2. The (infinite) sum of these areas is

$$\zeta(c, N) = \sum_{i=0}^{\infty} 1/(i+N)^c$$

where  $\zeta(c, N)$  is the Hurwitz zeta function (see Wiki or other for an account of its properties).

Convergence of the sum requires  $c > 1$ . When  $N = 1$  this becomes the Riemann zeta function.

3. Form a new sequence of areas

$$A_i = \frac{A}{\zeta(c, N)(i-1+N)^c}$$

( $i = 1, 2, 3, \dots$ ). By construction, these areas sum to the total area  $A$  and thus the result is space-filling if the algorithm does not halt.

4. Let  $i = 1$ . Choose a shape for area  $A_i$ , and find its linear dimension(s) from its area (e.g., for a circle  $r = \sqrt{A/\pi}$ ). Place this shape at random within area  $A$ , such that it does not overlap the boundary at any point. This is the "initial placement". Increment  $i$ .

5. Choose a shape with area  $A_i$  and place it at random within area  $A$  such that it does not overlap any boundary. Test this shape for overlap with any previously-placed shape. If it overlaps any previous shape, repeat step 5. This is a "trial".

6. If the new shape does not overlap any previous shape this is a "placement"; place its coordinates  $x, y$  and its linear dimension(s) in the placed-shapes data base, increment  $i$ , and return to step 5.

Stop at a specified number of placed shapes, a specified fill factor, or other.

This is a very simple algorithm. It appears to work for any shape or sequence of shapes obeying the power-law area rule above. It also works for different shapes of the bounding area.

One can legitimately ask "Doesn't this process eventually halt when there isn't enough space remaining?" The statistical finding is that the average number of trials needed to place the  $n$ -th shape increases as a power law in  $n$ , i.e., the process never stops, although it slows greatly for large  $n$ . Rigorous proof of this could be challenging. By construction the process is space-filling in the limit  $n \rightarrow \infty$ .

In two dimensions the usable range of  $c$  is from  $1^+$  ( $c$  must be  $> 1$ ) on up to 1.15-1.5. The maximum value of  $c$  depends on the shape, with less-compact shapes having lower maximum  $c$ . One can choose  $c$  freely within its range.  $N$  can be any number  $> 0$  (but is usually taken as an integer here). The fractal dimension  $D$  is  $D = 2/c$ .

The algorithm also works in 1 and 3 physical dimensions with the obvious adjustments.